JIMMA UNIVERSITY

JIMMA INSTITUTE OF TECHNOLOGY

SCHOOL OF CHEMICAL ENGINEERING

MASTERS OF SCIENCE IN PROCESS ENGINEERING

Process Intensification of Hydroxylation of Epoxied Waste Cooking Soybean Oil for Polyether Polyol Synthesis Using Micro Channel Technology

A Research Thesis Submitted to School of Graduate Studies of Jimma University Jimma Institute of Technology School of Chemical Engineering in Partial Fulfillment of the Requirement for the Degree of Masters of Science in Process Engineering.

By: - Selihom Birhanu (B.Sc.)

Main advisor: - Dr.-Ing. Wondwosen Sime

Co advisor:- Mr Fekadu Abera(MSc.)

September, 2026

JIMMA, OROMIA, ETHIOPIA

JIMMA UNIVERSITY

JIMMA INSTITUTE OF TECHNOLOGY

SCHOOL OF CHEMICAL ENGINEERING

MASTERS OF SCIENCE IN PROCESS ENGINEERING

This is to certify that the thesis prepared by Selihom Birhanu entitled as "Process intensification of hydroxylation of Epoxied waste cooking soybean oil for polyether polyol synthesis using micro channel technology" and submitted in partial fulfillment of the requirement for the award of degree of masters in process engineering complies with the regulation of universities and meets the accepted standards originality and quality.

Approved by the examining board

Dr. Gedefaw Asmare (Assistant professor)		9/2/2026
External examiner	Signature	Date
Dr. Ermias Girma (Assistant Professor)	----------	----------
Internal Examiner	Signature	Date
Dr.-Ing. Wondwosen Sime (Assistant Professor)	----------	----------
Main Advisor	Signature	Date
Mr. Fekadu Abera (MSc.)	----------	----------
Co Advisor	Signature	Date
Mr. Ketema Beyecha (Assistant professor)	----------	----------
Chairperson	Signature	Date
Dr. Edo Begna (Assistant Professor)	----------	----------
School Dean	Signature	Date

DECLARATION

I, Selihom Birhanu, declare that this research thesis entitled as "Process intensification of hydroxylation of epoxied waste cooking soybean oil for polyether polyol synthesis using a micro channel technology" is my original work. This research has not been presented for any other degree in any university. This research was conducted under the supervision of Dr.-Ing.Wondwosen sime (Assistant professor) and Mr. Fekadu Abera (M.Sc.). All woks and materials taken from other sources have been credited.

Submitted by

Selihom Birhanu	----------	----------
	Signature	Date

Approved by

Dr. Wondwosen Sime (Assistant Professor)	----------	----------
Main advisor	Signature	Date
Mr. Fekadu Abera (MSc.)	----------	----------
Co Advisor	Signature	Date
Mr. Tafere Aga (Assistant professor)	----------	----------
Program Coordinator	Signature	Date

ACKNOWLEDGMENT

At the beginning of everything, I want to give my deepest gratitude to the almighty God for giving me patience and strength in every step of my life. Then, I am glad to give the honor to Jimma University, Jimma Institute of Technology and School of Chemical Engineering for giving me this M.Sc. scholarship. I also want to express my heartfelt appreciation and gratitude to my advisors Dr.-Ing. wondwosen sime (Assistant Professor) and to Mr. Fekadu Abera (M.Sc.) for their kindness and support.

I want to give my respect and gratitude to the staffs of Addis Ababa University, College of Natural Science and Department of Chemistry for the collaboration that they have made with me in doing this research. I would like to be thankful to my family for their endless support, encouragement and for being there with me in every difficulty of my life.

I am very indebted and thankful to Mr. Dagnachew Teshome, Mr, Demmise Adugna, Mr. Shimeles Abera, Mr. Nasir Aman and Mr. Abdhurhaman kedir for helping me in achieving successful fabrication and assembly of micro channel reactor along with a micro channel reactor heat sink. Finally, I want to acknowledge all individuals and groups who were willing in helping me for the successful completion of this research.

ABSTRACT

The synthesis of bio based polyols from epoxied vegetable oil has gained significant interest of as a sustainable alternative to petroleum-derived feed stocks. However, the hydroxylation process of producing soy-based polyether polyol from Epoxide waste cooking soybean oil (EWCSBO) is an exothermic process, conventional reactors often suffers from heat and mass transfer limitation, leading to lower hydroxyl (OH) number. To address these limitations, this study aimed to intensify the hydroxylation of EWCSBO using a micro channel reactor integrated with a micro channel heat sink designed from hydrodynamic, mass and heat transfer literature models of 15cm width, 30cm length and 4mm diameter was fabricated. The intensified hydroxylation of EWCSBO was carried out 75 ^{O}C-90 ^{O}C utilizing ethylene glycol ($C_2H_6O_2$) following initial synthesis and refining of EWCSBO at 65 ^{O}C. System performance was evaluated by dimensionless number governing transport phenomena and hydrodynamics while response surface methodology was employed to optimize process parameter. The dimensionless numbers has directly illustrated the performance of the micro channel reactor and micro channel heat sink has performed in similar standard range way with other micro channel reactions. The statistical analysis demonstrated high reaction efficiency, yielding high OH number ranging from 390.12 mgKOH/g-441.14 mgKOH/g. Structural and thermal resistance of raw waste cooking soybean oil (WCSBO), intermediate epoxied waste cooking soybean oil (EWCSBO), and final product soy-based polyether polyol were characterized using Fourier transform infrared spectroscopy (FTIR), proton nuclear magnetic resonance (^{1}H-NMR), and Thermo gravimetric analysis (TGA). This research demonstrates a viable green chemistry approach for up cycling waste cooking oil in to bio-polyol suitable for polyurethane production in industrial several applications. It is highly essential for like textile, automotive, medical, and pharmaceutical industries. This research also gives a valuable insight for process intensification of polymer synthesis.

Keywords: Hydroxylation, Process Intensification, Micro Channel Heat Sink, Micro Channel Reactor, Soy-Based Polyether Polyol

Table of Content

DECLARATION iii
APPROVAL ..... **Error! Bookmark not defined.**
ACKNOWLEDGMENT iv
ABSTRACT v
Nomenclature xiii
INTRODUCTION 1
1.1. Background 1
1.2. Statement of the Problem 3
1.3. Objectives 4
1.3.1. General Objective 4
1.3.2. Specific Objectives 4
1.4. Research Questions 5
1.5. Scope of the Research 5
1.6 Significance of the Research 5
2. LITERATURE REVIEW 7
2.1. Vegetable oil (VO) 7
2.2. Waste cooking soybean oil (WCSBO) 7
2.3. Chemical transformations in waste cooking soybean oil 8
2.3.1. Epoxidation reaction of waste cooking soybean oil 8
2.3.2. Hydroxylation of Epoxide waste cooking soybean oil 10
2.4. Polyether Polyol 11
2.5. Applications of polyether polyol 11
2.6. Micro reactors 12
2.6.1. Micro channel reactors 12
2.6.2. Micro channel heat sink 13
2.7. Fabrication techniques of micro channel reactor system 14
2.8. Heat transfer in a micro channel reactor and micro channel heat sink 15
2.9. Mass transfer in a micro channel reactor 19
2.9. Hydrodynamics in micro channel reactor and micro channel heat sink 20
2.10. Pressure drop in a micro channel reactor and micro channel heat sink 21

2.11. Reaction kinetics in a micro channel reactor 22
2.12. Summary 23
3. MATERIALS AND METHODS 24
3.1. Materials and Chemicals 24
3.2. Apparatus and Equipment 24
3.3. Methods 25
3.3.1. Design of micro channel reactor and micro channel heat sink 25
3.3.2. Fabrication of micro channel reactor and micro channel heat sink 27
3.3.3. Pretreatment of waste cooking soybean oil 29
3.3.4. Epoxidation of refined waste cooking soybean oil 29
3.3.5. Performance test by Hydroxylation reaction of EWCSBO 30
3.4. Physic chemical characterizations of WCSBO, EWCSBO and soy-based polyether polyol 31
3.4.1. Acid value and free fatty acid determination 31
3.4.2. Iodine value determination method 32
3.4.3. Saponification value of determination method 33
3.4.4. Peroxide value determination method 34
3.4.5. Epoxy value determination for EWCSBO 35
3.4.6. Hydroxyl number determination for soy-based polyether polyol 36
3.4.7. Determination of density of WCSBO, EWCSBO and soy-based polyether polyol 36
3.4.8. Determination of specific gravity of WCSBO, EWCSBO and soy- based polyether polyol 37
3.4.9. Determination of viscosity of WCSBO, EWCSBO and soy-based polyether polyol 37
3.4 10. Moisture content determination for WCSBO, EWCSBO and soy-based polyether polyol 37
3.4.11. Refractive index for WCSBO, EWCSBO and Soy-based polyether polyol 38
3.5. Experimental and numerical evaluation of micro channel reactor and heat sink system 38
3.5.1. Heat transfer analysis for a micro channel heat sink 38
3.6. Heat Transfer Assessment of Micro Channel Reactor 42
3.7. Pressure drop determination of micro channel reactor 46
3.8. Thermodynamic assessment of micro channel reactor 46
3.9. Mass transfer measurement of micro channel reactor 46

3.10. Kinetic Study determination for hydroxylation reaction of EWCSBO 47
3.11. Statistical method 47
3.12 One factor at a time (OFAT) sensitivity analysis for hydroxylation reaction 49
3.13. Fourier infrared spectrophotometer analysis 49
3.14. Nuclear magnetic resonance analysis 49
3.15. Thermo gravimetric analysis (TGA) 49
4. RESULT AND DISCUSSION 50
4.1. Acid value and free fatty acid value determination of refined WCSBO and EWCSBO ... 50
4.2. Iodine values for refined WCSBO and EWCSBO 51
4.3. Saponification value results for WCSBO and EWCSBO 51
4.4. Peroxide values determination of WCSBO and EWCSBO 52
4.5. Epoxy value (E.V) for EWCSBO 53
4.6. Physic-chemical property values for WCSBO and EWCSBO 53
4.7. Acid values for Soy-based polyether polyol 54
4.8. Iodine values determination of soy based polyether polyol 55
4.9. Saponification value determination for soy-based polyether polyol 56
4.10. Peroxide values for soy based polyether polyol 56
4.11. Hydroxyl number (OH) number determination of soy-based polyether polyol 57
4.12. Physic-chemical properties of soy-based polyether polyol 58
4.13. Hydrodynamic properties for micro channel reactor 58
4.13.1. Reynolds number and pressure drop analysis for a micro channel reactor 58
4.13.2. Reynolds number and pressure drop for micro channel heat sink 60
4.14. Experimental Evaluation of Micro Channel Reactor 61
4.14.1 Heat transfer analysis of micro channel reactor 61
4.15. Heat transfer for micro channel heat sink 64
4.16. Thermodynamic properties for micro channel heat sink 66
4.17. Thermodynamic analysis for micro channel reactor 67
4.18. Mass transfer for hydroxylation of EWCSBO 68
4.19. Kinetic study 70
4.20. Kinetic study for micro channel reactor 70
4.21. Comparison of dimensionless numbers for micro channel reactor and micro channel heat sink with existing literatures 71

4.22. Statistical Method 73
4.22.1. ANOVA results 75
4.22.2. Model equation for OH number 76
4.22.3. Diagnostic plots 76
4.22.4. Impact of operation parameters with final OH number 77
4.22.5.Perturbation plot for process parameters for final OH number 80
4.22.6. Optimization of reaction parameters 81
4.22.7. Model validation 82
4.23. FTIR analysis for WCSBO, EWCSBO and soy-based polyether polyol 83
4.24. TGA graph for WCSBO 85
4.25. TGA graph for EWCSBO 86
4.26. TGA analysis for soy-based polyether polyol 87
4.27. H-NMR graph for WCSBO 88
4.28. NMR for EWCSBO 89
4.29. NMR for soy-based polyether polyol 90
5. CONCLUSION AND RECOMMENDATION 91
5.1. CONCLUSION 91
5.2. Recommendation 91
APPENDIX 93
Reference 97

List of tables

Table 1 Reynolds number with flow regime 19
Table 2 Literature Design parameter and Physical properties for micro channel reactor and micro channel heat sink 25
Table 3 Table for justification of design parameters selection 26
Table 4 Table for justification for selecting micro channel reactor design parameter 27
Table 5 Design specification for micro channel reactor and micro channel heat sink 28
Table 6 Process parameters for statistical analysis 48
Table 7 Acid value of WCSBO and EWCSBO 50
Table 8 Iodine values for WCSBO and EWCSBO 51
Table 9 Saponification value for WCSBO and EWCSBO 52
Table 10 Peroxide values for WCSBO and EWCSBO 52
Table 11 Epoxy value for EWCSBO 53
Table 12 Physico chemical properties of WCSBO and EWCSBO 53
Table 13 Acid value of soy-based polyether polyol 54
Table 14 Iodine values for soy-based polyether polyol 55
Table 15 Saponification value for soy-based polyether polyol 56
Table 16 Peroxide value for Soy-based polyether polyol 56
Table 17 Hydroxyl number for soy-based polyether polyol 57
Table 18 Physicochemical properties of soy-based polyether polyol 58
Table 19 Table for Re number and pressure drop determination 59
Table 20 Re number and pressure drop determination for micro channel heat sink 60
Table 21 Temperature deviation and velocity in a micro channel reactor 62
Table 22 Heat transfer analysis for micro channel reactor 62
Table 23 Data's for Temperature and velocity in micro channel heat sink 64
Table 24 Heat analysis for micro channel heat sink 64
Table 25 Thermodynamic properties for micro channel heat sink 66
Table 26 Thermodynamic properties 67
Table 27 Mass transfer analysis 68
Table 28 Comparison table for micro channel heat sink with literature results 71

Table 29 Comparison of micro channel reactor with literature values 72
Table 30 Central composite experimental design for hydroxylation of EWCSBO 73
Table 31 ANOVA results of quadratic model……..….75
Table 32 Fit statistics table 75
Table 33 Table for process optimization 82
Table 34 OFAT table for temperature 82
Table 35 OFAT table for molar ratio 82
Table 36 OFAT for reaction time 83

List of figure

Figure 1 Pretreatment techniques of WCSBO. 8
Figure 2 Epoxidation reaction mechanism. 9
Figure 3 Application of polyether polyol. 12
Figure 4 Micro channel reactor. 13
Figure 5 Micro channel heat sink. 14
Figure 6 Hydroxylation reaction of EWCSBO 30
Figure 7 Process flow diagram for hydroxylation reaction 31
Figure 8 Graph for Re number and pressure drop. 59
Figure 9 Graph Re number and pressure drop for micro channel heat sink. 61
Figure 10 Heat transfer of micro channel reactor. 63
Figure 11 Heat transfer for micro channel heat sink. 65
Figure 12 Graph for thermodynamic graph. 66
Figure 13 Graph for thermodynamics of micro channel reactor. 67
Figure 14 Re and sh number for micro channel reactor. 69
Figure 15 Sc number for micro channel reactor. 69
Figure 16 Normal plot of residuals 77
Figure 17 Predicted versus actual plot. 77
Figure 18 3D plot for impact of process parameter on OH number. 80
Figure 19 Perturbation plot. 80
Figure 20 Optimization of reaction parameters. 81
Figure 21 FTIR Graph for WCSBO, EWCSBO, and polyether polyol. 84
Figure 22 TGA graph for WCSBO. 85
Figure 23 TGA graph for EWCSBO. 86
Figure 24 TGA graph for soy-based polyether polyol. 87
Figure 25 ^{1}H-NMR graph for WCSBO. 88
Figure 26 ^{1}H-NMR graph for EWCSBO. 89
Figure 27 ^{1}H-NMR graph for soy-based polyether polyol. 90

Nomenclature

Roman Letters

A_C	Cross sectional area (m^2)
Al_2O_3	Aluminum Oxide
C	Concentration (mol/l)
Ca	Capillary number
CCl_4	Carbon tetrachloride
$CHCl_3$	Chloroform
CH_2O_2	Formic acid
CH_2O_3	Per formic acid
CH_3COOH	Acetic acid
CH_3CO_3H	Per acetic acid
CH_3OH	Methanol
C_2H_4O	Ethylene Oxide
C_2H_5OH	Ethanol
$C_2H_6O_2$	Ethylene glycol
C_3H_6O	Propylene oxide
$C_3H_{10}O_5$	Starch soluble
$C_4H_6O_3$	Acetic anhydride

d_H	Hydraulic diameter (m)
D	Diffusion coefficient (m^2/s)
E_a	Activation energy (J/mol)
F	Friction factor
G	Acceleration due to gravity (m^2/s)
Hr	Hour
H	Enthalpy change (J)
H_{wall}	Height of micro channel wall (m)
H_2	Hydrogen
H_2O	Water
H_2O_2	Hydrogen peroxide
H_2SO_4	Sulfuric acid
H_3PO_4	Phosphoric acid
Hcl	Hydrochloric acid
Icl	Iodine mono chloride
K	Thermal conductivity (W/m.K)
K_A	Mass transfer coefficient

KI	Potassium iodide
KOH	Potassium hydroxide
Kn	Knudsen number
L	Length of micro channel (m)
M_w	Molecular weight (Kg/mol)
M	Given mass (kg)
M	Meter
Mm	Millimeter
NaOH	Sodium hydroxide
$NaHCO_3$	Sodium bi carbonate
$Na_2S_2O3.H_2O$	Sodium thiosulfate
Nu	Nusselt number
N	Number of mole
O_3	Ozone
P	Static Pressure (Pa)
$\triangle P$	Pressure drop (Pa)
Pe	Peclet number
Pr	Prandtl number
Q	Volumetric flow rate (l/s)
Q	Heat released/absorbed (J)

R	Channel radius (m)
R	Reaction rate (mol.L^{-1}.S^{-1})
Re	Reynolds number
Sg	Specific gravity
T	Time (s)
T_i	Initial temperature (^{O}C)
TiO_2	Titanium oxide
T_f	Final temperature (^{O}C)
ZnO_2	Zinc oxide
3D	Three dimensional

Greek symbols

µ	Viscosity (Cp)
µm	Micro meter
A	Aspect ratio
℘	Density (kg/l)
Λ	Free molecular Path

Acronyms

ANOVA	Analysis of variance
ASTM	American society testing of materials
AV	Acid value

CASE	Coatings, adhesive, sealants, elastomers
CCD	Central composite design
CFD	Computational fluid dynamics
CNC	Computer numerated machine
EWCO	Epoxied waste cooking oil
EWCSBO	Epoxied waste cooking soybean oil
FFA	Free fatty acid
FTIR	Fourier transform infrared spectroscopy
GCM	Gas chromatography
^{1}H-NMR	Proton nuclear magnetic resonance
IR	Infrared ray
IV	Iodine value
ODE	Ordinary differential equation
OFAT	One factor at time
OH	Hydroxyl number
PE	Polyethylene
PET	Polyethylene terephthalate
ppm	Parts per million
PU	Polyurethane

RSM	Response surface methodology
RTD	Residence time distribution
SBO	Soybean oil
SMR	Small modular reactor
SV	Saponification value
TGA	Thermo gravimetric analysis
UV	Ultra violet
VO	Vegetable oil
WCO	Waste cooking oil
WCSBO	Waste cooking soybean oil

Subscripts

B	Blank
F	Final
G	Gravity (m/s^2)
H	Hydraulic
Hcl	Hydro chloric acid
I	Initial
Lit	Literature
NaOH	Sodium hydroxide
O	Outlet
S	sample

INTRODUCTION

1.1. Background

Polyols are widely used intermediate chemicals that are mostly synthesized from crude oil resources. However, the traditional synthesis method negatively impacts environmental sustainability and accelerates the depletion of fossil fuel reserves. Thus, replacement of crude oil resources by waste cooking oils (WCOs) is demanded. This approach mitigates the rapid consumption of non-renewable resources and substantially reduces carbon foot print (Dedy suhendra, 2023). WCO possess higher amount of carbon-carbon double bonds (C=C) that lead to unsaturated or unstable properties and helps to use it as a tool for further modification of other chemical reactions. These reactions include like polymerization, auto-oxidation, hydroxylation, acrylate formation, epoxidation, halogenation, hydrolysis, dimerization and others. Therefore, the presence of higher unsaturated fatty acid in WCO made it a great potential candidate to produce bio-based polyols via epoxidation and hydroxylation (Clak, 2020).

Epoxidation is a commonly used chemical reaction to produce value-added oleic chemicals using a wide range of WCOs. The resulting epoxied waste cooking oils (EWCOs) serves as useful precursors for coatings, adhesives, sealants and elastomers (CASE). Furthermore, they act as primary chemical intermediates for synthesis of bio-based polyol via ring opening reaction (Cogliano Tommaso, 2024).

Hydroxylation is an exothermic, ring opening reaction of EWCOs utilizing nucleophile reagents to cleave the oxarine rings formed during epoxidation. The process introduces hydroxyl (OH) functional groups into polyol backbone, imparting necessary thermal resistance, flexibility, or rigidity when reacted with isocyanides during polyurethane (PU) synthesis. However, hydroxylation is exothermic reaction, the fact that conventional one or two pot synthesis methods are constrained by poor thermal control localized overheating and high reagent concentrations. These limitations trigger undesired side reactions, lower conversion rates, and cause significant quality degradation in the PU product. To overcome these challenges process intensification, specifically using micro channel heat sinks, offer viable solution. In this reaction, nucleophile reagents open the epoxy ring formed by epoxidation. Additionally, the hydroxylation reaction

forms hydroxyl (OH) group in polyols that gives them thermal resistance, flexibility or rigidity when it reacts with isocyanates in polyurethane (PU) synthesis (Kim et al., 2026).

In recent years, process intensification has emerged as a paradigm shift in chemical engineering aiming to miniaturize process equipment while simultaneously boosting conversion efficiency, energy performance, and resource utilization. Traditional reactors suffer from severe heat and mass transfer bottlenecks; Consequently, small, confined micro reactor have gained significant research attention as tools for process intensification (Mastroianni et al., 2022).

Micro reactors are miniaturized reaction systems featuring sub-millimeter fluidic dimensions that confine chemical reactions with in precisely defined micro environment. The differences between micro reactors and conventional reactors are mainly their unique small size and geometry (Feng, 2023). These features of micro reactors give them a good qualified operational performance. The name micro reactors generalize a variety of reactor types like micro channel reactor , micro tubular reactor, micro packed reactors , micro trickle bed reactor and others (Gustavo V, 2023).

Micro channel reactor is highly considerable area of researches for the last four decades as a means of process intensification due to their narrow engraved channels. The reduced physical dimensions and high surface area to volume ratio enforce rapid mixing, significantly enhancing mass and heat transfer rates. This facilitates to manage the exothermic nature of several reactions that are highly difficult to be controlled. Furthermore, micro channel reactors can be seamlessly integrated with dedicated micro channel heat sinks, an innovative cooling system that utilizes a circulating medium to rapidly absorb and dissipate heat generated by continuous reactions (Sharma, 2023).

Therefore, this research focuses on process intensification of hydroxylation reaction of EWCSBO. The study aims to enhance hydroxylation performance by employing a micro channel reactor integrated with a micro channel heat sink. The methodology involves design, fabrication, and performance evaluation based on literature bench marked micro transport characteristics. This study aimed to intensify the process of the hydroxylation of EWCSBO and evaluation of the intensified performance. The methodology that was employed in this study was fabricating micro channel reactor and micro channel heat sink using literature driven design parameters by micro

machining system. The validation of the reactor system was tested by intensified hydroxylation of EWCSBO. Further performance of the reactor system was evaluated by physic-chemical characterization of soy-based polyether polyol. The final improvised product namely soy-based polyether polyol was examined by physicochemical characterizations. Moreover, molecular structure identifications were taken by proton magnetic resonance (^{1}H-NMR); Fourier transforms infrared spectroscopy (FTIR). The thermal stability analysis of the resulting soy-based polyether polyol was examined by thermo gravimetric analysis (TGA). Interactions of reaction parameters with OH number were studied using Response surface methodology (RSM). Additionally, the performance of the reactor system was evaluated using dimensionless number for mass and heat transfer efficiency.

1.2. Statement of the Problem

In recent years, the global consumption of cooking oil increased and has reached to 228 million metric ton. The annual amount of volume released of WCO reached from 29 million to 34 million metric ton globally(Salarvand et al., 2023). Thus valorization of this waste to bio based polyol is needed. However, Hydroxylation reaction of epoxide plant oils in traditional batch reactors suffers from severe mass and heat transfer limitation. Because the hydroxylation reaction is strongly exothermic, standard batch system accumulate excess thermal energy, Causing uncontrolled temperature spikes during operation. Furthermore, the immiscible nature of multiphase reactants forms a boundary film layer, presenting a major barrier to interfacial mass transfer. Consequently, these combined transfer resistance phenomena lead to incomplete reaction s and significantly reduced OH number in synthesized polyether polyol (Siti Nurzubadia, 2021) .

Polyether polyol serves as an essential precursor for PU production, an industry critical to sectors such as automotive manufacturing, textiles, and medical devices. A diminished OH value directly impairs the cross linking density and structural integrity of resulting polymer. As a result, the physic chemical properties of PU product including its thermal resistance, mechanical flexibility, structural rigidity, and plasticity are substantially compromised (Bahandari, 2023). To address these limitations, process intensification offers a promising alternative through micro reaction technology.

In this study, the hydroxylation of EWCSBO was investigated using a micro channel reactor integrated with micro channel heat sink. The micro scale channel dimensions dramatically reduce diffusion distance that enhances interfacial contact between immiscible phases and increase mass transfer rate. Additionally, the micro channel heat sink provides precise temperature control to safely manage the heat of reaction, overcoming the thermal hazards associated with exothermic nature. This research evaluates the performance and operational functionality of micro channel system, providing valuable insights into process intensified polymer synthesis.

1.3. Objectives

1.3.1. General Objective

The General objective of this research was to intensify and to evaluate the performance of a hydroxylation reaction of EWCSBO using micro channel reactor and micro channel heat sink configuration.

1.3.2. Specific Objectives

1. To synthesize epoxide waste cooking soybean oil.

2. To produce a soy-based polyol (soy-based polyether polyol) using the fabricated micro channel reactor system.

3. To evaluate the performance and thermal behavior of the micro channel reactor and micro channel heat sink system using experimental parameter measurement and dimensionless hydrodynamic analysis.

4. To characterize WCSBO, EWCSBO and, the resulting soy-based polyether polyol in terms of of physical properties (density (ρ), specific gravity (S.g), and viscosity (μ), chemical properties (A.V, S.V, I.V, Epoxy equivalent weight (EW), and OH number), and analytical profiles (FTIR, NMR, and TGA).

5. To analyze the main and interactive effects of independent process parameters (Temperature, time and molar ratio of EWCSBO to $C_2H_6O_2$) of hydroxylation of EWCSBO on OH value of synthesized.

1.4. Research Questions

1. Is it feasible to generate a value-added product from WCSBO through the epoxidation process?
2. How to further process a EWCSBO in to other value-added product in the fabricated micro channel reactor to test the performance of the reactor system?
3. How to evaluate the performance of a micro channel reactor and a micro channel heat sink system using experimental method?
4. What techniques need to utilize to identify WCSBO, EWCSBO and soy-based polyether polyol by their physicochemical properties?
5. What methods to use to analyze the interdependence of independent reaction parameters of hydroxylation reaction of EWCSBO with final OH value of soy-based polyether polyol?

1.5. Scope of the Research

This research focuses with the range of utilization of literature based micro channel reactor and micro channel heat sink for process intensification and performance evaluation of hydroxylation of EWCSBO. The design parameters for micro channel reactor and micro channel heat sink was set using literature based data. Then, lab scale prototype for micro channel reactor and micro channel heat sink was fabricated using micro machining tools. Then, the fabricated and assembled micro channel reactor system was tested by intensified hydroxylation of EWCSBO. EWCSBO was produced in a three necked reactor prior to the performance test. The process performance evaluation was done using physicochemical characterization of soy-based polyether polyol characterization using A.V,S.V,I.V,P.V, EW,OH number, FTIR, ^{1}H-NMR, and TGA analysis. The interaction of process parameter with final OH number was studied using RSM specifically CCD technique. The performance analysis of micro channel reactor and micro channel heat sink was analyzed by dimension less numbers. Therefore, the scope of this research was process intensification and process evaluation of hydroxylation reaction of EWCSBO using small scale micro channel reactor and micro channel heat sink.

1.6 Significance of the Research

This research served as a way to provide a foundation framework for decentralized process intensification in green chemistry. The application of literature based micro channel reactor and

micro channel heat sink reduces mass and heat transfer limitation for the hydroxylation of EWCSBO. The synthesis of soy-based polyether polyol with more enhanced OH value will have a direct essence on production of thermal resistant, rigid and flexible PU foams. This would benefit several industries like automotive, medical, textile, construction and other industries. Moreover, this research has enormous significance in waste valorization. The usage of WCSBO as an input for production of EWCSBO enhances green chemistry and circular economy.

2. LITERATURE REVIEW

2.1. Vegetable oil (VO)

Vegetable oils (VO) are cooking oils that mainly derived from natural plant sources like flax seed, sesame seed, soybean, nut, palm, sunflower, olive, and others. These VOs are composed of triglycerides and fatty acid chains. This composition includes higher amount of mono, polyunsaturated fatty acids and antioxidants that reduce the risk of several diseases and make them preferable for ingestion (Nasser R.Abd E Rahan, 2021).

The composition and characterizations soybean oil (SBO) is studied and found those (20-30%) oleic chains, (7-10%) linoleic acid chains, palmate acid (6-10%), stearic acid (4-5%) and 78% triglycerides. Linoleic and oleic chains are unsaturated fatty chains. These structures made it a great potential chemical substrate for further chemical modification (Wei Han foo, 2022).

2.2. Waste cooking soybean oil (WCSBO)

WCSBO is a used cooking SBO from several repetitive frying actions. WCSBO after repetitive usage and heating processes contains many free fatty acid chains (FFA). Furthermore, the unsaturated fatty acid forms polymerization, oxidation and hydrolysis reaction in the course of repetitive usage. The reaction of unsaturated fatty acid of WCSBO with atmospheric oxygen (O_2) forms an oxidation reaction. As a result, this creates smoke while frying. On the other hand, the reaction of unsaturated fatty acid creates polymerization. This reaction causes rancidity and alters the properties of the oil including lubricity, viscosity, density and stability. Thus, further pretreating techniques are needed to be employed to improve its properties. This is also useful to make it ready for further transformation technologies by creating a space for effective collision of molecules. Those pretreatment techniques include biological, chemical and physical methods (Halima kerras, 2023).

Physical methods: - The physical methods are mainly applicable to remove impurities from the WCSBO through several unit operations. These include heating, membrane separation, filtration and sol-gel adsorption that help to remove impurities and moisture resulted from a number of usages (Wei Han foo, 2022).

Chemical methods: - Chemical treatment methods involve enormous transformation reactions that further change the refined WCSBO in to some other newly formed products. WCSBO can

be transformed in to bio-based energies like biodiesel, bio-based polyols and other fine chemicals through these techniques (Beghetto, 2025).

Biological methods: Biological methods involve microbial action/Enzymatic activity of microorganisms like bacteria. These are needed to degrade triglycerides to glycerol and to produce methyl ester in biodiesel production of WCSBO. These techniques are very essential to reduce waste and pollution with minimal cost (Jermy ong shung sheng, 2024).

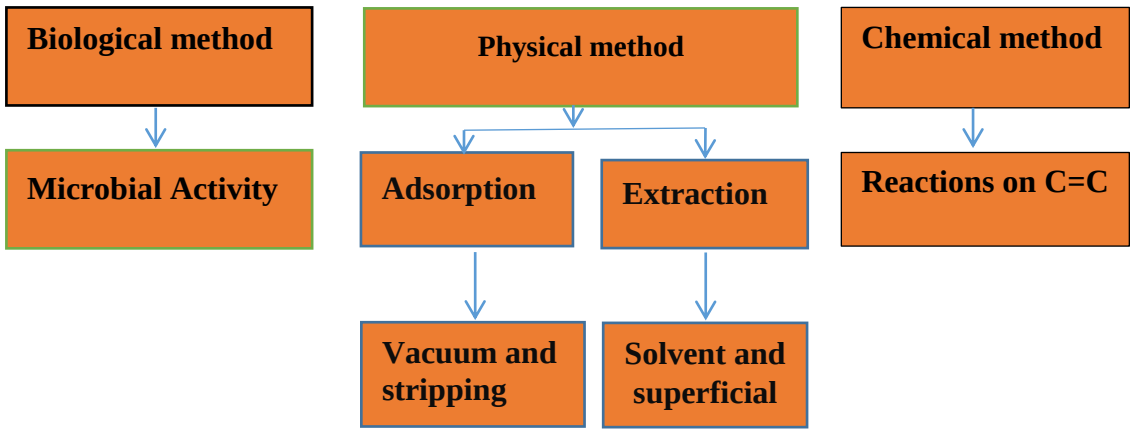


Figure 1 Pretreatment techniques of WCSBO (Himanshi Soni, 2023).

2.3. Chemical transformations in waste cooking soybean oil

There is an immense application of WCSBO in chemical transformations in which WCSBO served as great precursor for a reaction of hydrogenation, trans-esterification, ozonlysis, hydrolysis, polymer production via epoxidation and hydroxylation. WCSBO as an oil phase and aqueous phase yield many bio-based products (Beghetto, 2025).

2.3.1. Epoxidation reaction of waste cooking soybean oil

Epoxidation is a chemical reaction used to form an epoxy ring from carbon-carbon double bond of WCSBO. Epoxidation reaction takes place using carboxylic acid reaction namely acetic acid (CH_3COOH) or formic acid (CH_2O_2) as an oxygen acceptor. On the other side, hydrogen peroxide (H_2O_2) acts as an oxygen donor. This forms per-acetic acid (CH_3CO_3) or per-formic acid (CH_2O_3) which used as a main tool to form epoxy ring using homogenous and heterogeneous catalyst (Helbling et al., 2023).

A reaction of epoxidation of SBO with a blend of rapeseed oil using a homogenous catalyst of sulfuric acid(H_2SO_4) has been studied and an optimum process parameters were obtained at 65 ^{O}C (Hong phuoug 2023) have performed epoxidation of a blend of SBO and rapeseed oil using a homogeneous catalyst of sulfuric acid (H_2SO_4) to produce epoxied oil. This study also revealed the optimum process parameters.

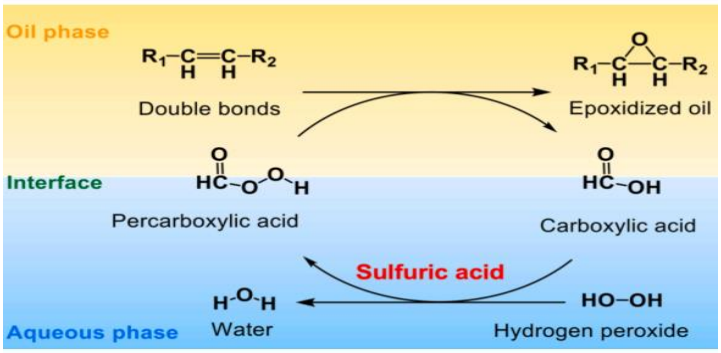


Figure 2 Epoxidation reaction mechanism (Juliana cardenas, 2025).

In this reaction, Temperature, catalytic activity, time and molar ratio of WCSBO to H_2O_2 play a significant role for the performance of the reaction. These reaction parameters have a huge impact on the overall performance of the reaction (Suhendra et al., 2023). The reaction of epoxidation of WCSBO can be performed using aluminum Oxide (Al_2O_3), Titanium oxide (TiO_2) as heterogeneous catalyst in a three necked reactor with one side thermometer and one side condenser at 50-60 ^{O}C for an average of 3-4 hrs (Fengyan zhang, 2023).

The effect of molar ratio of the oil phase to aqueous phase also has a significant impact on final epoxy ring formed. The optimum molar ratio ranges from 1:1-1:3. Higher molar ratio beyond the optimum value resulted rapid consumption of the limiting reactants and consequently reversibility of chemical reactions occurred (Ibrhaima Balde, 2022).

Moreover, the application of heterogeneous catalyst like metallic oxides, zeolite, and amberlite-120 is common in a reaction of epoxidation. The presence of these types of heterogeneous catalysts reduces viscosity and enhances lubricity. The action of enhancing lubricity of epoxide oil by heterogeneous catalyst is performed by speeding the reaction time. As the reaction proceeded, the viscosity increased. Thus heterogeneous catalysts play a significant role in

enhancing lubricity by lowering reaction time (Ji et al., 2022). While several studied on epoxidation reaction, the fact that epoxidation reaction is exothermic reaction and the difficulty of temperature regulation still remains a delicate point to gain qualified epoxide oil products.

2.3.2. Hydroxylation of Epoxide waste cooking soybean oil

Hydroxylation is a reaction that serves as a milestone to produce bio-based polymers. This epoxy ring-opening reaction uses hydrogen-containing reagents like H_2O, methanol (CH_3OH) , and $C_2H_6O_2$. Hydroxylation generally has been done using homogeneous or heterogeneous catalyst for hydroxylation of EWCSBO. Hydroxylation can take places in one or two-pot synthesis reaction. In both one and two pot synthesis the reaction open up an epoxy ring but the main difference is the time it takes to produce the soy-based polyether polyol (Gabriel L.O. Carmo, 2023).

One step synthesis of hydroxylation reaction using a heterogeneous catalyst of osmium tetra oxide (OsO_4) was done. It had a reaction time of 1 hr to produce polyether polyol. Significant amount of OH number increment was observed due to reaction time decrement. However, the toxicity of the catalyst imposes difficulty on catalyst separation (Rahmadi et al., 2024). Hydroxylation reaction can also be performed in two pot synthesis where epoxidation and hydroxylation occurs in two separate reactors. Here, in this reaction, a wide range of catalysts including metallic oxides, sulfated polystyrenes resins, and zeolite are used. Furthermore, homogeneous catalyst like H_2SO_4 and phosphoric acid (H_3PO_4) were used (Leszczynska et al., 2021).

Literatures on hydroxylation reaction manly rely on conventional reactors that suffer from hotspot and severe heat management problem. Even though studies have shown better performance of hydroxylation reaction with heterogeneous catalyst reactions, the toxicity and rare availability of the catalyst raise other critical issues on difficulty of catalyst separation on post processing. Thus, there is a crucial gap on the utilization of effective process intensification for this specific reaction. Therefore long reaction hours and poor performance is resulted.

2.3.2.1. Factors affecting efficient hydroxylation reactions

The performance of hydroxylation reaction heavily depends on the process parameters in which the reaction takes place. Temperature, reaction time, catalytic activity and molar ratio are key

factors that affect hydroxylation reaction. The temperature range for hydroxylation ranges with 75-110 ^{O}C (Kuang et al., 2023).

Longer reaction time for hydroxylation reaction beyond the optimum point lowers the performance of ring opening reaction. It has been revealed that the optimum reaction time is 1-3 hrs. As the time proceeds the reaction temperature increases more that hinders the performance more (Wazed et al., 2023).

Furthermore, catalysts role in conventional reactors is quite significant for both homogenous and heterogeneous case. For biphasic reaction like hydroxylation, the viscosity of reactants matters significantly. Therefore, in most studies, using sulfated based solid catalysts and metallic oxides catalyst used to reduce viscosity of reactants (Salarvand et al., 2023).

The study on optimization of hydroxylation reaction has found that optimum reaction parameters depend heavily on the reactor ability (Morales-Cerrada et al., 2021). However, conventional reactors are highly exposed for mass and heat transfer barriers. These resulted long reaction hours, higher reaction temperature and poorer performance. Thus, there is a critical gap in mitigation of such inconsistent process parameters.

2.4. Polyether Polyol

Polyether polyols are commonly used polyols in production of PU. PUs are manufactured by addition reaction of cyclic ethers like epoxides, Ethylene oxide ($C_2H_6O_2$)**,** Propylene oxides (C_3H_6O) with a wide range of isocyanides. Polyether polyols mainly used in PU rigid foam, soft foam and molding foam synthesis. This is due to their nature of enhanced characteristics of abrasion, resistance, heat resistance and chemical resistance and shock absorption (Jinhua Yi, 2021).

2.5. Applications of polyether polyol

Hydroxylated polyether polyol can serve as a precursor for production of PU that used to produce rigid and flexible foams with the reaction of isocyanides and polyether polyols. This is essential for matter and fabrics production. This serve in textile, medical, automotive industries (Kim et al., 2026). Moreover, Polyether polyols has been shown as effective tools for coatings, adhesives, sealants, and elastomers (CASE) due to its oily base and nature (Zafiah, 2023).

Additionally, pharmaceutical usage of poly ether polyol was studied; polyether polyol can be used for synthesis of gelatins, ointments and capsules. The bio based origin of polyether polyol made it suitable for safe assimilation (Azilatul Nabilla Zakwan, 2022).

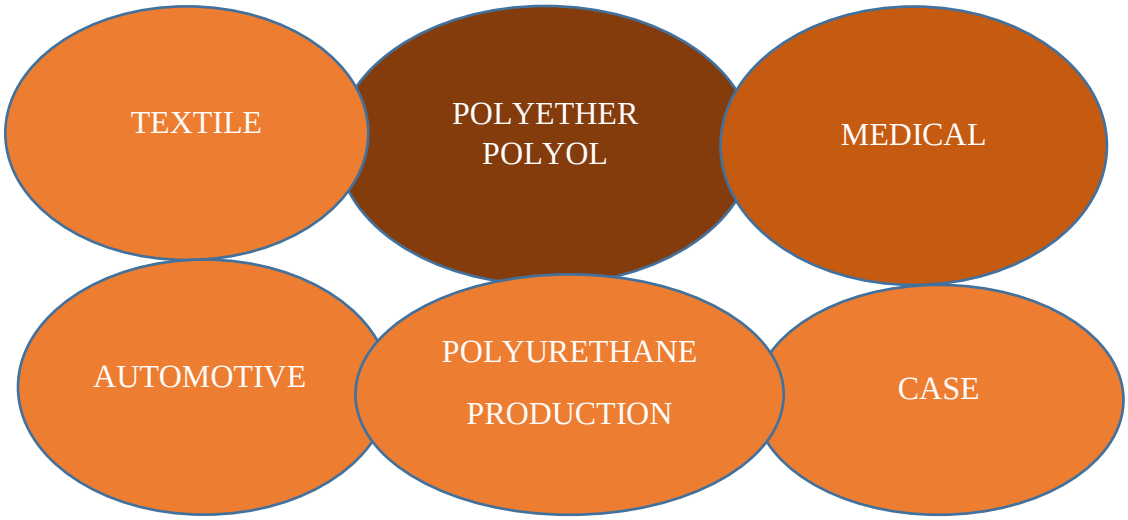


Figure 3 Application of polyether polyol (Alienor Delavardar, 2024).

2.6. Micro reactors

Micro reactors are small modular reactors (SMRs).They are noted by small dimension that ranges with 10 to 10 ^{4}µm. Micro reactors have obtained a huge attention of academic and industrial areas due to their higher surface area to volume ratio. These tools have reduced volume, more specialized and unique configuration. These features resulted improved reaction control of temperature increment, concentration, pressure drop and reaction time (Shaojie Tan, 2023). Micro reactors has an enormous application regarding on catalytic and non- catalyzed reactions, power generation, military application due to its ability for power generation (Aloisyus Yuli widianto, 2023).

2.6.1. Micro channel reactors

Micro channel reactors are small- reactors with narrow channels that have small hydraulic diameters for enhanced thermal performance, almost constant pressure drop and excellent mass transfer. These features of the reactor grant several additional merits that change the complete performance of the reactor system (Zhang & Yue, 2025).

Speedy reactions: - These small dimensions result fast reactions with improved mass and heat transfer. The rate at which raw materials changed to products is very high. This directly has a potential to form a qualified product with lesser byproduct (mastroani luca, 2022).

Enhanced conversion of product: - A number of factors including mass, and heat transfer rate, moderate reaction parameters facilitate enhanced performance of the reactor. As a result, shorter reaction time is achieved and prevents reversible reaction (mendonza, 2025).

Portability and scalability: - The modularity nature of the reactor makes it to be easily compacted and portable. Furthermore, the portability of the reactor helps to transport it to remote off- grid areas for case of power generation plant. The micro channel reactors are also suitable for perfect scaling up through numbering up process (Lee et al., 2021).

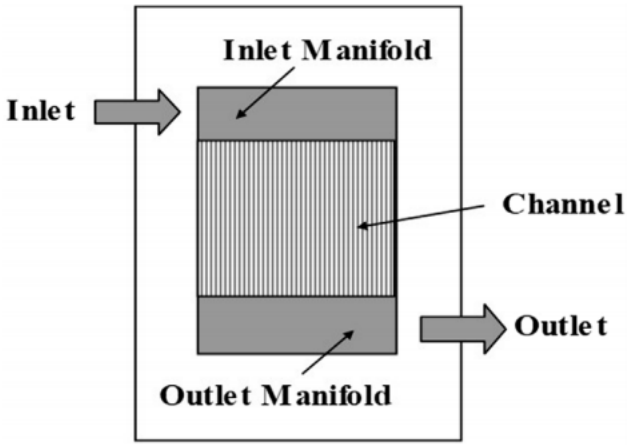


Figure 4 Micro channel reactor (Enhong Cao, 2021).

2.6.2. Micro channel heat sink

Micro channel reactor has been studied for decades majorly on its applications in electronics industry. A micro channel heat sink is a relatively tiny and advanced cooling technology that helps to dissipate heat with its unique geometry and cooling medium by absorbing a heat of reaction (Zhang & Yue, 2025).

The application of micro channel heat sink in electronics industry with an extended fin structure made it to be highly applicable for purpose of heat dissipation using Nano fluid as a cooling

medium (G Marsegila, 2024). The fact that micro channel heat sink have unique dimension has made it to be a great potential candidate for cooling medium in electronics industries. However, the applications of micro channel heat sink in chemical reactions are limited in electronics industry.



Figure 5 Micro channel heat sink (Xu ming, 2025).

2.7. Fabrication techniques of micro channel reactor system

The micro channel reactor and micro channel heat sink have enormous techniques of fabrication including micro machining, lithography, wet itching, dry itching, laser ablation and 3D (three-dimensional) printings are the prominent. These methods do vary based on their applications and the material of construction used to develop the reactor or the heat sink (Naveen Anthuvana, 2024).

A. **Micro machining: -** It is a method of developing a reactor system using grinding, grooving and cutting tools with specific size and shapes. Micro machining uses rotor, cutter, drills and computer numerated controller (CNC) machine to produce the desired geometry. It is the one of effective methods of fabrication to produce a desired system with a given precision (Boss et al., 2015).
B. **Lithography: -** This method uses light and electron beams to create a desired pattern then etched with an acid to remove all the impurities. Most of semi-conductor industries used such type of micro-electron lithography technology to get precise shape and size of the heat sink chip (Afzal et al., 2022).
C. **Laser Ablation:** - This method uses laser technology to develop a MRT for a construction material of metal, polymer and ceramic. Laser machine with a precise 3D design produces a reactor with exact dimension (Xu ming, 2025).

D. **3D Printing: -** It is a cost effective method to produce a micro channel reactor and a micro channel heat sink with accessories. This method mostly used to visualize reactor system in prototype sampling stage (Kai Han, 2022).

E. **Extrusion: -** This type of reactor development technique is not commonly used. Nevertheless, it helps in fabricating micro channels that are embossed with polymer materials in specific dimension (Koosha Karimi, 2024).

F. **Injection molding: -** Injection molding is other way to fabricate micro channel reactor and heat sink. The construction material of the reactor is injected, molded and designed with a given shape and size. Injection molding is mostly applicable for development of micro channel made from polymers (Devahdhanush et al., 2021).

G. **Dry and wet etching: -** Dry and wet Etching process are used to remove impurities from the micro channel reactor and heat sink using plasma and liquid acid solutions respectively. Mostly, the wet etching medium for micro channels reactors and heat sink is H_2SO_4 (Yan et al., 2022).

2.8. Heat transfer in a micro channel reactor and micro channel heat sink

The heat transfer in a micro channel reactor and heat sink can be achieved in main two modes of transfer namely conduction and convection. Conduction mode of transfer defined as a heat transfer between compacted inter molecular particles, while convection is a heat transfer in fluid phase between slightly far parted molecules. Heat transfer in convection mode achieved using either an external force (Forced convection) or convection heat transfer using natural density difference (Natural convection) (Saadouni et al., 2026).

The impact of micro channel reactor on the thermal performance of exothermic reactions is studied by its ability to create its space for conductive and convective heat transfer. This resulted to maintain the temperature at nearly constant ranges and provide isothermal reaction condition (Pontes. P, 2022). The heat transfer in a micro channel reactor and heat sink depend on the geometry of the reactor, fluid properties like ρ, μand the conductivity of the wall (K). Modes and efficiency of heat transfer in the reactor system examined numerically and experimentally. The experimental analysis uses thermo couples to measure the temperature distribution (Yu et al., 2024).

Nusselt number (Nu):- This is a dimensionless number that represent the ratio of convective heat transfer to conductive heat transfer. Higher Nu number shows the heat transfer mode resembles to convection. Small Nu number shows more conductive transfer mode. It serves as a reference of mode of transfer of a given heat transfer system (Jarred Wilhite, 2024).

$$Nu = \frac{hL}{k} \qquad (2.1)$$

Where

Nu-Nusslet number

h- Connective heat transfer coefficient ($W/m^2.K$)

k- Conductive wall (W/m.K)

ΔT- Change in temperature (^OC)

L- Length of the reactor (m)

Knudsen number (Kn): - It is a dimensionless number that determines fluid flow and heat management efficiency. Kn number is mostly applicable for single-phase flow of a given system. The value of Kn number determine the flow regime and molecular behavior. Kn number can be calculated as shown on equation (2.2).

$$Kn = \frac{\lambda}{n} \qquad (2.2)$$

Where ʎ-free path of a fluid molecule

L-Characteristic length (m)

When Kn >1, the molecular collision is higher than channel diameter or characteristic length. In such case, microscopic properties play a significant role. When Kn <1, the molecular movement of the fluid are not that much significant thus macroscopic properties are taken to consideration (Udom & Lappa, 2025).

Peclet number (Pe):- Peclet number is one of dimensionless number that implies the heat transfer mechanism in a microfluidic system. Pe number is a ratio of convection force over diffusion force. The higher Pe number shows a flow that smoothly passes through the channel.

Pe number is mostly used as a parameter to design a micro channel reactor and micro channel heat sink (Sharma, 2023).

$$Pe = \frac{uL}{D} \qquad (2.3)$$

Where

u- Velocity (m/s) D-Diffusivity-constant (m^2/s)

L- Length of the channel (m)

When Pe>1, convection heat transfer is more dominated rather than diffusion. In this case, parallel flow with uniform velocity is observed. When Pe<1, Diffusion heat transfer is more dominated. Here, homogenous and efficient mixing is enhanced.

Biot number (Bo):- Biot number (Bo) is also a dimensionless number that shows the way of heat transfer in a micro channel reactor and micro channel heat sink. The ratio of Bo number shows their comparison of conductive internal resistance to convective external resistance (Udom & Lappa, 2025).

$$\mathrm{Bo} = \frac{\mathrm{hL}}{\mathrm{k}} \qquad (2.4)$$

Where

h- Heat transfer coefficient ($W/m^2.K$)

L- Length of the micro channel (m)

K- Conductivity of the wall of the channel (W/m.K)

Higher Bo number shows that conductive heat transfer mechanism is more observed. The small Bo number implies the conductive resistance is higher. Thus, Heat transfer rate approximate to convective heat transfer (Shaojie Tan, 2023).

Fourier number (Fo):- Fourier number (Fo) number shows the heat conductivity rate of a micro channel reactor and a micro channel heat sink. When Fo number is higher, higher conductive

heat transfer rate is observed. Most of the time higher Fo number is preferable for effective performance (Subramaniya, 2022).

$$Fo = \frac{K \triangle T}{L} \qquad (2.5)$$

Where

K- Thermal Conductivity constant of the wall (W/m.K)

L-Length of the channel (m)

ΔT-Temperature difference (^{O}C)

Higher Fo number for both micro channel reactor and micro channel heat sink indicates the higher tendency of K. This is an essential feature of the system, which promotes the absorbance, release of heat of reaction in faster rate. Smaller Fo number indicates lower conductivity of the system. This directly affects the heat transfer rate (Devahdhanush et al., 2021).

Reynolds number (Re):- Reynolds number indicates the flow regime and fluid mixing efficiency. This dimension less number shows that if a given flow type is turbulent or not. Re number shows the mixing rate. If Re number is higher, it shows turbulent mixing. However, if Re number is lower, laminar flow is more dominant. In a micro channel reactor and in a micro channel heat sink the common flow type is laminar flow due to small dimension of the reactor and the heat sink (Bai & Torii, 2024).

$$Re = \frac{\rho U d_H}{\mu} \qquad (2.6)$$

Where

ρ– Density (Kg/l)

d_H- Hydraulic diameter of the channel(m)

u- Velocity of fluid (m/s)

μ-Viscosity (Cp)

Where d_H is expressed as

$$d_H = \frac{2wH}{w + H} \qquad (2.7)$$

Where W- Width of the channel (m) H- Height of the reactor of the heat sink (m)

Table 1 Reynolds number with flow regime.

Type of flows	Value of Re number
Laminar flow	Re<2300
Transition flow	2300<Re<4000
Turbulent flow	Re>4000

2.9. Mass transfer in a micro channel reactor

The mass transfer in micro channel reactor can directly imply the conversion rate of the reaction. The mass transfer depends on volumetric flow rate (Q), channel dimension, pressure drop (ΔP), and flow pattern in the channel. The mass transfer in a micro channel reactor has two forms either convective or diffusion (Pierre Albrand, 2023).

The mass transfer in a heterogeneous catalyst in a micro channel reactor is done using diffusional mass transfer of sulfated catalyst. The small diffusional distance resulted shortened time needed for interior and exterior diffusion (Enhong Cao, 2021). The experimental analysis of mass transfer can be done using calculation of mass transfer coefficient (K_A). This coefficient mostly analyzed by using concentration data from the reaction experiments. The analysis of concentration in a micro channel reactor can be experimentally done using FTIR or GCM (Gas chromatography) resulted value. K_A can be analyzed as shown below (Widianto et al., 2024).

$$KA = Ac(CA_1 - CA_2) \qquad (2.8)$$

Where

Ac-Cross sectional area (m^2) CA_2- Final concentration at outlet (mol/l)

CA_1-Intial concentration at inlet (mol/l)

The mass transfer for a micro channel reactor can also be examined by the relation it has with Re number. As Re number is increased, the fluid mixing in the reactor is high, as a result the mass transfer rate of the reactants increased. Laminar flow (with small Re number) also show higher tendency of reactant mixing in slow or smooth manner (Bouras, 2021).

Pe number also imply mass transfer rate. Smaller Pe number means there is more diffusion force than convective force. Therefore, for heterogeneous catalysis reaction, smaller Pe number is preferred. On the other hand, for homogeneous reaction, where convective mass transfer is more dominant, Higher Pe is a good performance indicator (Fu, 2023).

2.9. Hydrodynamics in micro channel reactor and micro channel heat sink

Hydrodynamics is a general term that collectively describes behaviors like flow pattern, ΔP and fluid mixing of a micro channel reactor and in a heat sink. The hydrodynamic characteristics of a given reaction in a micro channel configuration depend on Physic-chemical properties, type of micro mixer, channel geometry and phase of the fluid. There are different flow patterns in a micro channel reactor, and micro channel heat sink. These include slug flow, annular flow, segment flow; churn flow, bubbly flow, and slug-annular flow are commonly used flow patterns. These flows serve in both single-phase flow and multi-phase flow (Gao et al., 2022).

Slug flow: - Slug flow is mostly noticeable in two immiscible liquid-liquid multi- phase reactions and gaseous reactions that create bubble. Consequently, this results large interface area formation. Slug flow is highly characterized by elongated liquid or bubble flow that relatively move in slow movement (Fu, 2023).

Droplet flow: - Droplet flow usually observed in dispersed immiscible phase flow that form droplet caused by the dispersion of liquid. The shear stresses between the droplets create intensive molecular collision and mixing. The droplets form a complete immiscible flow in the reaction that lead to constant reaction volume (Shen et al., 2023).

Parallel flow: - In this flow type, parallel movements of liquid that have uniform velocity distributions are the main characteristics. As a result, effective mass and heat transfer with shorter residence time is achieved. This flow mainly involves in polymerization reaction (Alina Niculescu, 2022).

Annular flow: - Annular flow is in both liquid and gaseous phase reaction where there is a film thickness formed between the reactants. Annular flow can be significantly seen in H_2O_2 formation. Annular flow is suitable for two-phase flow where one phase forms a thin layer where the other is moving. In this case, annular flow forms two distinctive phase regime due to layer formation (M.B et al., 2024).

Churn flow: and bubbly flow: – Churn type of flow is very essential in single gaseous phase reaction. In this flow, there is a formation of large gas bubbles. Bubbly type of flow is also a type flow in a micro channel reactor and heat sink used in single gaseous phase flow where gaseous form small bubbles (Benrabah, 2025).

Slug-annular flow: - This is a transition flow between slug and annular flow. It has intermediate properties of annular and slug. In this type of flow, both long liquid bubbles with higher interface area and formation of thin layer between immiscible phases are observed (Giri, 2023).

The range of Re number shows the rate of fluid mixing in the reactor. If the reactor has a turbulent flow, higher Re number is observed. The contact or mixing in small d_H of cross ponds to higher efficiency. Thus, Greater Re number is more preferable for a qualified and fast production process (Gaikwad & Mohite, 2022).

Pe and Ca number can also further analyze the hydrodynamics efficiency of micro channel reactor and micro channel heat sink. Higher Pe number has more dominant convection force than diffusion force. This means that Q of the system is very high. When Pe <1, the Q may not be that much higher but higher fluid mixing and molecular collision is attained (Yu et al., 2024).

2.10. Pressure drop in a micro channel reactor and micro channel heat sink

The analysis of ΔP is a critical factor for the overall performance analysis of the micro channel reactor and heat sink. ΔP influences the rate of mixing of reactants throughout the channels. Micro channel reactors and heat sinks mostly involve either active or passive mixing system. In active mixing system, micro channel reactor uses a pumping source. On the other hand, Passive micro channels use the geometry of the reactor like Tesla shape or Y-shape for mixing of the reactants. The ΔP in active system is nearly constant because of small size of the reactor and heat sink. Nevertheless, passive mixing system show significant ΔP (Feng, 2023).

The experimental measurement of △p of system at inlet and outlet-section can be performed with the help of pressure gauges or transducers. For active micro channel system, pressure sources like syringe pumps or micro pumps are mostly used to pump the fluid through the channel (chen, 2022).

In most micro channel reactor and micro channel heat sink, the short diffusion distance of the channel result rigorous mixing and higher. This benefits heat and mass transfer rate. For Passive mixing system, the flow is laminar. Therefore, the appropriate equation is Hagen possiulie equation in (2.9) (Enhong Cao, 2021).

$$\triangle P = \frac{8\mu LQ}{\Pi r^4} \qquad (2.9)$$

Where

ΔP- Pressure drop (Pa)

Q-Flow rate (L/min)

μ-Viscosity (Cp)

r- Radius of the channel (m)

2.11. Reaction kinetics in a micro channel reactor

In a micro channel reactor, the reaction kinetics is intrinsic. This is due to efficient mass and heat transfer rate of the reactor. This caused short reaction time for changing raw materials to desired product. The residence time distribution (RTD) of a micro channel reactor resembles to an ideal flow due to its contact area of reactants. Kinetic study of a micro channel reactor can be analyzed using In-line or off- line analysis. In - line analysis usually done by the collaboration of the experimental setup and spectra photometers. These spectra photometers are ultra violet (UV) and IR (infrared) analysis (Zhang & Yue, 2025).

Off-line analysis involves taking concentration of the reactant at inlet and outlet points (Yan et al., 2022).The concentration data are examined by GCM analysis techniques. Consequently, mass transfer coefficients (K_L) get analyzed. The RTD can be measured by tracer observation of experiments (chen, 2022).

2.12. Summary

In summary, while the usage of WCSBO for production of sustainable epoxide oil and polyether polyols via epoxidation and hydroxylation is a quite established topic in many existing researches, there is a crucial remaining gap. Specifically, the hydroxylation of EWCSBO has unsolved bottleneck on mass and heat transfer barriers in conventional reactor. The reaction temperature of hydroxylation of EWCSBO mostly ranges from 1-3 hrs and temperature of 100-105 ^{O}C. Thus maintain reaction parameters using micro channel technology are demanded. Furthermore, despite the immense application of micro reactor technology on several areas, the process intensification of hydroxylation reaction of EWCSBO using integrated micro channel reactor and heat sink is missed. Most studies of micro channel heat sink studied its role in electronics industry. The application of heat sink with integration of micro channel reactor for optimization of reaction performance is underrated. The utilization of water as a cooling medium for specific reaction of hydroxylation of EWCSBO is uncommon. Thus, this research addressed these gaps by process intensification hydroxylation reaction of EWCSBO for polyether polyol synthesis using micro channel technology.

3. MATERIALS AND METHODS

3.1. Materials and Chemicals

In this study, the sample of WCSBO was collected from local restaurants in Addis Ababa, Ethiopia. All chemicals and reagents used were in analytical reagent grade. The reagents and chemicals used are glacial acetic acid (CH_3COOH purity 99.5%, India), hydrogen peroxide (H_2O_2, Purity 30%, National peroxide Ltd., India), ethylene glycol ($C_2H_6O_2$, India glycol Ltd., Purity 99%, India), titanium oxide (TiO_2, Travancore titanium products, India). Potassium hydroxide(KOH, Jay Dinesh chemicals, china),Hydrochloric acid (Hcl, purity 37%,Thermo FischerscientificTurkey),sodiumthiosulfate($Na_2S_2O_3.H_2O$,vinipulLtd.,India),Carbontetrachloride (CCl_4,purity99.5%,mercklifescience,India),chloroform($CHCl_3$,oxychem,USA),Aceticacidanhydride($C_4H_6O_3$ purity 99.95%,Jubilant, India), starch soluble($C_6H_{10}O_5$, Thermo Fischer scientific Ltd., India), sodium bi carbonate ($NaHCO_3$ purity 37%, GHLC Ltd., India), distilled water (H_2O, Ranchem chemical Ltd., India), Iodine mono chloride (Icl, purity 99%,Muby chemicals, India) phenolphthalein indicator ($C_{20}H_{14}O_4$, Macsen Laboratories, India), potassium iodide(KI, Calibre chemicals , India) all were purchased from Sida chemicals Ltd. in kirkos, Addis Ababa, Ethiopia.

3.2. Apparatus and Equipment

In this research, for fabrication of micro channel reactor and micro channel heat sink a laser machine (Hans Laser, china) was used for both parts. A rotor machine (Ronald DGA, Japan) has been used as a tool for engraving the channels. For experimental process parameters control 2 k-type thermocouples (Basstor, China), 2 temperature controllers (Fuji electric, Japan), 2 contactors (Fuji electric, Japan) and 4 small pressure gauges (Shanghai automation, China) have been used. For laboratorial synthesis and titration were three-necked flask(Glassco laboratories, India), burette(Glassco laboratories, India), measuring cylinder(Glassco laboratories, India), conical flask(Glassco laboratories), Erlenmeyer flask(Glassco laboratories, India), pipette, funnel(Glassco laboratories, India) ,condenser(Glassco laboratories, India), separator funnel (Glassco laboratories, India), universal indicator(Macsen laboratories, India), thermometer(Glasco laboratories, India), capillary meter(Glassco laboratories, India), prism(

Trioptics, Germany), hot plate with a magnetic stirrer(Bio base manufacturer, china) are all used in synthesis and characterizations of WCSBO, EWCSBO and soy-based polyether polyol.

3.3. Methods

3.3.1. Design of micro channel reactor and micro channel heat sink

The design of micro channel reactor and micro channel heat sink was designed using literature hydrodynamics, mass transfer, and heat transfer. The validation of the micro channel reactor and micro channel heat sink were analyzed by performance metrics of dimensionless numbers. These design parameters have been chosen carefully after critical review articles that have been made on development and process intensification of micro channel reactor for multiphase reactions. Consequent, validation on micro channel reactor and micro channel heat sink using dimensionless analysis have been done. The design parameters were based on process intensification of epoxidation of used cooking oil by acid catalyst (Ramirez, 2025) and investigation of micro channel heat sink using experiment , numerical and ANN networking (Surendera Barhatte, 2024) .

Table 2 Literature Design parameter and Physical properties for micro channel reactor and micro channel heat sink.

No	Parameters	Micro channel reactor (Juliana cardinas ramirez, 2025)	Micro channel Heat sink value (Surendera Barhatte, 2024)
1	Diameter	2 mm	2.5 mm
2	No of channels	10	15
3	Residence time	10 min	10 min
4	Volume	$1.57*10^{-3}$ m^3	$4.9*10^{-5}$ m^3

6	Area	0.02355 m^2	$4.9*10^{-6}$ m^2
7	Volumetric flow rate	15.7ml/min	4.9 ml/min
8	Shape	Spiral	Squared pattern
9	ρ_{mix}	1.01 g/ml	1g/ml
10	μ_{mix}	25.62 cP	1Cp

Table 3 Table for justification of design parameters selection.

No	Design parameters	(Surendera Barhatte, 2024)	Study value	Justification
1	Hydraulic diameter	2.5 mm	4 mm	Larger diameter was selected to smooth flow of coolant
2	No of channel	15	15	The number of channel was kept similar in number to maintain residence time
3	Channel shape	Squared pattern	Zigzag engraved	The shape of micro channel heat sink was selected according to the fact for its suitability for fabrication
4	Height	1.5 cm	1.5 cm	The height of micro channel heat sink was selected to 1.5cm similarly for same performance
5	Area	$4.90*10^{-6}$ m^2	$12.56*10^{-5}$ m^2	The area of micro channel heat sink was made to increase to increase

				cooling efficiency
6	Volume	$4.90*10^{-5}$ m^3	$1.88*10^{-3}$ m^3	The volume of the heat sink also made to slightly increase by increase the diameter for better performance

Table 4 Table for justification for selecting micro channel reactor design parameter.

No	Design parameter	(Juliana cardinas ramirez, 2025)	Study value	Justification
1	Hydraulic diameter	2 mm	4 mm	Wider hydraulic diameter is selected to prevent clogging due to viscous nature of reactants.
2	Number of channel	10	15	The number of channel was taken equal to maintain optimal residence time.
3	Channel shape	Spiral	Engraved zigzag channels	The engraved zigzag shape was selected purposely to create curves for effective mix of reactant and for suitability of micro machining tool.
4	Length	20 cm	30 cm	The length of micro channel and channel number increased for higher contact time and space.
5	Area	0.02355 m^2	$12.56*10^{-5}$ m^2	In this study relatively higher area is obtained with intention attain effective reactant collision.
6	Volume	$1.57*10^{-3}$ m^3	$1.88*10^{-3}$ m^3	Again relatively higher volume of reactant is chosen for higher performance.

3.3.2. Fabrication of micro channel reactor and micro channel heat sink

The fabrication of micro channel reactor and micro channel heat sink began with the selection of appropriate construction material for both components. Stainless steel SS1 316 was chosen for micro channel reactor because of its excellent mechanical strength, high temperature resistance,

and superior corrosion resistance making it suitable for demanding operating conditions. For micro channel heat sink aluminum 6061 was chosen due to its higher thermal conductivity which rapids heat absorption and heat dissipation, thereby enhancing the overall thermal performance. Then, both the aluminum and stainless steel were cut by laser machine (Hans Laser, China) with 30cm length and 15 cm width. Then both the heat sink and the reactor were engraved by a rotor machine (Ronald DGA, Japan) with a hydraulic diameter (d_H) of 4 mm. The inlet and out let tubes with diameter of 4mm of each on the heat sink and on the reactor were welded by arc-welding machine. Then the micro channel reactor and micro channel heat sink were arranged in parallel counter current flow arrangement for effective thermal energy transfer. Moreover, the micro channel reactor and the heat sink were arranged with an inclined configuration using gears and bolts. Finally, the micro channel reactor system was assembled with 4 small pressure gauges (Shangai automotive, china) and 4 temperature control systems with K-type of thermocouple (Basstor, china). The design specifications for both micro channel reactor and micro channel heat sink are listed table 5.

Table 5 Design specification for micro channel reactor and micro channel heat sink.

Specifications	Micro channel reactor	Micro channel heat sink
Construction materials	Stainless steel SS1316	Aluminum 6061
Reactor type	Rectangular plate with engraved channels	Rectangular-plate engraved channels
Length	30 cm	30 cm
Width	15 cm	15cm
Channel shape	Zigzag engraved channels	Zigzag engraved channels
Channel diameter	4 mm	4 mm
Inlet and outlet tubes diameters	1cm	1cm

Junction shape	T-junction	T-junction

3.3.3. Pretreatment of waste cooking soybean oil

The pretreatment techniques for enhancing the physicochemical properties of the WCSBO were applied in various sequential manners (Juliana Cardenas Ramirez, 2025). First, samples of WCSBO were collected from local restaurants in Addis Ababa, Ethiopia. Then, 500 ml sample of WCSBO was measured by measuring cylinder. Next, it was filtered by using No. 1 Whatman filter paper and funnel for repeated 5 times to remove impurities. Then, the next pretreatment procedure after filtration was heating. The sample of WCSBO was heated for 30 mins at 110 ^{O}C to remove moisture resulted from repetitive frying on a magnetic hotplate. The pretreated WCSBO was left to be cooled at a room temperature.

3.3.4. Epoxidation of refined waste cooking soybean oil

An epoxidation reaction for WCSBO was performed with method on (Mariana del valle, 2022) with slight modification. First, 200 ml of refined WCSBO was measured by a measuring cylinder and then added into 250 ml of three -necked flask with one necked condenser and another neck with thermometer. Then, 50 ml of glacial CH_3COOH was measured by a measuring cylinder and added into the three necked flask. 0.2 g of TiO_2 was measured by measuring balance and added in to the same three-necked flask. The reaction temperature was heated to 65 ^{O}C on magnetic hot plate. When the reaction temperature reached to 50 ^{O}C, 11.5 ml of H_2O_2 was added to the reaction in drop wise manner and left the reaction to be performed for 4 hrs. After the epoxidation reaction got completed, the EWCSBO left to be cooled at room temperature. Then after the EWCSBO was cool, EWCSBO was filtered four times using No. 1 Whatman filter paper and funnel to remove impurities and the catalyst used. The filtered EWCSBO was neutralized by using $NaHCO_3$ to neutralize unreacted CH_3COOH by dropping it using dropper until the EWCSBO turned the universal indicator into light green color. The next step was that excess $NaHCO_3$ was washed by 100 ml of warm H_2O for 4 repeated times. Then, warm H_2O and the EWCSBO became separated using separator funnel. The remained trace amount of H_2O was removed by heating.

3.3.5. Performance test by Hydroxylation reaction of EWCSBO

An intensified hydroxylation of EWCSBO was done using a method on (Wazed M.A, 2023) with a slight modification. First before the hydroxylation reaction took place, the stainless steel micro channel reactor was properly washed to remove impurities. Then, the micro channel reactor was left to be heated to 90 ^{O}C. Then, 100 ml of EWCSBO and100 ml of $C_2H_6O_2$ was measured by a measuring cylinder separately and added in to flask. The reactant mixture was heated on magnetic hot plate for preheating to reduce the viscosity at 65 ^{O}C. Then the mixed reactants were allowed to follow in to a gravity driven micro channel reactor. At the same time, 300 ml of H_2O was added in to gravity driven micro channel heat sink as a cooling medium. The system was a passive system that was driven by gravity inclined techniques. All the reactants and cooling mediums were made to smoothly flow through the engraved channels for 5 min. The final soy-based polyether polyol was collected at the outlet side. The collected soy-based polyether polyol was washed with 200 ml of warm H_2O to remove impurities. Then, the H_2O and EWCSBO were separated using a separator funnel. The remained small amount of H_2O in EWCSBO was separated by heating at 100 ^{O}C.

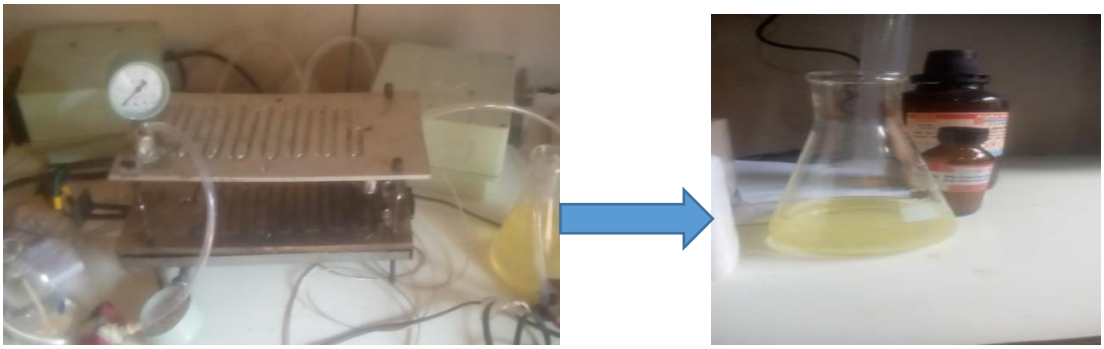


Figure 6 Hydroxylation reaction of EWCSBO.

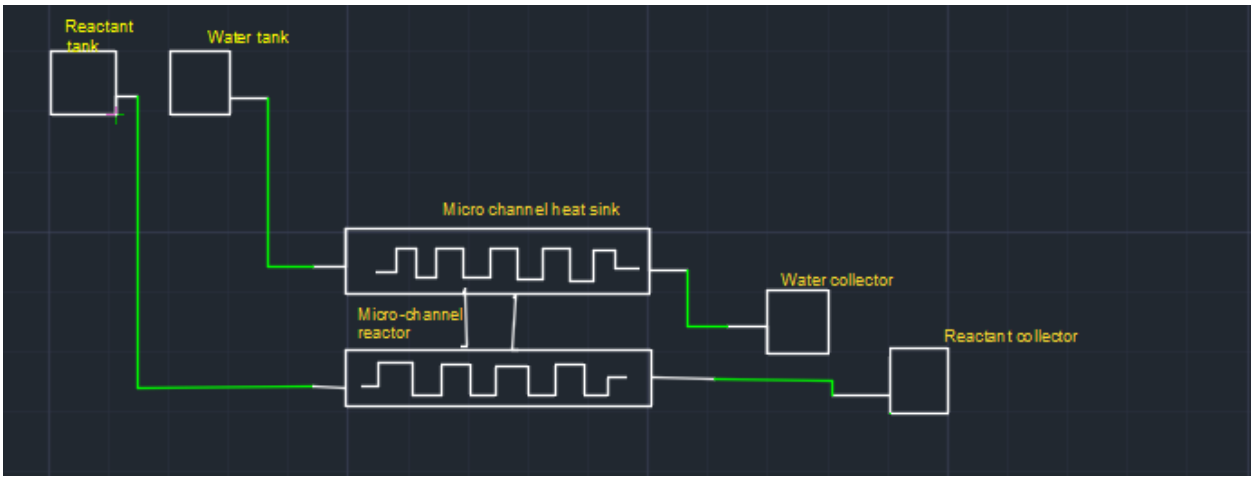


Figure 7 Process flow diagram for hydroxylation reaction.

3.4. Physicochemical characterizations of WCSBO, EWCSBO and soy-based polyether polyol

The physicochemical properties of WCSBO, EWCSBO and soy-based polyether polyol were determined using standard analytical procedures. The analysis included A.V, S.V, I.V, P.V, E.W (for EWCSBO only), and OH number (for soy-based polyether polyol only). All determinations were carried out in triplicate according to relevant ASTM (American society for testing materials) standard method. The determinations of these properties were determined in triplicate experiments to increase certainty and to analyze the impact of reaction parameters on these parameters.

3.4.1. Acid value and free fatty acid determination

The determination of A.V was determined by a dual titration method (Wazed et al., 2023) with small modification, First, 2 g of sample of $C_{20}H_{14}O_4$was measured by measuring balance and dissolved into 100 ml of C_2H_5OH through gentle shaking. Then, 0.1 N of 4 g of KOH pellets were measured by a measuring balance. Then, it was dissolved in other conical flask in 900 ml of H_2O by vigorous shaking. Then the solution was left to be cooled. Next 15 g of refined sample was measured by measuring balance and added in conical flask. Then, 50 ml of C_2H_5OH was measured by measuring cylinder and was added in to the other conical flask. Next, 2 drops of $C_{20}H_{14}O_4$ was added in to the C_2H_5OH sample until crystal violet color appeared. The sample and the titrated C_2H_5OH solution was heated until the solution completely dissolved. Then, the

solution cooled after it was heated and dissolved. Then, the KOH solution was dropped from the burette until light pink color observed by vigorous agitation. The final step was calculation was taking after final burette reading was recorded. Then, the value of FFA was calculated by dividing A.V by 2.

$$A.V = \frac{Mw_{KOH} Nv}{W_s} \qquad (3.1)$$

Where

M_{wKOH} -Molecular weight of KOH (mol/l) Ws-Sample-weight (g)

V-Volume of the KOH solution in burette used to neutralize the sample (ml)

$$FFA = \frac{A.V}{2} \qquad (3.2)$$

This titration method served for all samples of WCSBO, EWCSBO, and soy-based polyether polyol for triple experiments.

3.4.2. Iodine value determination method

Iodine value (I.V) was determined by duplicate titration method as (Say et al., 2024) with a slight modification. To determine I.V, 2.5 g of $C_6H_{10}O_5$ was dissolved in 50 ml of distilled H_2O on a magnetic hotplate. The solution was cooled and filtered using filter paper and funnel. The next step was 0.1 N of 3 g of $Na_2S_2O_3$ was measured by a measuring balance and it was dissolved in 1000 ml of H_2O. Then, $Na_2S_2O_3$ solution was added in to a burette and initial reading was recorded. Then, 5g of sample was measured by a measuring balance. On separate conical flask, 25 ml of CCl_4 was measured and added to a flask. Then, 10 ml of CH_3COOH and 10 ml of Icl was measured by a measuring cylinder and added in the same flask. Then, sample flask was prepared by adding CCl_4, mixture of Icl and CH_3COOH, and the sample. The blank flask was also prepared in the same manner with the sample flask except the addition of sample. After the sample and the blank flask were prepared, 2 g of KI powder was measured by a measuring balance and dissolved in 100 ml of H_2O and added in to both sample and blank flask. Next, Both the sample and blank flask were titrated by $C_6H_{10}O_5$ until blue black color observed. Then again,

both sample and blank were back titrated by $Na_2S_2O_3$ until milky solution formed. I.V was calculated as shown below in equation (3.3).

$$\text{I.V} = \frac{(\text{vb} - \text{vs})\text{N} * 12.69}{\text{W}_\text{s}} \qquad (3.3)$$

Where

Vb-Volume of blank (ml) Ws- Sample of weight (g)

Vs-Volume of sample (ml)

12.69- M_W of $Na_2S_2O_3$

The average for three runs of determination of S.V was performed for all three samples of WCSBO, EWCSBO, and soy-based polyether polyol.

3.4.3. Saponification value of determination method

The determination of saponification value based on (Putri et al., 2020) with a slight modification using triplicate runs. S.V of sample was done by back titration of KOH that neutralizes the amount of FFA found in the sample. First, 10 g of sample was measured by a measuring balance and put in a conical flask. 4 g of KOH pellets were measured and dissolved in 100 ml of C_2H_5OH. The solution was first placed in both sample and blank flask. Then, both blank and sample flask were connected to a three necked flask with one side thermometer and one side condenser and heated on a magnetic hot plate for 1 hr separately. After the heating process was performed, the solution was left to be cooled at room temperature. 100 ml of C_2H_5OH was measured by a measuring cylinder and added to a conical flask. A solution of KOH was placed in a burette and initial reading was taken. The $C_{20}H_{14}O_4$ solution titrated the 100 ml of C_2H_5OH sample with KOH solution until crystal violet color observed. The titrated solution was mixed with the sample and heated to get dissolved. The back titration of the mixed solution by a $C_{20}H_{14}O_4$ was done and ended as the color of the solution changed into light pink color was done. The same titration process was performed for the blank sample. The formula of S.V was described as the following in equation (3.4).

$$S.V = \frac{(v_{blank} - v_{sample})N * 56.1}{W_S} \qquad (3.4)$$

Where

V_b-Volume of blank (ml) N-Normality of KOH (meq/ml)

Vsample- Volume of sample (ml)

56.1-Molecular weight of KOH

The determination of S.V has been utilized for all samples of WCSBO, EWCSBO, and soy-based polyether polyol and the average value for three experiments were taken for WCSBO, EWCSBO.

3.4.4. Peroxide value determination method

The peroxide value(P.V) of sample was determined by a titration method as mentioned (Xylem) with a slight modification with two runs. First 0.5 g of $C_6H_{10}O_5$ was measured by a measuring balance. Then, 50 ml of H_2O was measured by a measuring cylinder. Then, the $C_6H_{10}O_5$ was dissolved in the H_2O in heating on magnetic hotplate through vigorous stirring. A mixture was prepared using mixing 90 ml and 60 ml of CH_3COOH and $CHCl_3$ respectively. Then, 10 g of sample was measured by measuring balance and added in to conical flask. Next, 2.5 g of $Na_2S_2O_3$ was measured by a measuring balance and it was dissolved in 1000 ml of H_2O through vigorous shaking. Then, the solution was left to be cooled. The cooled solution was added in to a burette. In a test tube 0.3 g of KI was mixed and dissolved in 10 ml of H_2O. Then the sample of WCSBO in conical flask was mixed with mixture of $CHCl_3$ and CH_3COOH. Then, the prepared KI solution was added in to a sample and blank flask. Then, the final mixed solution was titrated by a $C_6H_{10}O_5$ solution until dark blue black color observed. Then, again the sample and blank flasks were back titrated by $Na_2S_2O_3$ until its color changed to milky color. The P.V was calculated as shown (3.5)

$$P.V = \frac{v * N * 1000}{W_s} \qquad (3.5)$$

Where

V=Initial burette reading-Final burette reading (ml)

N-Normality of $Na_2S_2O_3.H_2O$ (meq/g)

Ws-Sample-weight (g)

The determination of peroxide value (P.V) was used for all samples of WCSBO, EWCSBO, and soy-based polyether polyol and an average value for all triplicate experiments was taken.

3.4.5. Epoxy value determination for EWCSBO

The epoxy value (E.V) for EWCSBO was determined by two titration measures with a slight modification (Dominguez-Candela et al., 2022). First; 5 g of EWCSBO was measured by a measuring balance and added in to a conical flask. Then, a mixture of CH_3COOH and acetone was prepared in a conical flask with 1:1 molar ratio and formed a final volume of 50 ml. On the other side, 3 g of KOH pellets were measured by a measuring balance and it was dissolved in 800 ml of H_2O by vigorous shaking. Then after the KOH solution was cooled, it was added in a burette. Initial reading was taken. Next, the prepared mixture of CH_3COOH mixture was added in both sample and blank in which both flasks contain 25 ml of the mixture. Both sample and blank flask were placed on magnetic hot plate for 30 mins for 140 ^{O}C. Then, both flasks were cooled. They were titrated KOH solution until blue violet color was observed. E.V was calculated as shown below in equation (3.6).

$$E.V = \frac{(v_{blank} - v_{sample}) * N}{W * 10} * 100 \qquad (3.6)$$

Where

V_b-Volume of blank (ml)

Vs-Volume of sample (ml)

W-Weight of sample (g)

N-Normality of KOH (meq/g)

3.4.6. Hydroxyl number determination for soy-based polyether polyol

The determination of OH number for soy-based polyether polyol can be determined by triplicate titration methods (Kim, 2026) with slight modification. First, 10 g of soy-based polyether polyol was measured by measuring balance and added to conical flask. 10 ml of CH_3COOH and 10 ml of pyridine solution were measured by a measuring cylinder and the solution was added in to other conical flask. Both sample and blank were prepared using CH_3COOH –C_5H_5 solution with and without soy-based polyether polyol respectively. Next, both the sample and blank flasks were connected to a reflux condenser and placed on magnetic hot plate to be heated at 100 ^{O}C for 1 hr. After the reaction was performed for the first 30 mins, 10 ml of distilled water was used for performing hydrolysis reaction and the reaction was preceded to the remaining 30 mins. For the titration step, 2 g of $C_{20}H_{14}O_4$ was measured by a measuring balance and got dissolved in 1000 ml of C_2H_5OH. Then 0.1N of KOH pellets were dissolved 900 ml of H_2O by gentle shaking. The solution was left to be cooled and added in to burette. The initial reading recorded was taken. Finally, both blank and sample flasks were titrated by $C_{20}H_{14}O_4$ until crystal violet color observed. Then they were back titrated by KOH solution until light pink color observed. Then final burette readings for both sample and blank flask were recorded. The OH number for soy-based polyether polyol was calculated as shown in equation (3.7).

$$OH = \frac{(V_{blank} - V_{sample}) * 56.1}{W_s} + A.V \qquad (3.7)$$

Where

OH-Hydroxyl number (mgKOH/g)

V_s-Volume of sample (ml)

V_b-Volume of blank (ml)

W_s-Weight of sample (g)

3.4.7. Determination of density of WCSBO, EWCSBO, and soy-based polyether polyol

The determination of $\mathcal{S}$ for WCSBO, EWCSBO and soy-based polyether polyol were calculated following a method on (Council, 2020) to asses structural changes by taking the ratio of mass of samples to their respective volume measurements. First, the 10ml of each sample of WCSBO, EWCSBO and soy-based polyether polyol were measured by a measuring balance and the

volumes of these samples were measured by a measuring cylinder at 25 ^{O}C. Then, their ratios were taken.

$$\mathcal{P} = \frac{m}{v} \qquad (3.8)$$

Where

m- Mass of samples (g)

v- Volume of samples (ml)

3.4.8. Determination of specific gravity of WCSBO, EWCSBO, and soy- based polyether polyol

The determination of Sg of WCSBO,EWCSBO and soy-based polyether polyol were obtained based on a method on (Eke Ejiofor, 2021) by dividing their $\mathcal{P}$ to the ϱ of water that is 1 g/l at 25 ^{O}C. The formula for specific gravity determination is expressed as the following in equation (3.19).

$$S.g = \frac{\mathcal{P}_{sample}}{\mathcal{P}_{H20}} \qquad (3.9)$$

Where $\mathcal{P}_{Sample}$- sample density (Kg/l)

$\mathcal{P}_{H2O}$-water density (Kg/l)

3.4.9. Determination of viscosity of WCSBO, EWCSBO, and soy-based polyether polyol

The viscosity of WCSBO, EWCSBO, and soy-based poly ether polyol were determined by the method (Gobbana, 2022). They were measured by capillary viscometer at 25 ^{O}C. 10 ml of samples were taken from each WCSBO, EWCSBO, and soy-based polyether polyol. Then, all the three samples were placed in a capillary tube and their respective viscosity were determined separately.

3.4 10. Moisture content determination for WCSBO, EWCSBO, and soy-based polyether polyol

The determination of moisture content (M.O) for all the three samples were determined with a guidance of method (Daha Retino swatiri, 2021) with a slight modification. A 5 g of each sample from WCSBO, EWCSBO, and soy-based polyether polyol was taken and put in separate test tubes. Then, each test tube was heated on a magnetic hot plate at 160 ^{O}C for 15 mins. Then, the

weight of each sample was taken after heating. The moisture content was calculated as shown below in equation (3.10).

$$M.O = \frac{M_{initial} - M_{final}}{M_{inital}} * 100 \qquad 3.10$$

Where

M_{intial}- Mass of sample before heating (g)

M_{final}- Mass of sample after heating (g)

3.4.11. Refractive index for WCSBO, EWCSBO and Soy-based polyether polyol

The refractive index (R.I) for WCSBO, EWCSBO and soy-based polyether polyol was made to characterize the physic-chemical properties by using prism (Gobbana, 2022). First 3-5 drops of samples of WCSBO, EWCSBO and soy-based polyether polyol were put in the prism and get exposed to a light refraction at 20 ^{O}C.

3.5. Experimental and numerical evaluation of micro channel reactor and heat sink system

The performance test for an intensified hydroxylation of EWCSBO was done to validate the micro channel reactor parameter through several reaction parameters. The experimental analysis for micro channel reactor and a micro channel heat sink was done using the following methods for mass transfer, heat transfer, thermodynamics, reaction kinetics, and pressure drop analysis.

3.5.1. Heat transfer analysis for a micro channel heat sink

For case of heat absorbance, a single rectangular micro channel heat sink with T- junction serpentine shape engraved channels with a hydraulic diameter of 4mm made of aluminum 6061 was used (F.Montazeri, 2023). The velocity of cooling medium is measured by manual measurement of distance travelled over time. The micro channel heat sink was made with 30 cm of length and 15 cm width. For experimental measurement of temperature, two K-type thermocouples at an inlet and outlet side of the channel for heat sink was used. The thermo couples were calibrated using 0 ^{O}C test method. The total q was determined by the formula used in equation (3.11). The average thermal conductivity (k) for micro channel heat sink was taken as

165 W/m.K at 25 ^{O}C. The reactions were performed in a five experiment runs with varying temperature.

$$q = \frac{K\Delta T}{L} \qquad (3.11)$$

Where

K- Thermal conductivity of aluminum plate (W/m.K)

L-Length of the micro channel heat sink (m)

3.5.1.1. Reynolds number (Re) determination of micro channel heat sink

The Re number for micro channel heat sink 4mm of hydraulic diameter with a cooling medium of water was determined by the method (Greener et al., 2021) on with a slight modification. The micro channel heat sink made of aluminum 6061 used water as cooling medium. Thus, the first step to compute Re number was done by measuring the flow rate of water in five experimental measures. This was done by dividing the distance traveled of water through the gravity-driven channels of the heat sink. Then, measuring μ of H_2O at 25 ^{O}C of reaction temperature was performed. Next, by taking 1 g/l of value taken as a $ƒ_{H2O}$, the Re number can be calculated as the following in five runs with different flow rate and temperature measurements.

$$Re = \frac{ƒud_H}{\mu} \qquad (3.12)$$

Where

ϱ-Density of H_2O (Kg/l)

Q-Flow rate of H_2O (ml/min)

μ-Viscosity of H_2O (cP)

d_H-Hydraulic-diameter (m)

3.5.1.2. Thermal resistance (R_{th}) determination of micro channel heat sink

The thermal resistance (R_{th}) of micro channel heat sink was determined to evaluate its thermal performance (Fu, 2023). The R_{th} was calculated using temperature measurements taken at the inlet and out let section with K-type thermocouple for over five consecutive runs. The using thermodynamic heat gain was calculated using specific heat capacity of H_2O 4.148 KJ/kg.^{O}KThe R_{th} was calculated as the following in equation (3.13).

$$R_{th} = \frac{Q}{\triangle T} \qquad (3.13)$$

Where

Q-Heat gain/loss (J) T_f-Final temperature (^{O}C)

Ti-Initial temperature (^{O}C)

3.5.1.3. Biot number determination of micro channel heat sink

The determination of Bo number was made by a method (H., 2024) with slight modification. For a rectangular micro channel heat sink, the determination of Bo number value was made a micro channel heat sink made up of aluminum 6061 as a construction material using water as a cooling medium to heat transfer analysis. The micro channel heat sink was developed by 30cm of length and 15 cm of width of dimension. The Bo number for a micro channel heat sink was computed by calculation of heat transfer coefficient. The thermal conductivity for aluminum 6601 micro channel heat sink is 165 W/m.^{O}K

$$\mathrm{B0} = \frac{\mathrm{hL}}{\mathrm{K}} \qquad (3.14)$$

Where

Bo-Biot number K-Thermal conductivity (W/m.K)

h- Heat transfer coefficient (W/m^2.K)

For Bo number determination, the heat transfer coefficient was made to analyze the micro channel reactor. The temperature measurements at inlet and at outlets were measured by K-thermocouples. The heat transfer coefficient was determined as shown below in equation (3.15).

$$h = \frac{Q}{A\Delta T} \qquad (3.15)$$

Where

Q- Heat gain/loss (J)

A- Area of the reactor (m^2)

T_i -Initial temperature (^OC)

T_f- Final temperature (^OC)

3.5.1.4. Determination of Nusselt number for a micro channel reactor

The thermal performance for the determination of Nu number used as a tool to serve for empirical efficiency measurement of micro channel heat sink as shown in the method (Hui ying yong, 2023). The micro channel heat sink was made with the dimension with 30 cm of length and 15 cm of width. A cooling medium of water in a micro channel heat is used. The thermal conductivity of water was 0.6 W/m.K. The average of heat transfer coefficient for the micro channel reactor at varying temperature was made for repetitive number of temperature. Nu number was computed as the following equation (3.16).

$$Nu = \frac{hd_H}{K_f} \qquad (3.16)$$

Where

Nu-Nusselt number

d_H- Hydraulic diameter (m)

K_f -Thermal conductivity of fluid (w/m.K)

3.5.1.5. Determination of pressure drop for micro channel heat sink

3.5.1.5.1. Empirical measurement of ΔP

The small pressure gauges were properly placed in tube of the micro channel at inlet and outlet. The pressure gauges were calibrated.

3.5.1.5.2. ΔP determination of micro channel heat sink

The Δp for a micro channel heat with a passive system using a gravity- driven technique showed a laminar flow through small d_H of the heat sink (Maleki & Bertola, 2025). The micro channel heat sink was prepared with dimension of 30 cm length and 15 cm of width. For gravity driven micro channel heat sink, the △P was highly determined by the height difference.

$$\triangle P = \rho gh \qquad (3.17)$$

Where

℘- Density (g/l) h- Height difference (m)

g- Gravitational force (m/s^2)

3.5.1.6. Thermodynamic measurement of micro channel heat sink

The thermo dynamic measurement for a single micro channel heat sink with a construction of material of aluminum 6061 using water as a cooling medium was determined according to a method with (Lee et al., 2021) a slight modification. First, for thermodynamic property measurement, the mass flow rate was computed by taking the ratio of mass measured for flown through the channel per given time at different temperature. Then the specific heat capacity (Cp) of water was taken as 4.18 KJ/ (Kg.K). The analysis of heat gain for thermodynamic properties was analyzed in triplicate manner by varying mass flow rate (Kruatian, 2020).

$$Q = mCp \triangle T \qquad (3.18)$$

Where

Q- Heat absorbed from the micro channel reactor (J)

Cp- Specific heat capacity (J/Kg.K)

ΔT-△Temperature difference (^OC)

m- Mass flow rate (kg/s)

3.6. Heat Transfer Assessment of Micro Channel Reactor

The heat transfer for a micro channel reactor was assessed by determining Fourier heat flux (q"), Re number, Ca number, Pe number and R_{th} of the reactor. For a single rectangular micro channel reactor made of stainless steel SS1316 with an electrical heater of 10 Kw the heat flux was determined by using two K-type thermocouple for measuring temperature at the inlet and outlet. The value of heat flux was determined.

3.6.1. Heat flux determination for micro channel reactor

The heat flux for a rectangular zigzag channels made of stainless steel made SS1 316 with 4mm hydraulic channels and with electrical heater of 10 Kw at the bottom of the reactor wall. Two K-thermocouples were used at inlet and outlet tubes to measure the inlet and outlet temperatures after they were calibrated with 0 ^{O}C test (F.Montazeri, 2023). The thermal conductivity for stainless is 17 W/m.K. The heat flux for micro channel for micro channel reactor was in triplicate manners with different average temperatures.

$$q = \frac{K \triangle T}{L} \qquad (3.19)$$

Where

K-Conductivity of micro channel reactor (w/m.^{O}K)

ΔT-Temperature difference (^{O}C)

L-Length of micro channel reactor (m)

3.6.2. Reynolds number determination of micro channel reactor

The Re number determination of micro channel reactor was computed by measuring the velocity of EWCSBO and $C_2H_6O_2$. The Re number for EWCSBO $C_2H_6O_2$ were calculated separately (Bouras, 2021). The velocity was computed by taking the ratio of distance travelled through the channel per time taken. Both EWCSBO and $C_2H_6O_2$ are Newtonian fluids. Thus the μ was considered as constant throughout the courses of the reaction.

$$Re = \frac{\rho u d_H}{\mu} \qquad (3.20)$$

Where

ϱ-Density of EWCSBO (Kg/l)

u -Velocity of EWCSBO (m/s)

d_H- Hydraulic diameter (m)

μ-Viscosity (cP)

3.6.3. Thermal resistance (R_{th}) determination of micro channel reactor

The thermal resistance for a micro channel reactor made of stainless steel SS1316 with an electrical heater of 10 Kw was calculated using a procedure mentioned of with (Kahdrawi, 2024) with a slight modification. For calculating R_{th}, first the inlet and outlet temperature measurements of the reactor were measured by K-type thermocouples. After, the K-type thermocouples were calibrated by 0 ^{O}C test. Next, the volumetric flow rate was computed by multiply velocity with A_c. The velocity has been measured by dividing the distance traveled per a given minutes. The R_{th} for a micro channel reactor in a five experimental runs with different velocity of the biphasic reactants.

$$R_{th} = \frac{Q}{\triangle T} \qquad (3.21)$$

Where

ΔT-temperature difference at inlet and outlet (^{O}C)

Q- Heat gain (J)

$$Q = A_c * u \qquad (3.22)$$

Where

Q- Volumetric flow rate (ml/s)

A_c- Cross-sectional area (m^2)

u- Velocity of bi-phasic reactants (m/s)

3.6.4. Biot number determination of micro channel reactor

The heat transfer efficiency analysis for determination of Bo number was done for a rectangular engraved of micro channel reactor based on the method (Feng, 2023). The micro channel reactor was developed with 30 cm length and 15 cm of width was determined by computational method with a slight modification. The value for thermal conductivity of the stainless steel is 17 W/m.K. The Bo number can be computed as the equation shown in equation (3.23).

$$\mathbf{Bo} = \frac{\mathbf{hL}}{\mathbf{K}} \qquad (3.23)$$

Where

Bo-Biot number

K-Thermal conductivity (W/m.K)

h- Heat transfer coefficient ($W/m^2.K$)

The evaluation of average heat transfer coefficient was determined for a micro channel reactor was determined at inlet and outlet section using K-type thermocouple measurements. The heat transfer coefficient was calculated as following equation shown in equation (3.24).

$$\mathbf{h} = \frac{\mathbf{Q}}{\mathbf{A\Delta T}}$$

Where

Q-Heat gain (J)

Ti- Initial temperature (^OC)

A-Area of micro channel reactor (m^2)

Tf- Final temperature (^OC)

3.6.5. Nusselt number determination of micro channel reactor

The assessment of Nu number for a micro channel reactor was performed based on the method on (Sharma, 2023). For the thermal performance evaluation of micro channel reactor with SS1 316 stainless steel by the dimension 30 cm length and 15 cm width was evaluated by Nu number. The determination of Nu number was made to evaluate the heat transfer characteristics. The thermo physical property for thermal conductivity of fluid the reactant mixture was taken as 2 W/m.K (Kim, 2026). The Nu number was evaluated in equation (3.25).

$$\mathbf{Nu} = \frac{\mathbf{hd_H}}{\mathbf{K_f}} \qquad 3.25$$

Where

h- Heat transfer coefficient ($W/m^2.K$)

K_f-Thermal conductivity of the fluid (W/m.K)

d_H- Hydraulic diameter (m)

3.7. Pressure drop determination of micro channel reactor

The Δp for a micro channel reactor made up of stainless steel SS1 316 was determined by using an experimental measurement (wang, 2024). First, for the experimental method two pressure gauges were placed at the inlet and outlet tube of the reactor. The pressure drop was computed by taking the deviation of pressure at inlet and outlet. For computational assessment of Δp, the pressure for micro channel reactor was highly dependent the height that drive the flow of the force.

$$\Delta P = \rho gh \qquad (3.26)$$

Where

ρ-density of reactant mixture (Kg/l)

h- Height of micro channel reactor (m) g- Gravitational force (m/s^2)

3.8. Thermodynamic assessment of micro channel reactor

The thermodynamic assessment of micro channel reactor was calculated using method expressed (Alina Niculescu, 2022) on with slight modification. The thermodynamic efficiency of the micro channel reactor was evaluated by assessing the amount of heat released. This was performed by first measuring the mass flow rate and taking the specific heat capacity (Cp) of EWCSBO and $C_2H_6O_2$ were the next procedures. The Cp for EWCSBO and $C_2H_6O_2$ were taken as 1.9KJ/kg.K and 2.5KJ/Kg.K respectively. This was computed as the following for EWCSBO and for $C_2H_6O_2$ separately (Ji, 2022).

$$Q = mCp\Delta T \qquad (3.27)$$

Where

Q- Heat loss (J) ΔT-temperature-difference (^OC)

m- Mass flow rate (Kg/s)

Cp- specific heat capacity (KJ/Kg.K)

3.9. Mass transfer measurement of micro channel reactor

For non-catalytic hydroxylation reaction of an EWCSBO in a micro channel reactor, the

mass transfer was evaluated by a dimensionless number including Schmidt number and Re number that directly imply the mixing of biphasic reactants of liquid-liquid reaction (Bouras, 2021).

3.9.1. Schmidt (Sc) value for micro channel reactor mass transfer

For micro channel reactors, for biphasic reaction of EWCSBO and $C_2H_6O_2$ the mass transfer was evaluated by Schmidt number (Sc) number. The evaluation of Sc number performed based on the method (Shaojie Tan, 2023). The value of Sc number was calculated by using thermo-physical properties like μ at 60 ^{O}C. For non-catalytic hydroxylation reaction of EWCSBO, it was computed as the equation (3.28).

$$Sc = \frac{\mu}{\rho DAB} \qquad (3.28)$$

Where

K-mass transfer coefficient

L-length of micro channel reactor (m)

d_H- Hydraulic diameter (m)

Dab-diffusivity-constant (m^2/s)

3.10. Kinetic Study determination for hydroxylation reaction of EWCSBO

The kinetic model for reaction of hydroxylation of EWCSBO in a micro channel reactor was developed. The kinetic model was derived assuming that the reaction is as elementary liquid irreversible reaction with pseudo 2nd order in which each reactant has first order (Yan et al., 2022). The chemical reaction equation for hydroxylation of EWCSBO is represented as shown in equation (3.29). The order of reaction is taken as 2nd order based on the results from literature.

$$C_{57}H_{98}O_9 + 3C_2H_6O_2 \rightarrow C_{63}H_{116}O_{15} \qquad (3.29)$$

3.11. Statistical method

The statistical analysis for an intensified hydroxylation of EWCSBO was performed using RSM particularly CCD technique (Iyan Sopyian, 2022). The interdependence of reaction parameters (Temperature, molar ratio of $C_2H_6O_2$ to EWCSBO, reaction time) with response variable OH

number was investigated using design expert software. These process parameters have been selected with literatures values. The temperature range for hydroxylation was performed with a range of 75 ^{O}C-90 ^{O}C (Kim et al., 2026). The temperature range for hydroxylation reaction in a micro channel reactor was lower than in conventional reactor. Molar ratio of $C_2H_6O_2$ to EWCSBO was ranged 1:1-1:3 (Ibrhaima Balde, 2022). The reaction time for the hydroxylation in a micro channel reactor was relatively smaller than in conventional reactors. It took in min (minutes) rather than hours unlike the traditional reactors. It ranged from 3 mins to 12 mins (Ji et al., 2022).

Table 6 Process parameters for statistical analysis

Name	Units	Low	High	-alpha	+alpha
Temperature (A)	^{O}C	75	90	69.89	95.11
Molar ratio $C_2H_6O_2$ to EWCSBO (B)	-	0.3	1	0.06	1.23
Time (C)	Min	3	10	-0.07	15.07

The total number of runs used in the statistical analysis is shown below in equation (3.30)

$$N = 2^n + 2n + n_c \qquad (3.30)$$

Where N is total number of runs, n represents independent variables. 2^n shows factorial run, 2n shows actual run and n_c implies central run. The total number of runs is 20 runs with 8 factorial runs, 6 actual runs and a total of 6 central runs. The quadratic model equation that was employed to analyze the interrelation of reaction parameters with response variable is shown in (3.31).

$$Y = \beta_0 + \beta ixi + \sum \beta ijxi + \varepsilon \qquad (3.31)$$

Where βo regression coefficient, βi denotes linear coefficient, βij denotes independent coefficient, ε shows value of error. X_i and x_j are denotation for independent variables

3.12 One factor at a time (OFAT) sensitivity analysis for hydroxylation reaction

The one factor at a time (OFAT) analysis was made to analyze and decide which factor has the most significant impact on response variable (OH number). This was done by keeping two reactants constant and studying the effect of the remaining by changing its magnitude. The OFAT sensitivity analysis was made using the equation (3.32).

$$S\% = \frac{\Delta Y}{\Delta X} \qquad (3.32)$$

Where

△y- response variable deviation.

△x- factor deviation

3.13. Fourier infrared spectrophotometer analysis

The determinations of FTIR results for WCSBO, EWCSBO and soy-based polyether polyol were done by (spectrum 65 FTIR, perkin Elemer, Massachuset, USA) using KBr pellets as a reference material.

3.14. Proton nuclear magnetic resonance analysis

The ^{1}H- NMR for WCSBO, EWCSBO and soy-based polyether polyol were determined by Burker avance 500 MHZ using deuterated chloroform (CDl_3) as a solvent.

3.15. Thermo gravimetric analysis (TGA)

The analysis of TGA for WCSBO, EWCSBO and soy-based poly ether polyol to test the thermal degradation of molecules in a sample were done by DTG-60Hz (Shimdazu, Japan). This was done with the temperature range of 0 ^{O}C-600 ^{O}C with heating rate10 ^{O}C/min in inert nitrogen (N_2) environment.

4. RESULT AND DISCUSSION

4.1. Acid value and free fatty acid value determination of refined WCSBO and EWCSBO

An A.V indicates the concentration of FFAs present in a chemical sample. Lower A.V level reflects reduced FFA content and superior purity, whereas higher values correlate directly with diminished stability and an increased susceptibility to oxidation, polymerization, and hydrolysis (Putri et al., 2020). Table 7 showed the titration results for an acid value determination for WCSBO, EWCSBO.

Table 7 Acid value of WCSBO and EWCSBO.

No	Sample	Average Temperature	Molar ratio	Average Time	A.V
1	WCSBO	105 ^{O}C	-	25 min	0.62±0.03 mgKOH/g
2	EWCSBO	70^{0} ^{O}C	0.75	4.5 hrs	0.6±0.32 mgKOH/g

Table 7 illustrates that the average A.V for WCSBO, EWCSBO from triplicate experiments with uncertainty values. These values showed the amount KOH in mg that are needed to neutralized FFA in a given sample weight. The A.V for WCSBO is with in standard range of 0.62±0.03 mgKOH/g (Wazed M.A, 2023).This value of A.V for WCSBO show good stability and the pretreatment step prior to the titration method was successful. The A.V for EWCSBO also implies very significant decrease in value. The A.V for EWCSBO is decreased when compared to WCSBO. This is due to the formation epoxy rings. Moreover, the amount of FFA that is presented in WCSBO were consumed and changed to epoxy rings. The A.V was found as 0.6±0.32 mg KOH/g that is a strong confirmation for successful epoxidation of WCSBO (Dhanavel & Nandakrishnan, 2024).

4.2. Iodine values for refined WCSBO and EWCSBO

An I.V shows the amount of saturation of the given chemical. As the I.V is increases the amount of unsaturated or readiness to further reaction also increases. But large I.V rate more than the range also implies poor pretreatment techniques (Say et al., 2024). Table 8 showed that the value for I.V for WCSBO and EWCSBO.

Table 8 Iodine values for WCSBO and EWCSBO.

No	Sample	Average temperature	Molar ratio	Average time	I.V
1	WCSBO	105 ^{O}C	-	25 mins	102.5±0.3 $I_2$100g
2	EWCSBO	70 ^{O}C	0.75	4.5 hrs	6±0.75 I_2/100g

Table 8 shows the average of I.V for WCSBO, EWCSBO form three number of runs. The I.V of WCSBO is found as 102.5±0.3 I_2/100g. This is an implication for higher amount of unsaturation C=C bonds. This implies the presence of unsaturated FFAs like linoleic and oleic FFA chains in sample of WCSBO. Thus, the pretreatment procedures were successful in treating oxidation and polymerization reactions resulted from number of usage. This attributed to the readiness of WCSBO for further epoxidation reaction (Navin Gautam, 2024). Then, the I.V for EWCSBO is much lower when compared with WCSBO. The I.V is obtained 6±0.75 I_2/g. This due to the transformation of C=C bonds to an epoxy rings. Thus EWCSBO was more stable than WCSBO (Holm, 2023).

4.3. Saponification value results for WCSBO and EWCSBO

S.V of WCSBO and EWCSBO show the amount of KOH needed to saponify unsaturated fatty acid presented in refined samples. They also show the shortness or length of FFA chains. Table 9 shows that S.V for WCSBO,EWCSBO and soy-based polyether polyol (Eke Ejiofor, 2021).

Table 9 Saponification value for WCSBO and EWCSBO.

No	Sample	Average temperature	Average molar ratio	Average time	S.V
1	WCSBO	105 ^{O}C	-	25 mins	186±0.5 mgKOH/g
2	EWCSBO	70 ^{O}C	0.75	4.5 hrs	185±0.3 mgKOH/g

As shown in the above table 9 from average S.V, there is small decrement of S.V from WCSBO to EWCSBO show the conversion of FFA chains to epoxy rings. The S.V the two samples are approximate values. This is due to the fact that the FFA chains length for the two compounds are almost similar. The similarity of S.V for WCSBO and EWCSBO comes from the presence of FFA chains in both samples. The length of the FFA chains is similar. Thus, S.V also falls in the similar range for both samples of WCSBO and EWCSBO (Leszczynska et al., 2021).

4.4. Peroxide values determination of WCSBO and EWCSBO

The P.V for WCSBO and EWCSBO were determined with a set of titration methods (Benbouriche et al., 2022). The P.V shows that the amount of stability of the product. The decrease in the amount of peroxides and hyper oxides shows the purity of the sample. On the other side, higher P.V cross ponds to lower quality and higher rancidity of the sample resulted from poor pretreatment and poor epoxidation (Firadousi, 2025). Table 10 illustrates the P.V for WCSBO and EWCSBO.

Table 10 Peroxide values for WCSBO and EWCSBO.

No	Sample	Average temperature	Molar ratio	Time	P.V
1	WCSBO	105 ^{O}C	-	25 mins	12.5±0.75 meq/Kg

2	EWCSBO	70 ^{O}C	0.75	4.5 hrs	6.25±0.5 meq/Kg

The P.V for both samples shows the amount of rancidity. The P.V for WCSBO obtained as 12.5 ±0.75 meq/Kg. This resulted from effective pretreatment techniques that reduced rancidity of WCSBO. As a result, the P.V for the WCSBO decreased. For EWCSBO, the P.V decreased from the value of WCSBO. This is a sign for stability of EWCSBO since the formed epoxy ring yielded reduction of rancidity (Chinemerm, 2024).

4.5. Epoxy value (E.V) for EWCSBO

The E.V was determined to evaluate the percentage of epoxy value that avails in EWCSBO. The E.V shows the percentage of epoxy ring presented in EWCSBO. The E.V is found 65 ±0.15 %, which is an average epoxy weight value from 3 experimental runs, this shows higher percentage of an epoxy ring presented in EWCSBO (Ivan Dominguez-Candela, 2022).

Table 11 Epoxy value for EWCSBO.

No	Sample	Average temperature	Molar ratio	Average time	E.V
1	EWCSBO	70 ^{O}C	0.75	4.5 hrs	65±0.15 %

4.6. Physicochemical property values for WCSBO and EWCSBO

The physicochemical property determination of WCSBO and EWCSBO was determined to evaluate the characteristics of the samples with the standard value to evaluate the effectiveness of the pretreatment techniques and epoxidation reaction.

Table 12 Physic chemical properties of WCSBO and EWCSBO.

Sample	℘ (g/ml)	S.g	μ (cP)	Moisture content (%)	Color	R.I
WCSBO	0.95±0.02	0.95±0.1	50±0.01	0.07±0.4	Faint Yellow	1.471
EWCSBO	0.94±0.2	0.94±0.1	320.6±0.7	0.02±0.01	Faint Yellow	1.47

Table 12 shows the physic-chemical properties namely ℘, S.g, μ and M.O were found within the standard range. This implies the successful practice of and pretreatment technique and reaction and it serve as a confirmation sign for the standard value (Council, 2020).

4.7. Acid values for Soy-based polyether polyol

The acid value of Soy based polyether polyol was determined by titration of samples of soy-based polyether polyol

The acid value of soy based polyether polyol was determined by triplicate experimental method to measure the amount of FFA values. This also served as measure for the intensification rate of hydroxylation reaction in a micro channel reactor system (Vrushali M, 2024).

Table 13 Acid value of soy-based polyether polyol.

Run	Temperature (^{O}C)	Time (min)	Molar ratio	Acid value (mgKOH/g)
1	75	4	0.5	0.6±0.01

2	80	6	1	0.5±0.05
3	90	8	1.5	0.3±0.02

The A.V for soy based polyether polyol got decreased as the temperature, molar ratio and time increases. The small hydraulic diameter channels (d_H) facilitated the heat and mass transfer through its vigorous performance. Therefore, the process parameters values got increased, the reaction efficiency become more intensified. Thus, the FFA chains become more and more consumed .Consequently, A.V got decreased. In conventional reactors, higher temperature and higher molar ratio and reaction time are a cause for poor reaction. However, in micro channel reactor, the higher A.V is obtained at higher due to the excellence of the reactor in managing the heat and mass transfer (Mohamed Ezzeldin, 2021).

4.8. Iodine values determination of soy based polyether polyol

The I.V determination of soy-based polyether polyol was performed to evaluate the presence of unsaturated FFA chains. The I.V determinations was made in series of reaction runs to indirectly measure the functionality of micro channel reactor and micro channel heat sink (Jain, 2023).

Table 14 Iodine values for soy-based polyether polyol.

Runs	Temperature (^{O}C)	Time (min)	Molar ratio	Iodine value (I_2/100g)
1	75	4	0.5	4±0.01
2	80	6	1	3.91±0.1’
3	90	8	1.5	2.95±.0.05

The I.V for soy based polyether polyol became decreased. This is due to the miniaturization performance of micro channel reactor and micro channel heat sink. This unique performance of micro channel reactor shaped the efficient performance of epoxy ring opening reaction at higher temperature. Thus, the C=C bonds become decreased. Consequently the I.V has decreased from 4±0.01 I_2/100g, 3.91±0.1 I_2/100g and 2.95±0.05 I_2/100g. Thus, for higher temperature of micro

channel reaction, the reaction become more intensified and I.V for soy-based polyether polyol decreased due to the conversion of C=C bond (Fengyan zhang, 2023).

4.9. Saponification value determination for soy-based polyether polyol

The S.V for soy based polyether polyol was determined to evaluate the amount KOH needed to saponify the FFA chains presented in soy based polyether polyol. The S.V has been determined by triplicate experiment runs at different process parameters.

Table 15 Saponification value for soy-based polyether polyol.

Runs	Temperature (^{O}C)	Time (min)	Molar ratio	Saponification value (mgKOH/g)
1	75	4	0.5	183±0.05
2	80	6	1	184±0.02
3	90	8	1.5	183±0.05

The S.V for soy-based polyether polyol show almost approximate values for all experimental runs due to the fact that FFA chains presented in soy based polyether has closer length regard less of the intensification of the hydroxylation of EWCSBO parameters. For all there experimental runs, the S.V ranges 183 mgKOH/g-184 mgKOH/g (Salarvand et al., 2023).

4.10. Peroxide values for soy based polyether polyol

The peroxide value of soy based polyether polyol was determined by a titration method to measure the amount of peroxides and hyper oxides that causes the rancidity and bad smell in the sample of soy-based polyether polyol.

Table 16 Peroxide value for Soy-based polyether polyol.

Runs	Temperature (^{O}C)	Time (min)	Molar ratio	Peroxide value
1	75	4	0.5	4.15±0.02
2	80	6	1	4.12±0.01
3	90	8	1.5	3.75±0.5

The P.V of soy-based poly ether polyol decreased as the operational parameters (temperature, molar ratio of EWCSBO to $C_2H_6O_2$, reaction time). The relative minute size of micro channel reactor and micro channel heat sink yield high contact surface area for the reactants. Thus, micro channel reactors and micro channel heat sink that has performed at 75 ^{O}C, 80 ^{O}C and 90 ^{O}C exhibited lowering of P.V due to effective eradication of degradation of soy-based polyether polyol by effective reaction. Thus, P.V was increased due to effective ring opening reaction of EWCSBO (Kuang et al., 2023).

4.11. Hydroxyl number (OH) number determination of soy-based polyether polyol

The OH number of soy-based poly ether polyol was determined by titration soy-based poly ether polyol. The OH number was to determine and obtained with the range of 410.5±0.01 mg KOH/g -440±0.6 mgKOH/g. These values indicated that the intensified hydroxylation of EWCSBO was successful. More OH number implicated higher thermal resistant behavior and effective stability. Thus, the produced soy-based polyether polyol can serves as qualified polyurethane input (Mariana del valle, 2022).

Table 17 Hydroxyl number for soy-based polyether polyol.

Run	Temperature (^{O}C)	Molar ratio	Time (min)	OH number (mgKOH/g)
1	75	0.5	4	410.5±0.01
2	80	1	6	421.3±0.5
3	90	1.5	8	440±0.6

The OH number obtained from triplicate experimental runs shows the quantification for the process intensification for hydroxylation of EWCSBO. The reported OH numbers are 410±0.01 mg/KOH, 421.3± 0.5 mgKOH/g and 440±0.6 mgKOH/g. These values have shown the increment of OH number by 50 % from the hydroxylation reaction in conventional reactors. Mostly, in batch reactor the OH number falls under the range of 200 mgKOH/g -250 mgKOH/g. The increasing value of temperature and molar ratio facilities higher conversion unlike the

reaction conditions in traditional batch reactors. As the temperature went from 75 ^{O}C-95 ^{O}C, the OH number also enhanced from 410.5±0.01 mgKOH/g to 440±0.6 mgKOH/g. The values of OH number are increased this much due to the attribute of the small channel geometry of the micro channel reactor and the micro channel heat sink (Ibrhaima Balde, 2022).

4.12. Physicochemical properties of soy-based polyether polyol

The physicochemical properties of soy-based polyol were determined in three sequential experimental runs to validate that the developed micro channel reactor system produced an intensified products. The values are for the confirmation of physicochemical properties of soy-based polyether polyol at different reaction parameters.

Table 18 Physicochemical properties of soy-based polyether polyol.

Runs	Reaction temperature (^{O}C)	Time (min)	Molar Ratio	℘ (g/l)	S.g	μ (cp)	M.O (%)	R.I	Color
1	75	4	0.5	0.93±0.005	0.93±0.005	330.1±0.6	0.05±0.004	1.36±0.01	Faint Yellow
2	80	6	1	0.94±0.01	0.94±0.01	332.9±0.4	0.03±0.001	1.32±0.2	Faint Yellow
3	90	8	1.5	0.94±0.01	0.94±0.01	335.6±0.08	0.01±0.002	1.3±0.05	Faint Yellow

4.13. Hydrodynamic properties for micro channel reactor

4.13.1. Reynolds number and pressure drop analysis for a micro channel reactor

The Re number for a micro channel reactor was determined to measure the hydrodynamics efficiency which consequently affects the pressure drop rate, mass and heat transfer efficiency. The determination of Re number was done in a gravity –driven T-junction micro channel reactor with hydraulic diameter (d_H) of 4 mm. The Values of Re numbers were examined at different flow rate and the average density ($℘_{aveg}$) was examined at room temperature and found to be 1.05

g/l and the average viscosity for this mixture 170.5 m.CP. The table 19 shows the values of Re number for different experimental runs.

Table 19 Table for Re number and pressure drop determination.

Runs	Height(Cm)	Velocity(ml/ min)	Re number	△P	Flow regime
1	2	5.2	0.12	20.6	Laminar
2	3	10.1	0.24	30.9	Laminar
3	5	12.3	0.31	51.25	Laminar
4	7.5	20.6	0.53	77.25	Laminar
5	10	25.4	0.62	103.05	Laminar

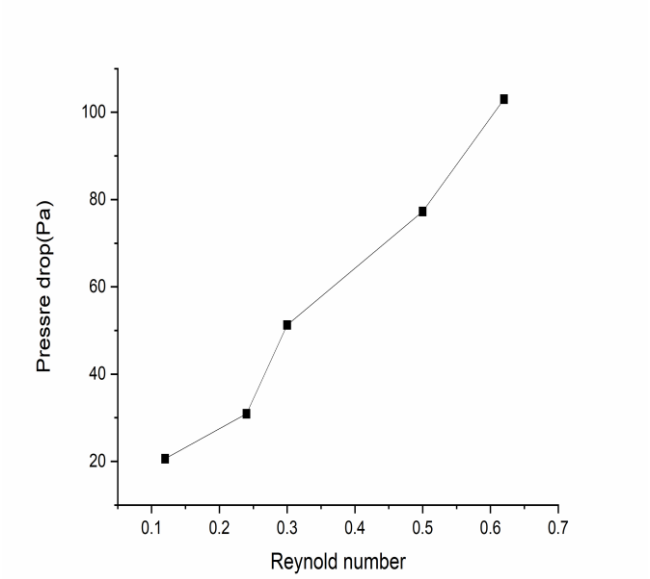


Figure 8 Graph for Re number and pressure drop.

The relation of Re number and the pressure drop with velocity of reactants in a micro channel reactor was examined to evaluate all heat transfer, hydrodynamics and pressure drop of the reactor system. As the height between the micro channel reactor and the micro channel heat sink increased, the velocity of EWCSBO and $C_2H_6O_2$ mixture went from 0.5 ml/min to 8 ml/min.

This has favored the smooth flow of the reactant along the length of micro channel reactor. The mixture of EWCSBO and $C_2H_6O_2$ is a viscous mixture. Therefore, the gravity-driven flow of micro throughout the channel facilitated the mixing without turbulence and over flow through the narrow channels. The Re number for the micro channel heat sink also went from 0.12 to 0.62. This implies laminar regime. This directly implicates slug flow for the mixture of reactants. Moreover, there are no significant eddies and vortices. The pressure drop also illustrates a significant loss starting from the inlet to the outlet. This is a direct implication of reactants throughout small the hydraulic diameter channels (4mm) have vigorous slow mixing (Bouras, 2021).

4.13.2. Reynolds number and pressure drop for micro channel heat sink

For a rectangular micro channel with zigzag shape with an hydraulic diameter of 4mm and using water as a cooling medium, the Re number was calculated in variety of experimental runs. The Re number was calculated.

Table 20 Re number and pressure drop determination for micro channel heat sink

Run	Height (cm)	u (m/s)	℘ (g/ml)	μ (Cp)	Re number	Pressure (Pa)	Flow regime
1	2	5.2	1	0.89	22.47	19.6	Laminar
2	2.5m	10.1	1	0.89	44.94	24.5	Laminar
3	5cm	11.5	1	0.89	51.6	49	Laminar
4	7.5cm	20.6	1	0.89	89.88	73.5	Laminar
5	10cm	27.3	1	0.89	122.69	98	Laminar

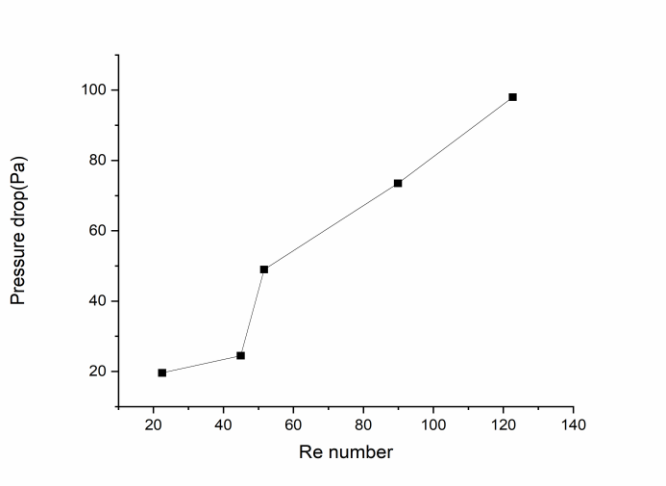


Figure 9 Graph Re number and pressure drop for micro channel heat sink.

The calculated Re number ranged from 22.47 to 114.15 showed the flow is in laminar regime (Re<2300) particularly slug flow in micro channel heat sink. This is an implication for strengthen of inertial force over the viscous one. The laminar flow of the cooling medium throughout the channel show higher heat transfer rate with smooth and stable performance. This is a preferable characteristic for a micro channel heat sink for exothermic nature of hydroxylation reaction to absorb heat of reaction. The increase of Re number in a micro channel heat sink also resulted increment in pressure drop. The fact that micro channel heat sink is gravity driven the pressure drop from inlet to outlet got increased throughout the channels along the increment of velocity gradient and the height between the micro channel reactor and the micro channel heat sink. Thus, high cooling medium velocity cross ponds to higher pressure drop and cooling effect. This is good implication for heat dissipation of the micro channel heat sink performance (F.Montazeri, 2023).

4.14. Experimental Evaluation of Micro Channel Reactor

4.14.1 Heat transfer analysis of micro channel reactor

The heat Transfer of Micro Channel Reactor was determined by calculation of dimensionless number including Re number, Nu number, $R_{th,}$ Nu number and Bo number. These dimension less numbers were calculated at different temperature and u for five consecutive runs (Widianto et al., 2024).

Table 21 Temperature deviation and velocity in a micro channel reactor.

Runs	Height (cm)	Temperature difference (^{O}C)	u (ml/min)
1	10	5.1	5
2	20	4.5	10
3	25	3.6	12.3
4	30	2.5	20.6
5	50	2.1	25.4

Table 22 Heat transfer analysis for micro channel reactor.

Runs	Re number	Nu number	R_{th} (K/w)	Heat flux	Bo number
1	0.12	5.33	0.003	19.6	0.254
2	0.24	15.2	0.012	13.7	0.72
3	0.3	25.89	0.0073	9.9	1.23
4	0.5	59.92	0.0031	7.19	2.86
5	0.62	140.13	0.0013	3..79	6.69

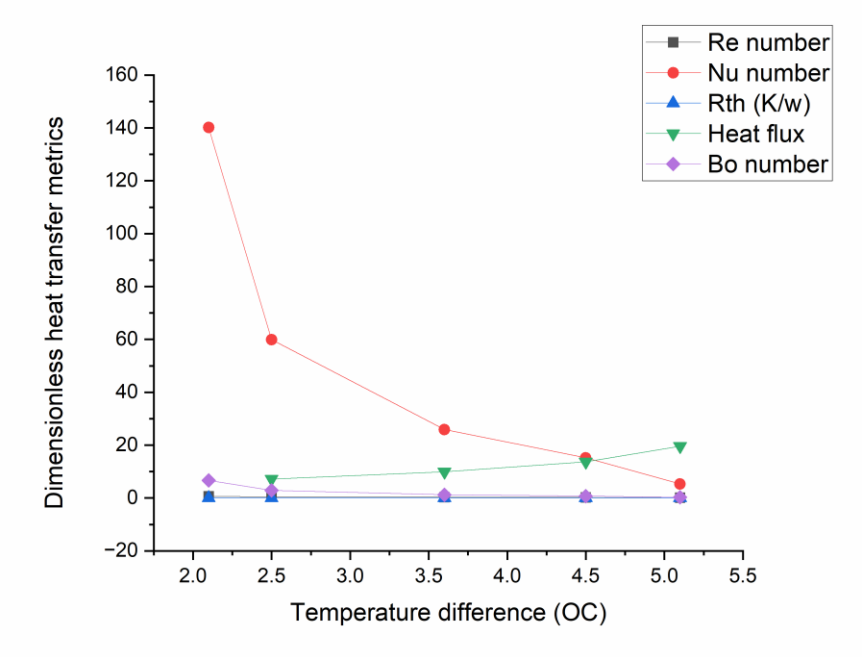


Figure 10 Heat transfer of micro channel reactor.

The heat transfer analysis for micro channel reactor was made at different velocities and temperature ranges. The Re number has been increased significantly throughout the increasing of velocity in the experimental runs. The values of Nu number increased through the process and as the processes of the hydroxylation proceed heat is being released. This directly implies the advancement of convective heat transfer as the temperature becomes regulated. Thus, the heat flux becomes decreased. This effect is due to the thermal performance of the micro channel reactor and micro channel heat sink. On the other side, the small dimension of the micro channel reactor provide excellent heat performance thus as the contact between reactants enhanced, the thermal resistance become decreased. The increment of Bo number also illustrates the heat transfer resembles more to convection rather than conduction heat transfer. Thus, the increment of Bo number confirms the heat exchange between the micro channel reactor and the micro channel heat sink. Additionally, the heat flus for the micro channel reactor become decreased as velocity increases. This is due to the reason that at higher height of the gravity channels and velocity, heat transfer rate is increased. Thus, the temperature gradient between the inlet and the outlet point decreased and come to the point of thermal equilibrium (Lee et al., 2021).

4.15. Heat transfer for micro channel heat sink

The heat transfer for a micro channel reactor was examined by calculation of dimension less number like Re, Nu and Bo. The effectiveness of micro channel heat sink in reducing heat transfer barrier was evaluated by thermal resistance at different temperature and velocity (Udom & Lappa, 2025).

Table 23 Data's for Temperature and velocity in micro channel heat sink.

Run	Height (cm)	Temperature difference (^{O}C)	u (mm /min)
1	2	5	5
2	2.5	4.5	10
3	5	3.6	11.5
4	7.5	2.5	20
5	10	2	27.5

Table 24 Heat analysis for micro channel heat sink.

Run	Re number	Nu number	Bo number	R_{th}	Heat flux
1	22.47	11.06	0.02	0.47	8350
2	44.94	22.12	0.07	0.23	7515
3	51.61	26.55	0.1	0.19	6012
4	89.88	33.20	0.2	0.15	4175
5	122.69	44.25	0.6	0.11	3340

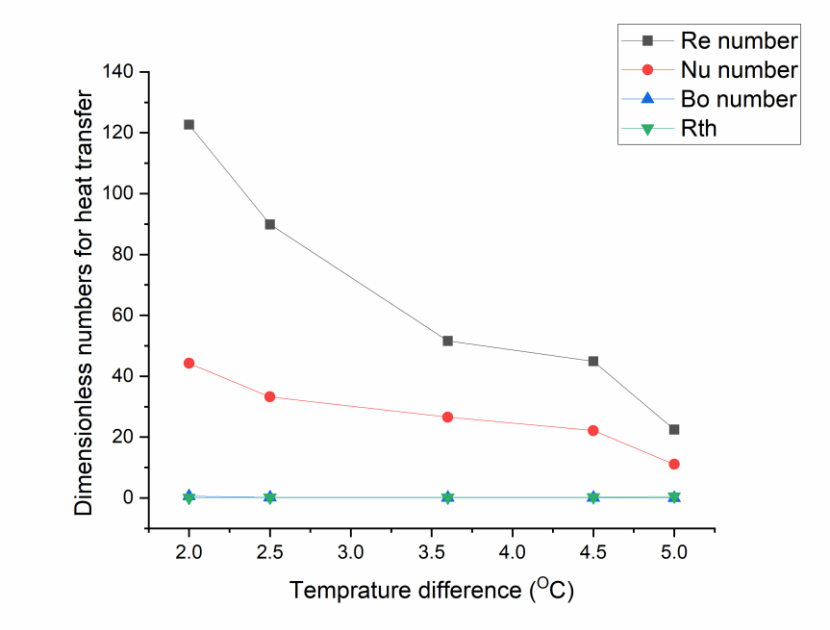


Figure 11 Heat transfer for micro channel heat sink.

The heat transfer analysis for a micro channel heat sink has been performed for five experimental runs. From experimental analysis made, the temperature difference between the inlet and outlet section decreased as the values for dimensionless numbers increased. The values for Nu and Re numbers increased as the height between the channels increased. This is a confirmation for enhancement of heat transfer coefficient and for excelling heat transfer rate. The R_{th} values ranges from 0.027-0.6. This is an implication for insignificant values of the barrier of thermal transfer. As R_{th} is inversely proportional with the thermal performance of the micro channel heat sink, lower values confirm the successful functionality of the micro channel heat sink. The lower Bo values have shown the dominance of conduction heat transfer over the convective one. This means the micro channel heat sink regulate the temperature across the longitudinal direction of the heat sink between the inlet and outlet tubes. The other metrics for thermal performance of micro channel heat sink is q. The value of q reduced as the velocity increases. The increment of velocity facilitates the mass transfer and speed up the reaction. So the heat regulation step becomes significantly improvised and temperature gradient narrows. Consequently, heat flux decreased (M.B et al., 2024).

The figure 11 which is a graph of micro channel heat sink showed constant increment of heat flux as the temperature range increased. This is due to the attribution of micro channel heat sink and micro channel reactor. The micro channel reactor and the micro channel heat sink excel almost uniform approximate temperature distribution.

4.16. Thermodynamic properties for micro channel heat sink

The thermodynamic analysis was used as a key feature in empirical assessment of micro channel heat sink. This directly showed the heat absorbed by the micro channel heat sink to regulate the exothermic nature of hydroxylation reaction. This was performed using water as a cooling medium. So the specific heat capacity (Cp) of water was taken for thermodynamic calculation.

Table 25 Thermodynamic properties for micro channel heat sink.

Run	Mass-flow rate (Kg/min)	Specific-heat capacity(KJ/Kg.K)	△T (K)	Heat absorbed (J)
1	0.005	4.18	5	10.46
2	0.01	4.18	4.5	18.82
3	0.012	4.18	3.6	18.07
4	0.015	4.18	2.5	15.69
5	0.02	4.18	2	18.67

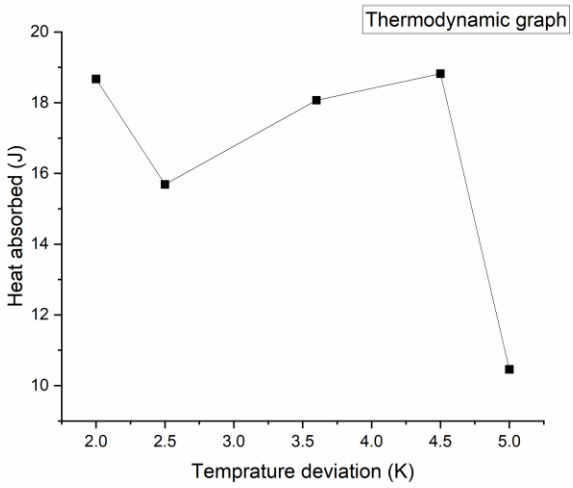


Figure 12 Graph for thermodynamic graph.

The heat transfer performance for micro channel heat sink was determined by analysis with a variety of mass flow rate and temperature difference. As the mass flow rate increased from 0.005 Kg/min to 0.015 Kg/min, the temperature variation went lower. Higher mass flow rate for a micro channel heat sink yields effective cooling. Thus, the variation of temperature from inlet and outlet become slightly decreased in the experimental runs due to effective temperature distribution. Consequently, Q got increased to regulate the temperature of micro channel reactor. Thus this attributes for the intensified hydroxylation of EWCSBO (Coman, 2023).

4.17. Thermodynamic analysis for micro channel reactor

Table 26 Thermodynamic properties.

Runs	Mass-flow rate (Kg/min)	T_i (K)	T_f (K)	Average Cp (KJ/Kg.K)	Heat loss (J)
1	0.004	348	351.31	2	5.1
2	0.006	351	354.62	2	9.3
3	0.008	353	357.35	2	8.6
4	0.012	358	364.63	2	7.5
5	0.015	362	370.81	2	8.1

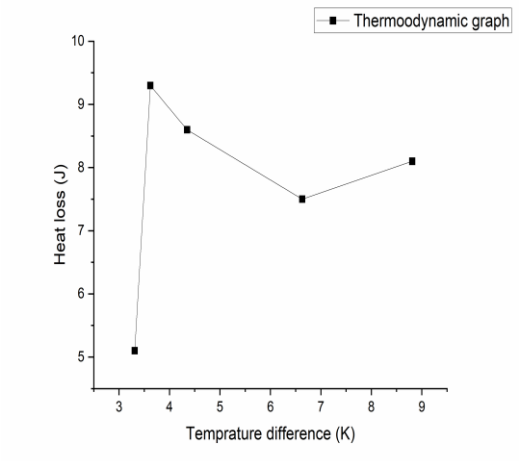


Figure 13 Graph for thermodynamics of micro channel reactor.

The thermodynamic properties of a micro channel reactor were examined to evaluate the performance of micro channel reactor. As the mass flow rate goes from 0.004 Kg/min to 0.015 Kg/min, the value heat released also has a range from 5.1 J to 8.1 J. The mass flow rate of the reactants mixture has a directly proportionality with the heat released. The average specific heat capacity (Cp) of the two reactants mixture has been used as a constant average values through the experimental runs .As the flow rate of the reactant mixture increased, the reaction started to consume more reactants. Thus, the reaction started to release more heat. Therefore, the heat loss will continuously rise. This shows the effectiveness of the reactor system to regulate the heat release due to exothermic nature of the hydroxylation reaction. Therefore, the thermal performance of a reactor resembled to isothermal reaction (Pontes. P, 2022).

4.18. Mass transfer for hydroxylation of EWCSBO

The mass transfer analysis for hydroxylation of EWCSBO was performed to test the functionality of the developed micro channel reactor. The following table shows different reaction conditions on analysis of micro channel reactor. The mass transfer analysis for micro channel reactor was conducted with ρ_{avg} of 1.05 g/l and μ of 0.89 Cp.

Table 27 Mass transfer analysis.

Runs	Height (cm)	Temperature difference (^{O}C)	Re number	Sc number	Sherwood number
1	2	15	0.12	1160327	42.97
2	2.5	10.5	0.24	1657610	57.13
3	5	7.6	0.31	2290120	69.36
4	7.5	5.5	0.52	3164529	144.41
5	10	2.9	0.62	6001693	115.16

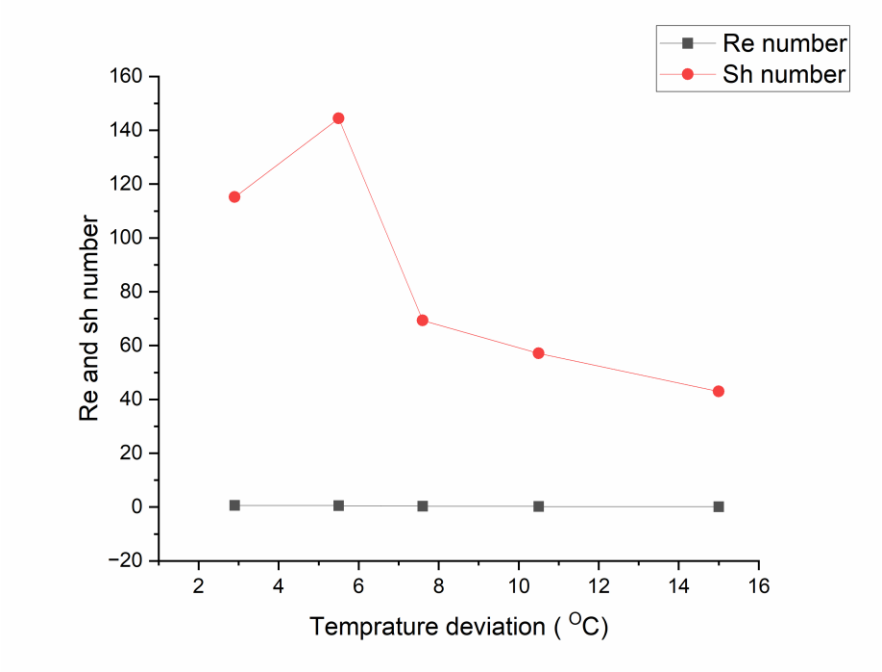


Figure 14 Re and sh number for micro channel reactor.

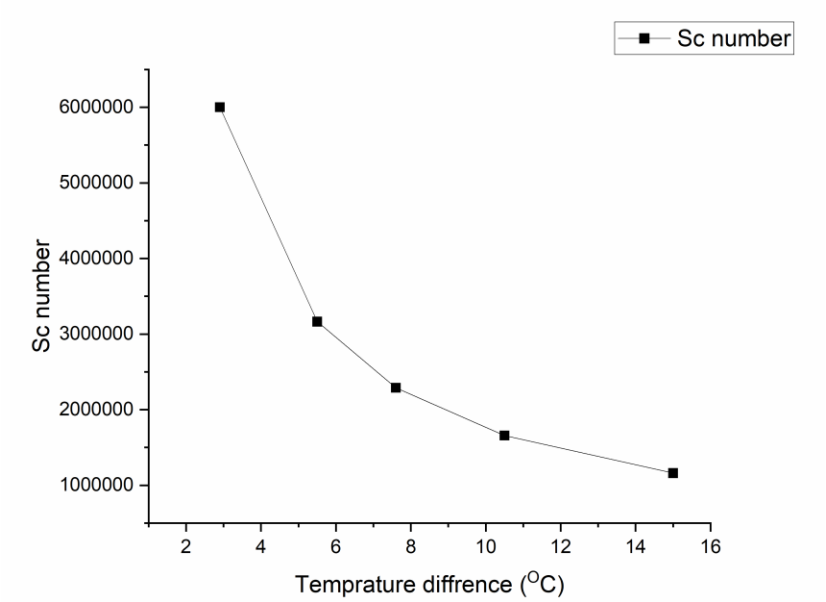


Figure 15 Sc number for micro channel reactor.

In the figure 15 mass transfer analysis for hydroxylation reaction of EWCSBO and soy-based polyether polyol, the value of Sc number, Re number and sh number were analyzed. The Re number for a micro channel reactor was obtained in smaller range of 0.12-0.62. This is due to viscous nature of the reactant mixture. Consequently, slow slug flow was enhanced. Viscous

force was far greater than inertia force. This is a good attribute for efficiency of micro channel reactor to mix reactants effectively. On the other side, the value of sc number increased dramatically. This is because of effective mass transfer of reactants in small diffusion distance of the grooved reactor. The value of Sh number increased as the velocity and the height between the micro channel reactor and the micro channel heat sink increased. The gravity driven passive micro channel reactor helped to enhance the flow even though, the reactants are viscous by their nature. Thus, unlike the conventional reactor, as the concentration increases, the mass transfer rate becomes increased due to the miniaturized reactor.

4.19. Kinetic study

4.20. Kinetic study for micro channel reactor

The kinetic study for a micro channel reactor was developed to analyze the rate of the hydroxylation reaction of EWCSBO. The kinetic study for a micro channel reactor as done as following

Assumptions

- Irreversible liquid –liquid phase elementary reaction
- Second order of reaction (First order for each reactant)
- Isothermal reaction condition

Mole balance: $\mathbf{Accumilation = \ input - output + genration - consumption}$

$$\mathbf{Fi_0 - F_i + ridv = \frac{dni}{dt}} \qquad (4.1)$$

$$\mathbf{\frac{dF_I}{dv} = ri} \qquad (4.2)$$

Rate law

$$\mathbf{-rA = KC_A\, C_B} \qquad (4.3)$$

For species B

$$\mathbf{-rB = -3KC_AC_B} \qquad (4.4)$$

For species C

$$\mathbf{rC = Kc_A C_B} \quad (4.5)$$

Where

$$\mathbf{K = Aexp(-\frac{Ea}{RT})} \quad (4.6)$$

$$\mathbf{-rA = -k\left(\frac{FA}{V_0}\right)\left(\frac{FB}{V_0}\right) = k/V0^2 FAFB} \quad (4.7)$$

Where

$$\mathbf{CA = \frac{FA}{V0}, CB = \frac{FB}{Vo}} \quad (4.8)$$

$$\mathbf{FB = FB_0 - 3(FA_0 - FA)} \quad (4.9)$$

Final equation

$$\mathbf{\frac{dFA}{dv} = -\left(\frac{k}{VO^2}\right) FA[FB_0 - 3(FA_0 - FA)} \quad (4.10)$$

4.21. Comparison of dimensionless numbers for micro channel reactor and micro channel heat sink with existing literatures

Table 28 Comparison table for micro channel heat sink with literature results

No	Measuring metrics	(Surendera Barhatte, 2024)	Study results
`1	Nu	120	44.97
2	Re	6633	22.24
3	Heat flux (q)	1522	3340 $w/m^2.K$
4	Area	$4.9*10^{-6}\ m^2$	$12.56*10^{-6}\ m^2$
5	Volume	$4.9*10^{-5}\ m^3$	$1.88*10^{-3}\ m^3$
6	Volumetric flow rate	4.9 ml/min	18.8 ml/min
7	Pressure drop	179,345 Pa	98 Pa

Table 29 Comparison of micro channel reactor with literature values.

No	Measuring metrics	(Juliana cardinas ramirez, 2025)	Study results
1	Residence time	10 min	10 min
2	Volumetric flow rate	15.7 ml/min	18.8 ml/min
3	Re number	1.65	0.62
4	Area	$0.02355\ m^2$	$12.56*10^{-5}m^2$
5	Volume	$1.57*10^{-5}\ m^3$	$1.88*10^{-3}\ m^3$
6	Sh number	40.01	42.67

From the above comparison table 28 and 29, it has been revealed that the comparison between micro channel reactor and heat sink with existing literature showed the prototype has performed in the same region with the existing literatures. The particular difference seen was on Re number for micro channel reactor. It shows immense difference. This is due to the literature has used an active system with pump power 294 W while this study uses a passive micro channel reactor and heat sink system with a gravity driven pressure drag force. This study has used passive system to reduce pulsation effect. In the comparison of micro channel reactor with literature, both showed strictly laminar regime which is an essential attribute of hydrodynamics for viscous fluid mixing. Comparing the Nu number for micro channel heat sink rom the literature versus the study, the Nu number in this study showed significant increment form the literature this may resulted from increase of channel number and hydraulic diameter. The Sh number comparison also showed approximate values that implies effective mass transfer. The other large deviation of pressure drop in micro channel heat sink also steamed from the fact that the literature used active pump while this study use passive gravity driven path. Thus as a conclusion, it can be stated that the chosen design parameters and the fabricated prototype yielded the performance with expected range.

4.22. Statistical Method

The statistical analysis of an intensified hydroxylation reaction of EWCSBO in a micro channel reactor was performed by design expert software. RSM particularly CCD was used to design, analyze and optimize reaction runs. The interaction of independent parameters (Temperature, Molar ratio of $C_2H_6O_2$ to EWCSBO, Time) with OH number was studied through 20 experiment runs.

Table 30 Central composite experimental design for hydroxylation of EWCSBO.

		Factor 1	Factor 2	Factor 3	Response 1
Std	Run	A:Temprature	B:Molar ratio	C:Reaction time	Hydroxyl number
		^{O}C		Min	mgKOH/g
14	1	82.5	0.65	12.3863	427.118

1	2	75	0.3	3	409
18	3	82.5	0.65	6.5	413.26
7	4	75	1	10	404.68
2	5	90	0.3	3	419.6
15	6	82.5	0.65	6.5	413.26
13	7	82.5	0.65	0.613725	390.12
10	8	95.1134	0.65	6.5	438.12
8	9	90	1	10	441.14
6	10	90	0.3	10	434.6
19	11	82.5	0.65	6.5	413.26
11	12	82.5	0.0613725	6.5	411.26
16	13	82.5	0.65	6.5	413.26
4	14	90	1	3	413.87
12	15	82.5	1.23863	6.5	416.12
3	16	75	1	3	396.86
5	17	75	0.3	10	392.6
9	18	69.8866	0.65	6.5	398.65
20	19	82.5	0.65	6.5	413.26
17	20	82.5	0.65	6.5	413.26

4.22.1. ANOVA results

Response 1: OH number
Transform: Power
Lambda: 1, Constant: 0

Source	Sum of Squares	df	Mean Square	F-value	p-value	
Model	3344.88	6	557.48	25.63	< 0.0001	significant
A-Temprature	2175.32	1	2175.32	100.00	< 0.0001	
B-Molar ratio	5.66	1	5.66	0.2603	0.6185	
C-Time	672.15	1	672.15	30.90	< 0.0001	
AB	0.1152	1	0.1152	0.0053	0.9431	
AC	324.36	1	324.36	14.91	0.0020	
BC	167.26	1	167.26	7.69	0.0158	
Residual	282.80	13	21.75			
Lack of Fit	282.80	8	35.35			
Pure Error	0.0000	5	0.0000			
Cor Total	3627.67	19				

Factor coding is **Coded**.
Sum of squares is **Type III - Partial**

The **Model F-value** of 25.63 implies the model is significant. There is only a 0.01% chance that an F-value this large could occur due to noise. **P-values** less than 0.0500 indicate model terms are significant. In this case A, C, AC, BC are significant model terms. Values greater than 0.1000 indicate the model terms are not significant. If there are many insignificant model terms (not counting those required to support hierarchy), model reduction may improve your model.

Fit Statistics

Table 31 Fit statistics table.

Std. Dev.	4.66	R^2	0.9220

Mean	413.67	Adjusted R^2	0.8861
C.V. %	1.13	Predicted R^2	0.7100
		Adeq Precision	19.0504

The **Predicted R^2** of 0.7100 is in reasonable agreement with the **Adjusted R^2** of 0.8861; i.e. the difference is less than 0.2.**Adeq Precision** measures the signal to noise ratio. A ratio greater than 4 is desirable. Your ratio of 19.050 indicates an adequate signal. This model can be used to navigate the design space.

4.22.2. Model equation for OH number

From experimental runs, OH number ranges 390.12 mgKOH/g – 441.14 mgKOH/g. Therefore, the equation 4.11 showed that the model equation for regression analysis for the interaction of reaction parameters with OH number.

$$Y = 1262A + 0.6439B + 7.02C + 0.12AB + 6.37AC + 4.57BC \quad (4.11)$$

In the equation (4.11), the temperature was represented by “A” and “B” for molar ratio and reaction time by “C”. The combined effect of temperature and molar ratio represented by “AB” , the combined effect for temperature and reaction time designated by “AC” has a positive impact on OH number. The other combined effect of molar ratio and time represented by letters “BC” also exhibited an increasing relation with final OH number.

4.22.3. Diagnostic plots

Diagnostic plots show the rate of suitability of the suggested quadratic model. The normal diagnostic plot evaluates the distribution of errors. As figure 16 shows, the normal plot of residual values resembled to a straight line pattern and the transform used is suitable. The resulted values were collected together around the diagonal straight line as shown below. Even though the plot is not perfectly straight line, it tended to straight line. This showed that the error has normal distribution. The second plot, as shown in figure 17 below, the plot of predicted versus actual values of OH number was found as a perfectly straight line graph. This shows that an excellent aproximity of real values with the predicted ones with no significant varation. Thus,

the second order polynomial model was suitable to compare experimental values with predicted values.

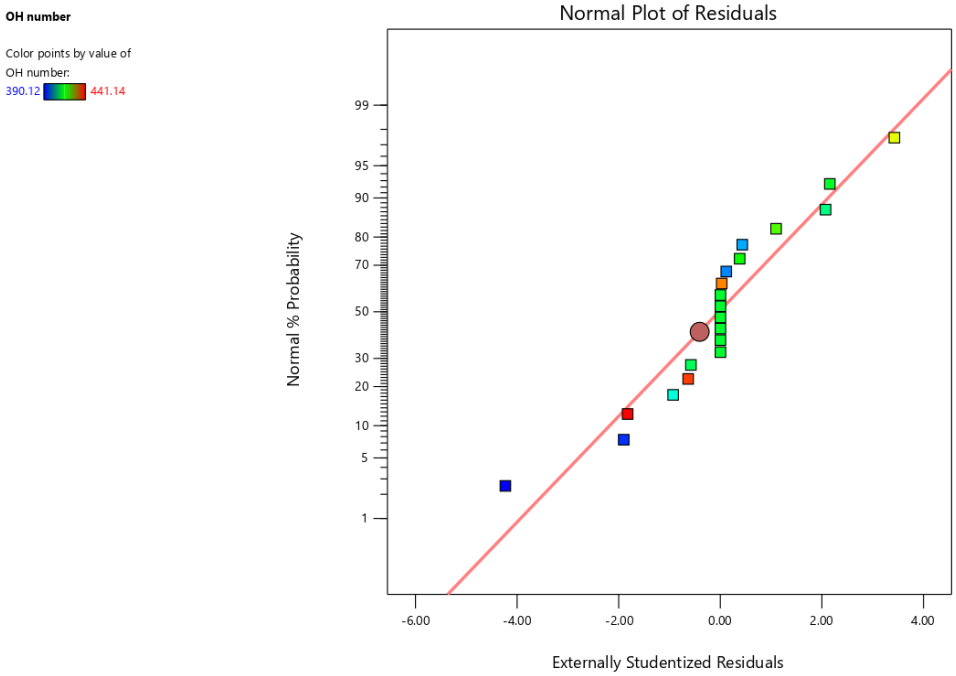


Figure 16 Normal plot of residuals

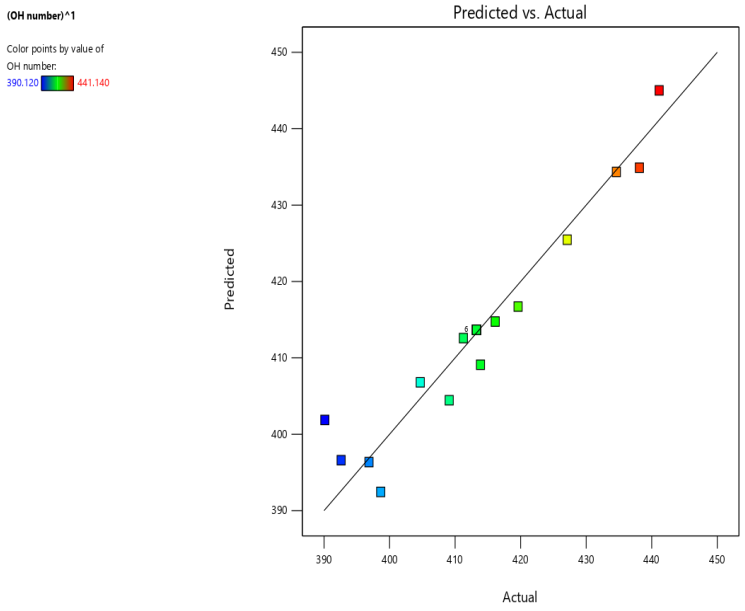


Figure 17 Predicted versus actual plot.

4.22.4. Impact of operation parameters with final OH number

3D plots for relation of process parameters with response variable were used and studied to analyze the significant impact of process parameters with OH number. This was done by studying the impacts of two process parameters on OH number, while keeping the remaining process parameter constant.As shown in the first figure 18, the combined effect of molar ratio and temprature on response variable while keeping the reaction time constant at 6.5 mins. In this graph, the combined effect of process parameters illustrate a slanted shape. This is an implication for the powerful effect of process parameters individually. This means the combined effect of molar ratio and temprature decoupled by individual property of time. This dueto the excellent performance of micro channel reactor and heat sink.

In other side, on, the second 3D plot shows the effect of molar ratio of EWCSBO to ethylene glycol and reaction time on OH number , keeping reaction time at 82.5^0C. Both these parameters have direct proportional relation with OH number. Both the individual paramaeters increased the result of OH number. However, the combined effect of individual parameters of molar ratio and reaction time is relatively lowcompared with the individual parameters of OH number. Thus an inclined plane graph is observed.

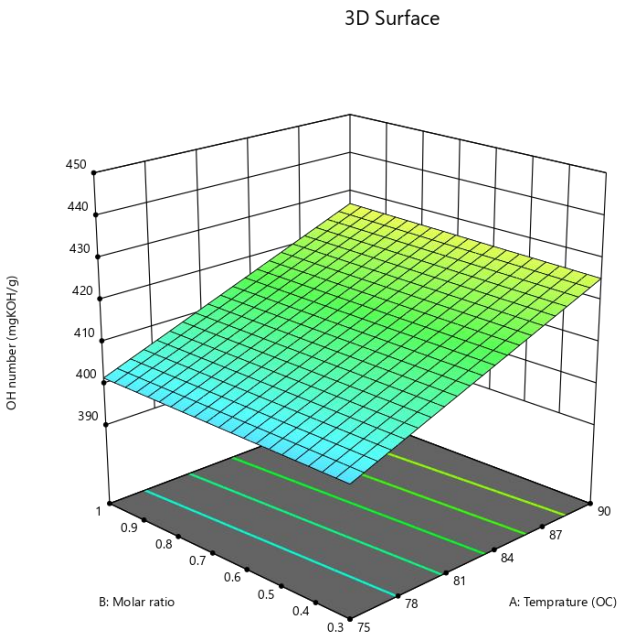
The last 3D plot shows the interaction of temprature and a reaction time on OH number at 0.65 molar ratio, this shows that the relation has a resultant postive impact on final OH number. In this case also the value of of temprature and reaction time exhibits the slightly inclined graph. This results are show proof for efficeny of micro channel reactor and micro channel heat sink. Thus, the mass and heat transfer performance caused high OH number. In which case, the temprature, molar ratio EWCSBO to $C_2H_6O_2$ and reaction time decouples combined effect.

Factor Coding: Actual

OH number (mgKOH/g)
Design Points
390.12 441.14

X1 = A
X2 = B

Actual Factor
C = 6.5

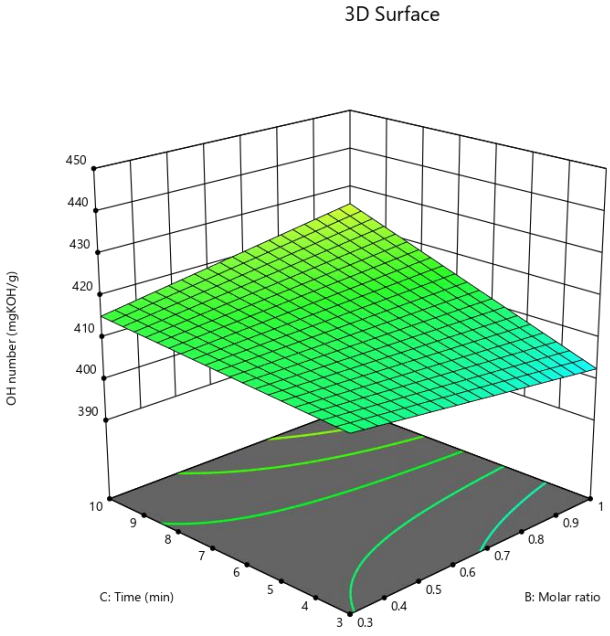


Factor Coding: Actual

OH number (mgKOH/g)
Design Points
390.12 441.14

X1 = B
X2 = C

Actual Factor
A = 82.5



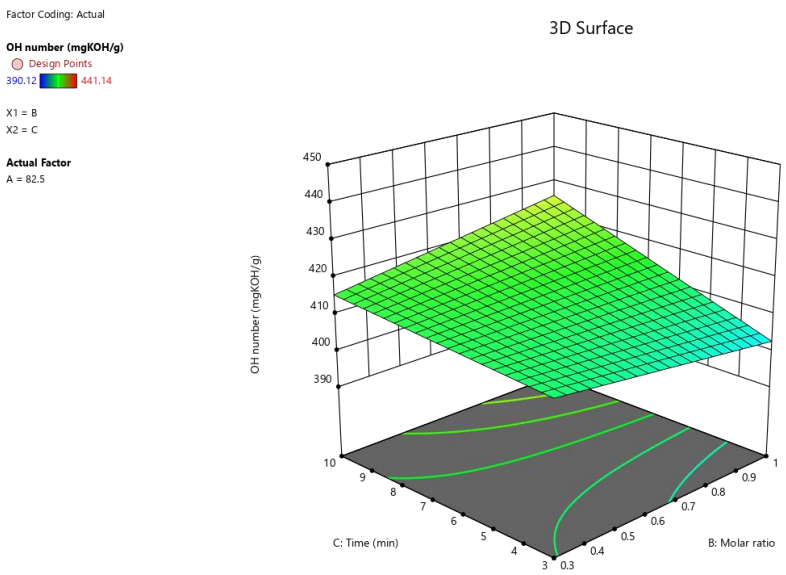


Figure 18 3D plot for impact of process parameter on OH number.

4.22.5. Perturbation plot for process parameters for final OH number

A perturbation plot was drawn by design expert software to analyze the effect of each parameter on main response variable of OH number for the studying which variable has a significant effect on the main result.

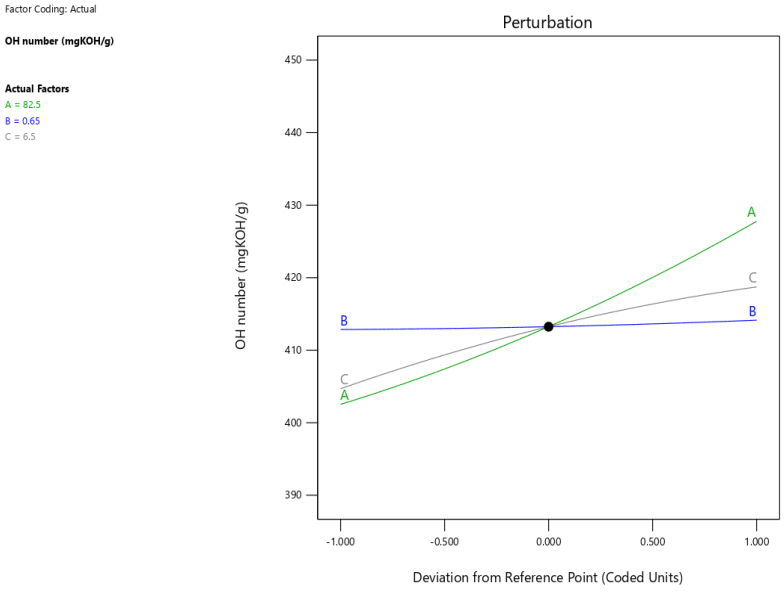


Figure 19 Perturbation plot.

This perturbation plot showed the effect of process parameters on final OH number by varying process the two process parameter while keeping the other constant. As shown on the above figure 19 on plot of perturbation, the process parameters temperature (A), Reaction time(C) has a significant impact on OH number. The other process parameter, Molar ratio (B) has a straight line perturbation plot. This means the effect of molar ratio was not that much significant on the resulted response variable. As the analysis on ANOVA showed individual effect of factor of temperature and reaction time has greater effect.

4.22.6. Optimization of reaction parameters

The statstical analysis of hydroxylation reaction of EWCSBO was assesed by CCD method. It was reveled that the optimum OH number was found to be 442.75 mgKOH/g at a temprature of 89.49 ^{O}C, a molar ratio of 0.97 and a reaction time of 9.91 mins.

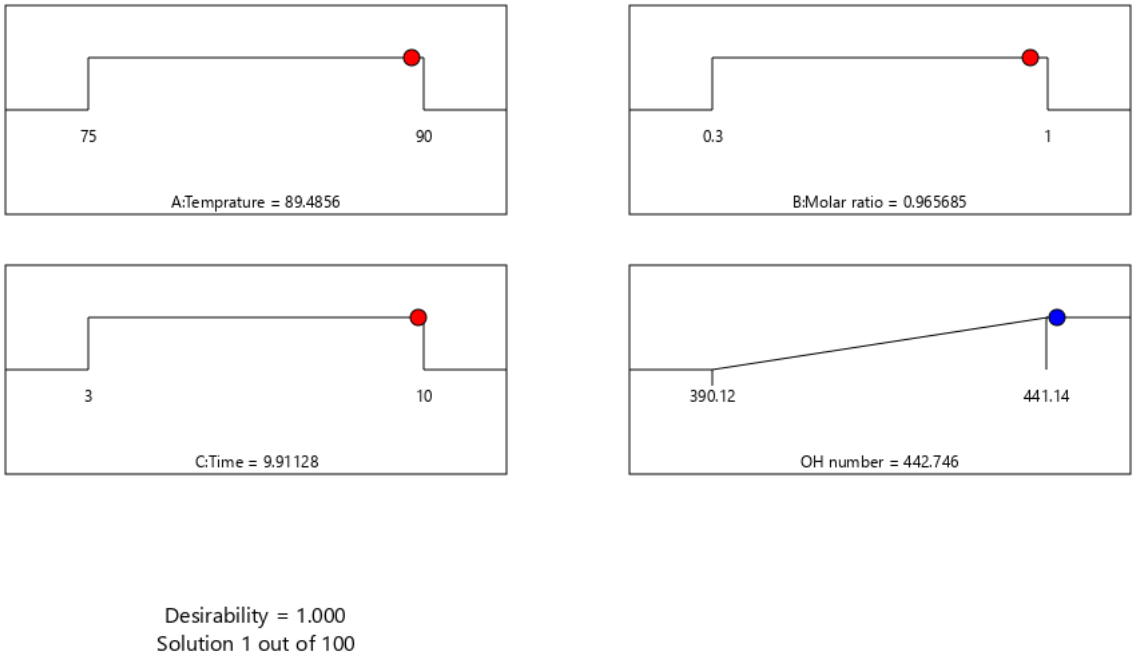


Figure 20 Optimization of reaction parameters.

4.22.7. Model validation

Triplicate experiments were taken based on predicted optimal process parameters that were recommended by the design expert software to confirm the developed model and its results. The recommended optimal values are 89.49 ^{0}C, 0.96 molar ration and reaction time 9.91min. An OH number of 436.511 mg KOH/g has been obtained. Consequently error percentage has been done.

$$\%Error = \frac{Pred.value - actual\ value}{pred.value} value \qquad (4.12)$$

Table 32 Table for process optimization.

Temperature(^{0}C)	Molar ratio of $C_2H_6O_2$to EWCSBO	Reaction Time (min)	Actual-OH number (mgKOH/g)	Predicted OH number (mg OH/g)	Error (%)
89.49	0.96	9.91	436.51	442.75	1.41

4.22.8. One factor at a time (OFAT) sensitivity analysis

The sensitivity analysis for an intensified hydroxylation of EWCSBO was analyzed using the analysis. One factor at time sensitivity an analysis was conducted by taking the ratio the deviation of the response variable per the difference of the independent variables.

Table 33 OFAT table for temperature.

No	Temperature (^{0}C)	Molar ratio	Time (min)	OH number (mgKOH/g)	Sensitivity analysis
1	90	1	3	434.6	1.68%
2	75	1	3	392.6	

Table 34 OFAT table for molar ratio.

No	Temperature (^{0}C)	Molar ratio	Time (min)	OH number (mgKOH/g)	Sensitivity analysis
1	75	1	3	396.86	6.07%
2	75	0.3	3	392.61	

Table 35 OFAT for reaction time.

No	Temperature(^{0}C)	Molar ratio	Time(min)	OH number (mgKOH/g)	Sensitivity analysis
1	82.5	0.65	6.5	413.26	3.92%
1	82.5	0.65	0.6	390.12	

From the table 34, 35, 36 sensitivity analysis for each single factor, a percentage was calculated and found that a molar ratio shows greater significance than temperature and time. Indeed all three factors are found to be significant that resulted 1.68, 6.07 and 3.92 times result increment on OH number has been observed with the increase of temperature, molar ratio and time respectively. Even though the statistical analysis in ANOVA and perturbation plot reported that molar ratio is in significant. Practically, from OFAT analysis, molar ratio has higher sensitivity analysis that resulted impact on OH value.

4.23. FTIR analysis for WCSBO, EWCSBO, and soy-based polyether polyol

The FTIR analysis for WCSBO, EWCSBO and soy-based polyether polyol were conducted to identify the functional groups using KBr pellets as a reference material. The FTIR for all WCSBO, EWCSBO, and soy-based polyether polyol were evaluated in the range 500-4000cm^{-1} as shown in figure 21.

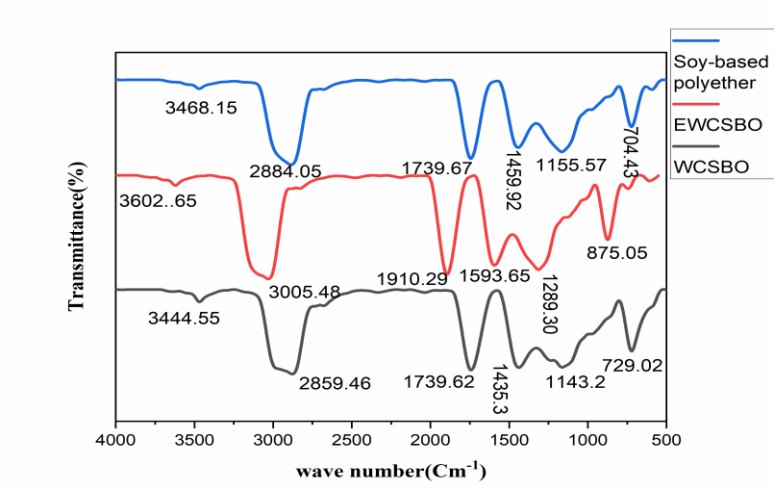


Figure 21 FTIR Graph for WCSBO, EWCSBO, and polyether polyol.

The projection peaks for WCSBO were observed at 3444.55 cm^{-1},2859.46 cm^{-1},1739.62 cm^{-1},1435.3cm^{-1},1143.2 cm^{-1},729.02 cm^{-1}. These crosspond to hydroxyl (O-H) streching bonds, streching carboxylic (-COOH-)group, streching C=O bond,bending, alkanes (C-H) group, bending alkyl amines (-NH_2) and bending alkyl aldehydes (–CHO-) bond respectiviely (Putri A.R, 2020). For EWCSBO, 3602 cm^{-1} was observed to due to hydroxyl (O-H) streching bond, 3005 cm^{-1} shows a functional group of bonded streching alkanes (C-H) bonds,1910.29 cm^{-1} and1593.65 cm^{-1} reveals the functional group of streching ketones(C=O) bond.The wave number for 1289.30 cm^{-1} show bending ketones(-C=O) group. Finally,875 cm^{-1} showed that the formation of epoxy group (Ibrahima Balde, 2022). For soy-based polyether polyol, 3468.15 cm^{-1} showed hydroxyl (O-H) streching bond, 2884.05 cm^{-1} is associated with streching carboxyl aci d(-COOH-) functional group,1739.67cm^{-1} and 1459.92 cm^{-1} is due to streching and bending ketones(-C=O) bonds respectively, 704.43 cm^{-1} was shown for bending hydroxyl (C-O) group that is resulted from ring openinig reaction. The FTIR graph for WCSBO, EWCSBO, and Soy-based polyether polyol exihbited approximate visual graph dueto structural similarty of glycerol back bone. Despite the fact that the micro channel techology intensified hydroxylation reaction, the functional group for soy-based polyether polyol has approximate structrual behavior with specfic wave number shift.

4.24. TGA graph for WCSBO

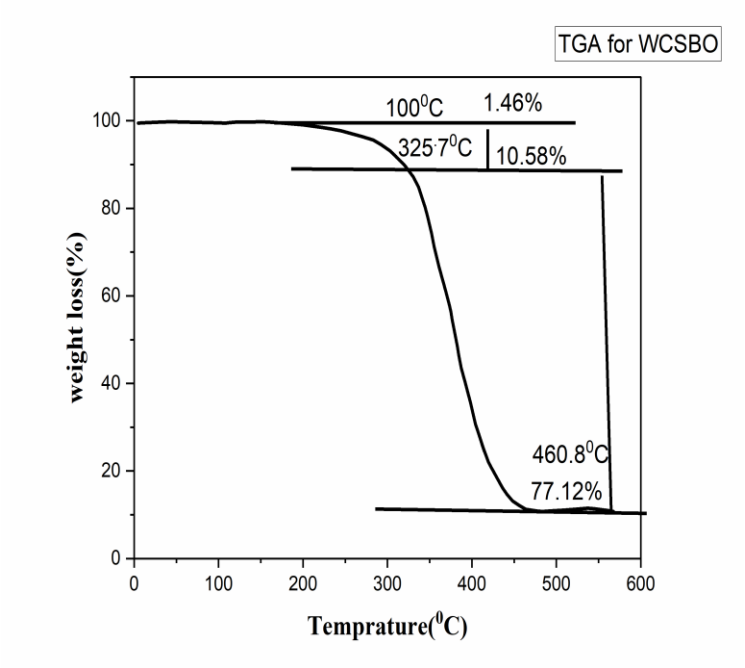


Figure 22 TGA graph for WCSBO.

The thermal stablity of refined WCSBO was examined by the TGA graph analysis. The graph showed that the measure of weight loss. The TGA graph illustrated the decompostion percentage of the compound against the temprature range from 0 ^{O}C-600 ^{O}C in controlled atmosphere. It has revelaed three distnict stages of decompostion. The first stage at 1.46 % and 100 ^{O}C shows the degradation of free water molecules. At 325.7 ^{O}C, the degradation percentage for WCSBO is 10.58 % which implies the primary degradation of poly unsaturated fatty acid like linoleic acid . The third stage of decompostion at 460.87 ^{O}C , has a weight loss of 77.12 %. This also reveals the degradation of Polymers mainly PET (polyehtylene tetra phatalte) and PE (Poly ethyelene). The higher decompostion rate of compounds by 77.12 % shows the release of unnecassary compounds. Consequently, it shows good pretreatment procedure and higher quality of WCSBO (Hui ying yong, 2023).

4.25. TGA graph for EWCSBO

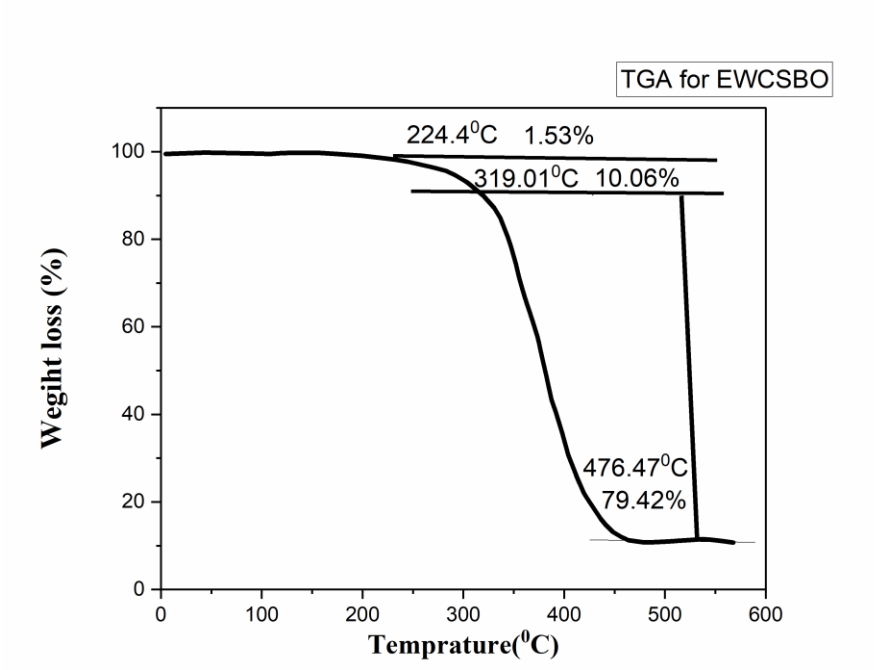


Figure 23 TGA graph for EWCSBO.

The effectiveness of epoxidation of WCSBO and the quality of produced EWCSBO was examined by TGA graph analysis. The TGA graph was drawn with the decomposition percentage versus temperature range of 0^{O} C-600 ^{O}C. It has three decomposition phases. In the first stage of decomposition, at 222.4 ^{O}C, 1.53 % rate of degradation for organic compounds was observed. These organic compounds include alkanes, alkenes and aldehydes that were adhered in the composition of EWCSBO. At the second stage of degradation, at 319.01 ^{O}C, 10.06 % decomposition rate was observed. This shows main degradation of ester bonds. At the last stage, 476.47 ^{O}C, a decomposition percentage of 79.42 % was obtained. This decomposition phase is again due to degradation of Polymer like PET. The TGA graph analysis for EWCSBO showed higher weight loss of 79.42 % decomposition. This shows the exact physic-chemical properties (Milena Leszcynska, 2021).

4.26. TGA analysis for soy-based polyether polyol

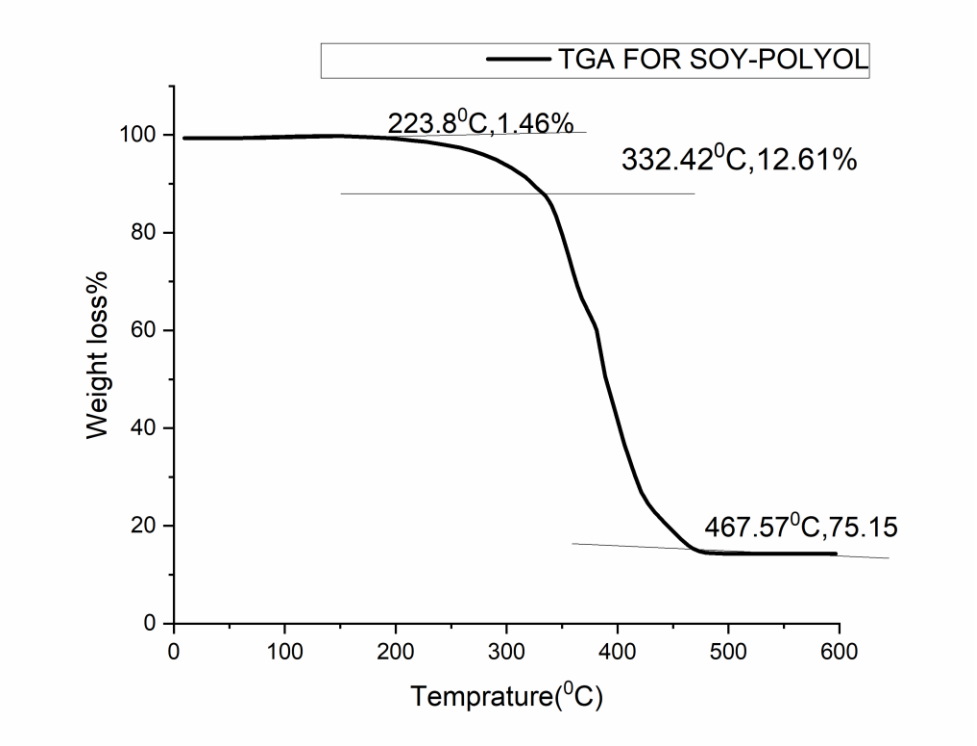


Figure 24 TGA graph for soy-based polyether polyol.

TGA analysis for soy-based poly ether polyol was used to evaluate the intensified hydroxylation process and quality of soy-based polyether polyol. In the soy-based polyether polyol, TGA graph, three degradation steps were observed. At the first step decomposition, at 223.8 ^{O}C, 1.46 % of degradation of organic additives like acetyl aldehydes and formic aldehydes were observed. The second stage of degradation, at 332.42 ^{O}C, 12.61 % of decomposition percentage, polymer degradation including PE and PET was observed. The final stage of decomposition, at 467.57 ^{O}C, 75.1 %, polymeric degradation namely dissociation of PE and PET are observed. The intensified hydroxylation of EWCSBO was evaluated and found successful by TGA analysis. This is due to the fact that higher percentage of degradation of soy-based polyether polyol shows the original property of soy-based polyether polyol (Bahandari, 2023).

4.27. ^{1}H-NMR graph for WCSBO

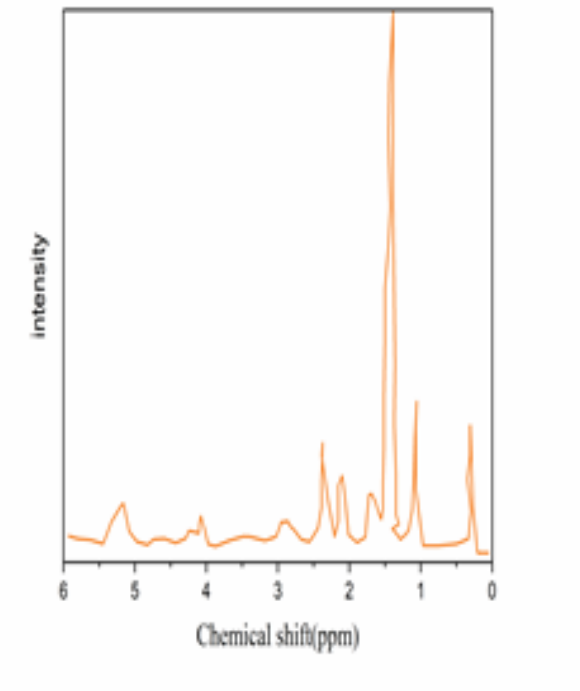


Figure 25 ^{1}H-NMR graph for WCSBO.

The ^{1}H-NMR spectrum of WCSBO was analyzed and showed by characteristic peaks for triglyceride structure. The highest peak for WCSBO has been illustrated at 1.5 ppm tht is a direct confirmation for structure of glycerol backbone in the sample. At 5.3ppm, illustrates the presence of unsaturated fatty acids like oleic acid, linoleic acid. The presence of peaks at 4.1ppm shows the olefin peaks. At 2.4ppm bis-allylic protons were observed in WCSBO. The presence of no peaks at 6 ppm in ^{1}H-NMR graph of WCSBO shows there is no contamination with aromatic compounds (Rahmadi et al., 2024).

4.28. ^{1}H-NMR for EWCSBO

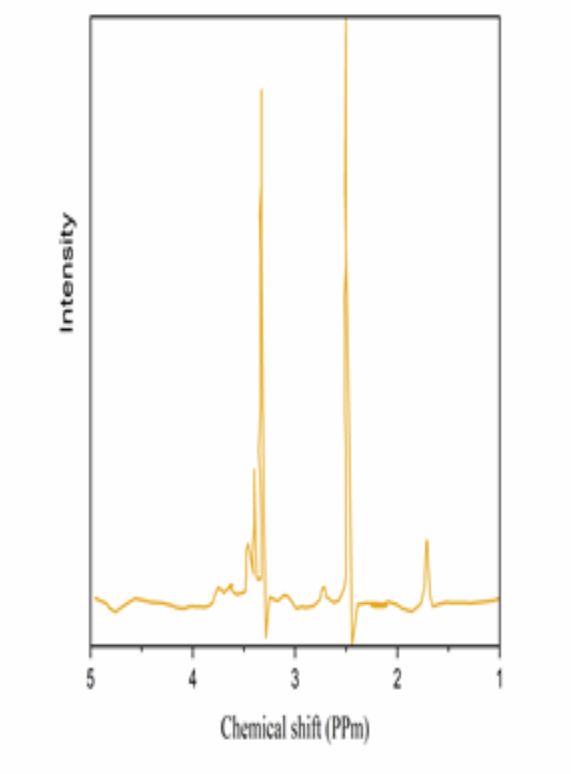


Figure 26 H-NMR graph for EWCSBO.

The ^{1}H-NMR spectrum for EWCSBO was presented in chemical shifts at different peaks as shown above. The strong peak at 2.9ppm illustrates the presence of epoxy ring in the sample. The other highest peak observed at 3.5 ppm shows glycerol backbone and implies its oil origin. Consequently, at 1.7ppm, the peak confirms the conversion of allelic protons in WCSBO to epoxy structure. The strong peak at 3.3 ppm in EWCSBO ^{1}H-NMR graph illustrates the methylene (-CH2-) group. This also confirms the consumption of unsaturated fatty acids (Peroline Helbiling, 2023)

4.29. ^{1}H-NMR for soy-based polyether polyol

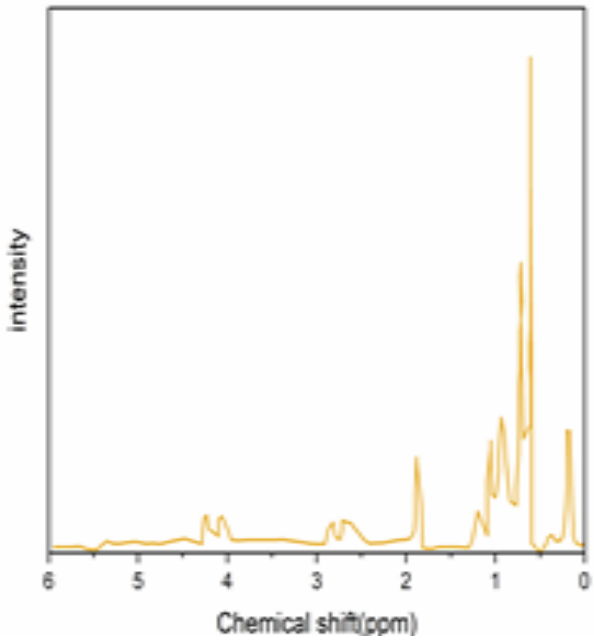


Figure 27 ^{1}H-NMR graph for soy-based polyether polyol.

The ^{1}H-NMR graph for soy-based polyether polyol shows the relation of chemical shift and signal intensity to identify the structural change occurred during the reaction. At 0.5ppm to 1.0 ppm, the peaks imply the presence of fatty acid methyl (-CH_3-) protons. The peaks at 2.9 ppm of EWCSBO diminished. Instead of the strong peak at 2.9ppm, the highest peak was observed at 1.6ppm that exhibits the structure of OH formed during ring opening reaction. This illustrates the epoxy ring have been disappeared due to the ring opening reaction. At 4.2 ppm, the peak shows glycerol (-CH_2-) intact. This consequently implies the bio-based origin of soy-based polyether polyol (Saadouni et al., 2026).

5. CONCLUSION AND RECOMMENDATION

5.1. CONCLUSION

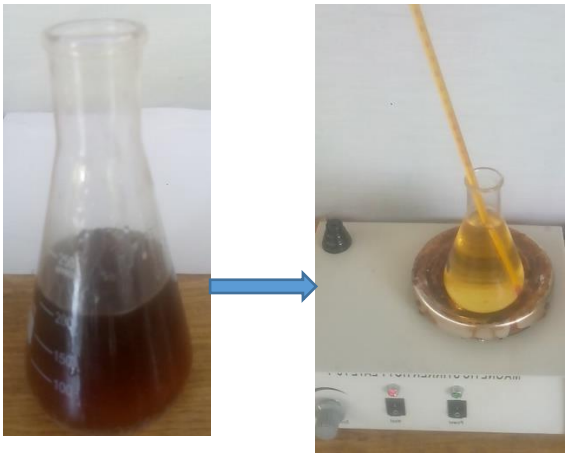
In this research, Process intensification of hydroxylation of EWCSBO was performed using integrated micro channel reactor and micro channel heat sink configuration. Consequently, it has enhanced better performance. The fabricated small dimension of the reactor helped to have higher contact area and enhanced diffusion of the reactants. This led to shorter residence time, higher conversion and good reaction control system. The micro channel heat sink along with a micro channel reactor helped the reaction to absorb the heat of the reaction and to cool it efficiently. The results of RSM revealed that the most optimum OH number was observed at 89.49^0C, 0.96 molar ratio and 9.91 mins of process parameters. The revealed OH number was 436.51mg KOH/g. This is a good implication of successful process intensification of hydroxylation reaction by applying the micro channel reactor and micro channel heat sink in regulating process parameters. In mass and heat transfer analysis procedure for micro channel reactor a Re number with a range of 0.12 to 0.62. This value of Re number for micro channel reactor imply the smooth mixing of reactants in small engraved channel of the reactor. This is an implication for slow flow in small dimension that implied strictly laminar condition. The Nu number for micro channel heat sink was obtained with range of 11.06 to 44.25. The thermal resistance for the micro channel heat sink was obtained from 0.003-0.0013. These values are a strong indication for effective performance system. For a micro channel heat sink, Re number for micro channel heat sink ranges was observed with range of 22.42 to 122.69. The cooling medium namely water was highly appropriated material in dissipating heat. The Re value for micro channel heat sink has shown slight increment from Re number of the reactor due to lower viscousity of the cooling medium. The Sh number also increases as velocity increases and molar ratio increment. Molecular structural identification of WCSBO, EWCSBO and soy-based polyol were identified by FTIR, NMR graph. For TGA analysis of soy-based polyether polyol was identified 75.1%. The efficiency of micro channel reactor increased. As a conclusion, a micro channel reactor was found as a promising tool for process intensification of a hydroxylation of EWCSBO.

5.2. Recommendation

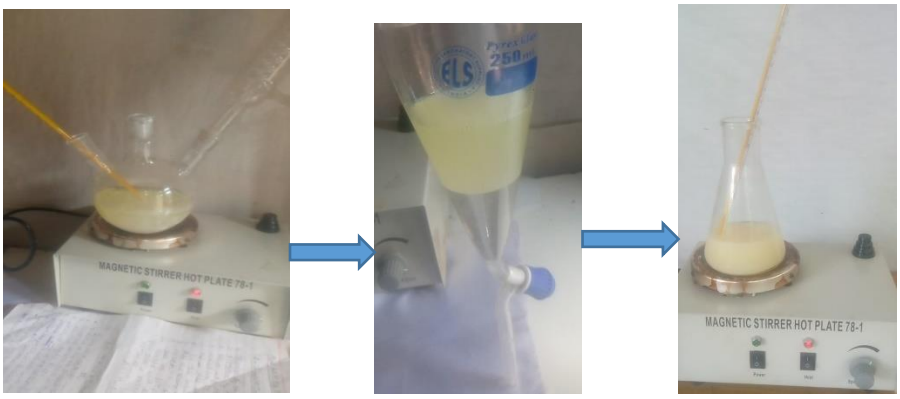
In this study, process intensification of hydroxylation of EWCSBO using micro channel reactor and micro channel heat sink was successfully studied. It has also resulted better performance. Future studies can focus on employing nano fluids as a cooling medium for more improvised thermal performance of the micro channel heat sink. Moreover, further studies on employing heterogeneous catalytic reaction using chemical vapor deposition or wash coating techniques is recommended. CFD modeling and machine learning for the employment of micro channel reactor system can also be done by done researchers. It is also recommended that to use phase change materials for the micro channel heat sink for best performance results.

APPENDIX

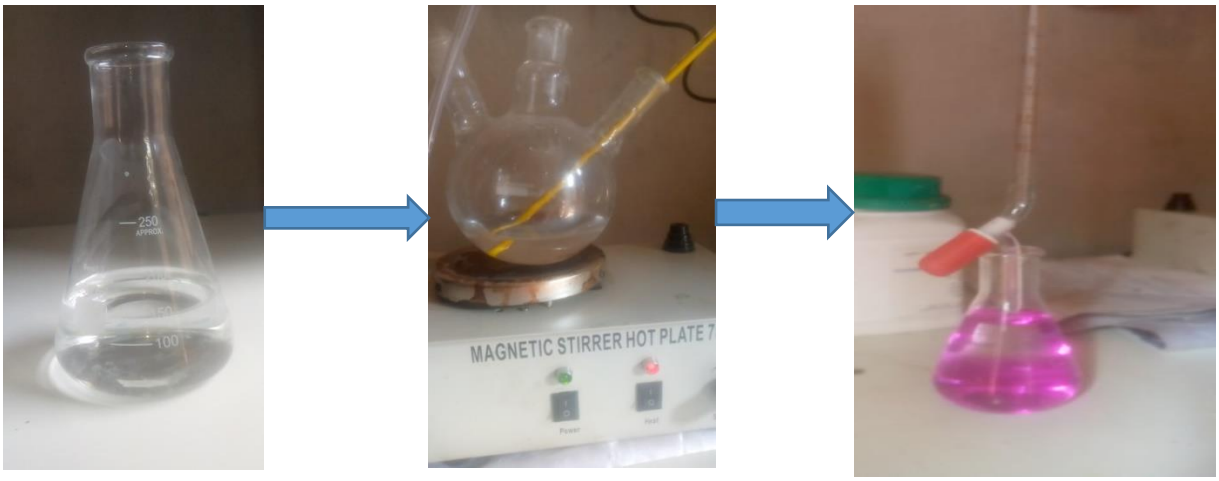
Appendix A: - Pretreatment laboratory photos



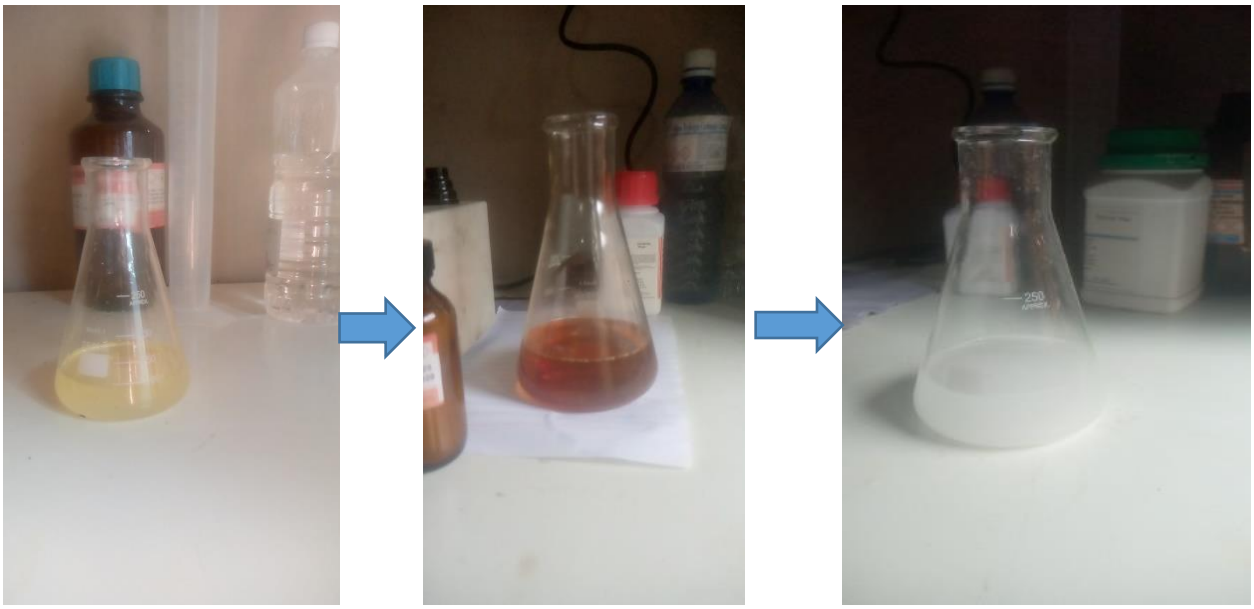
Appendix B: Laboratory photos for epoxidation reaction and titration methods.



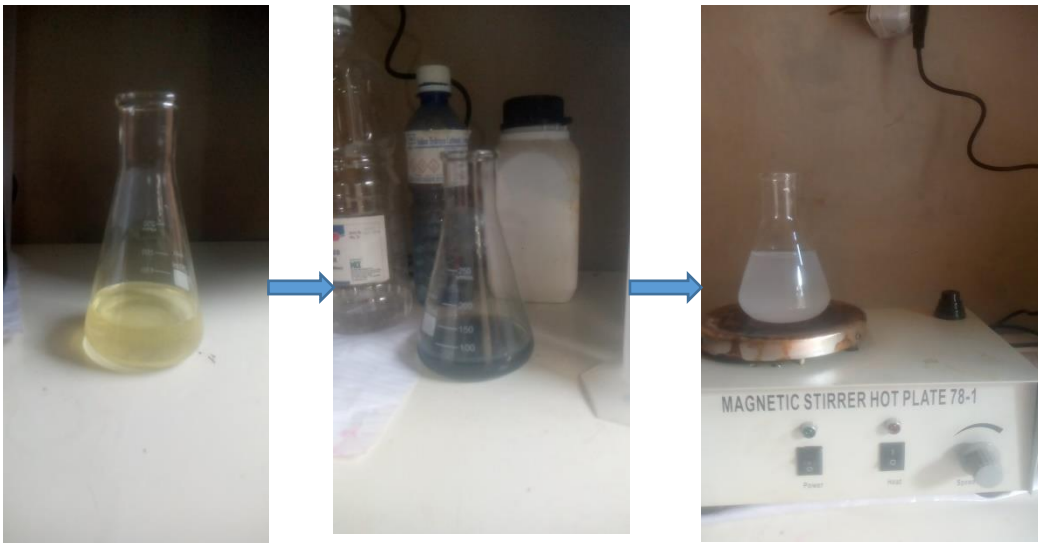
Appendix C: - Laboratory photos for saponification value determination.



Appendix D: - Laboratory photos iodine value determination.



Appendix E: - Laboratory photos for peroxide value determination.



Appendix F: - Design expert software results.

Fit Summary

Response 1: Hydroxyl number

Transform: Power
Lambda: 1, Constant: 0

Table F1 model summary statistics

Source	Sequential p-value	Adjusted R^2	Predicted R^2	
Linear	< 0.0001	0.7708	0.6422	
2FI	< 0.0001	0.9505	0.8857	Suggested
Quadratic	0.1504	0.9613	0.8364	
Cubic	0.2125	0.9724	-0.9218	Aliased

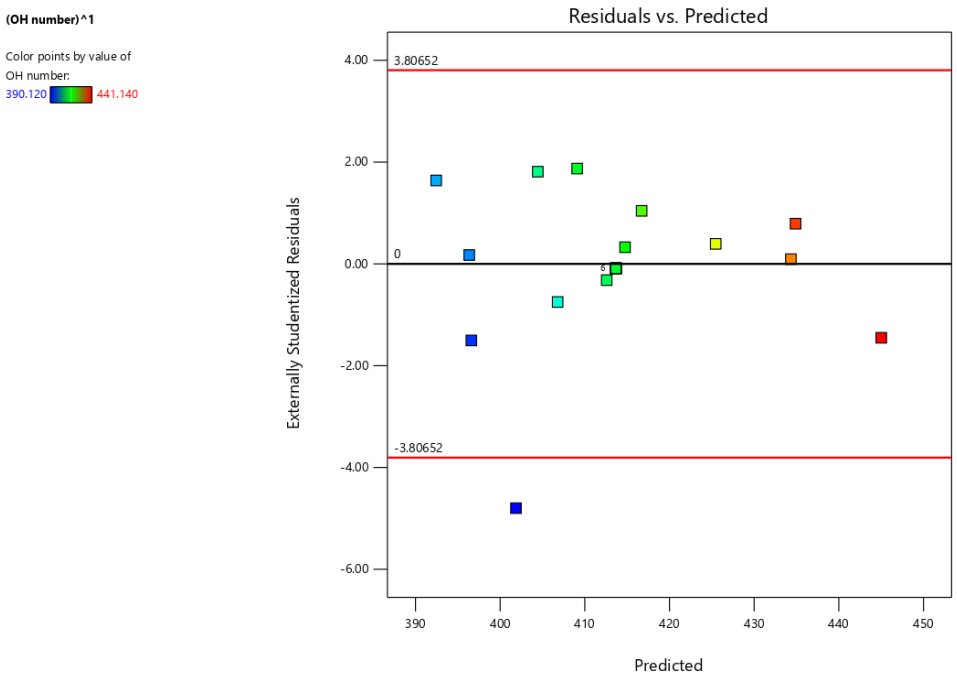


Figure F1 Residual versus predicted

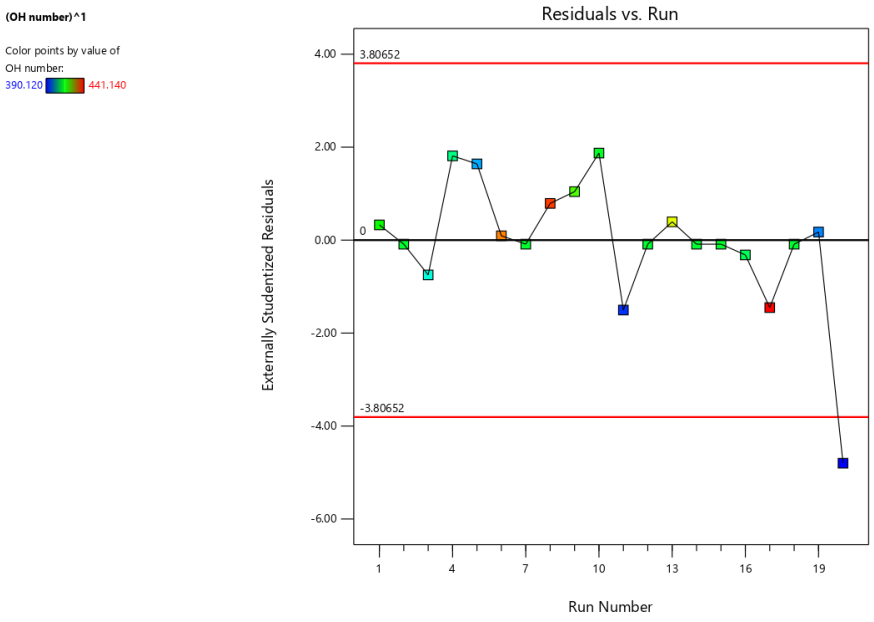


Figure F2 Residual versus run graph.

Reference

Afzal, M. J., Tayyaba, S., Ashraf, M. W., Khan, M. I., Javaid, F., Basher, M. K., & Hossain, M. K. (2022). A Review on Microchannel Fabrication Methods and Applications in Large-Scale and Prospective Industries. *Evergreen*, *9*(3), 764-808. https://doi.org/10.5109/4843111

Alienor Delavardar, G. S., Paul Dercenene,Marine Bourser, Roberto morales-cerrada, Benjamin Nottelet,julein Pinaud,Sylavin Caillol. (2024). Sustainable polyurthanes:towards new cutting edge opportunities. *151*. https://doi.org/10.1016/j.progpolymsci.2024.101805

Alina Niculescu, G. A., George Bulbuasa,Iuliana Stefan,Ciprian Bucur,Anisa Borena. (2022). Micro channel reactor for low level H_2 oxidation within o_2 stream: Prelimnary tests in view of integration in H_2 generator with in CECE process. https://doi.org/10.46390/j.smensuen.25122.444

10.46390/j.smensuen.25122.444

10.46390/j.smensuen.25122.444.1

Aloisyus Yuli widianto, v. L., Cindy,Clarisa,Reynaldo,valentio,Caralonia,Elfa,Lanny Sapei. (2023). <MASS TRANSFER PHENOMENA OF PARTIALLY MISCIBLE - ScienceDirect.pdf>.

Azilatul Nabilla Zakwan, R. s. f. N. H. (2022). Comparative Study on Optimization of Factors Affecting Epoxidation-Hydroxylation Reaction for The Production of Waste Cooking Oil Based-Polyol. *Scientific Research Journal*, *19*(2), 1-22. https://doi.org/10.24191/srj.v19i2.13748

Bahandari, M. G. a. V. (2023). Comparison on physico chemical parameters of five comerically avialable branded oils in Tansen Bazar. *11*.

Bai, R., & Torii, S. (2024). Numerical simulation and experiment of laminar heat transfer characteristics in micro-channel collector. *Thermal Science*, *28*(2 Part B), 1281-1286. https://doi.org/10.2298/tsci2402281b

Beghetto, V. (2025). Strategies for transformation of waste cooking oils in to high value proucts: A critical review. https://doi.org/10.20944/preprints202501.0911.v1

Benbouriche, A., Haddadi-Guemghar, H., Bachir-bey, M., Boulekbache-Makhlouf, L., Hadjal, S., Kouadri, L., Mehidi-Terki, D., Hamitri, M., & Madani, K. (2022). Improvement of thermo-resistance and quality of soybean oil by blending with cold-pressed oils using simplex lattice mixture design. *Ocl*, *29*. https://doi.org/10.1051/ocl/2022025

Benrabah, R. (2025). Hydrodynamics of gas-liquid micro reactor designed for oxidation kinetics of organnic compounds

Boss, E. F., Benke, J. R., Tunkel, D. E., Ishman, S. L., Bridges, J. F., & Kim, J. M. (2015). Public insurance and timing of polysomnography and surgical care for children with sleep-disordered breathing. *JAMA Otolaryngol Head Neck Surg*, *141*(2), 106-111. https://doi.org/10.1001/jamaoto.2014.3085

Bouras, H. (2021). Predictions of mass transfer performance in trickel bed reactors equipped with innovative catalyst shapes.

chen, J. (2022). Computitional study of transport phenomena in micro channnel reactors by hydrogen production by steam reforming.

Chinemerm, H. U., Paul eze Eme,Peretual Ngozi eze,Heney Asuhery,Obajaja and afoma emmanuela omeilli. (2024). Chemical assesment of the quality of palm oil and soldin major market in orlu zone in imo state, Nigieria. https://doi.org/10.30574/wjarr.2024.21.2.0529

Clak, A. O. a. J. (2020). Green Chemicals from used cooking; Trends, challenges and opportunities. *2452-2236*. https://doi.org/10.1016/j.cogsc.2020.100369

Cogliano Tommaso, R., vincenzo,Salmi,Tapio,Granen,Kari,Tesser,Richard. (2024). Epoxidation of vegitable oils in a continious device,kinetics,mass transfer,reactor and modelling. *120079*, *294*. https://doi.org/10.1016/j.ces.2024.120079

Coman, A. (2023). Synthesis and charachterization of renewable polyurethanes using different bio based polyols from olive oils.

Council, I. O. (2020). Determination of the peroxide value.

Daha Retino swatiri, p. m., Arief budhiman. (2021). Chemical epoxidation of oleic acid produce AB type monomer based polyester synthesis. https://doi.org/10.11113/jurnalteknologi.v83.16912|

Dedy suhendra, G. R., Sri seno Handayani and Herani. (2023). Syntehsis of polyol through epoxiation an hydroxylation reactions of Ricinus Communius L. Oil. *300-301*. https://doi.org/10.2991/978-94-6463-232-3_30

Devahdhanush, V. S., Lei, Y., Chen, Z., & Mudawar, I. (2021). Assessing advantages and disadvantages of macro- and micro-channel flow boiling for high-heat-flux thermal management using computational and theoretical/empirical methods. *International Journal of Heat and Mass Transfer*, *169*. https://doi.org/10.1016/j.ijheatmasstransfer.2020.120787

Dhanavel, N., & Nandakrishnan, M. (2024). An Ecofriendly Potentiometric Technique to Measure the Iodine Values of Animal Fats. *Brazilian Journal of Analytical Chemistry*, *12*(46). https://doi.org/10.30744/brjac.2179-3425.AR-102-2024

Dominguez-Candela, I., Lerma-Canto, A., Cardona, S. C., Lora, J., & Fombuena, V. (2022). Physicochemical Characterization of Novel Epoxidized Vegetable Oil from Chia Seed Oil. *Materials (Basel)*, *15*(9). https://doi.org/10.3390/ma15093250

Eke Ejiofor, B. E. A., Allen J.E. (2021). Effect of Variety on the quality parameters of crude soybean oil. https://doi.org/10.12691/ajfst-9-3-1

10.12691/ajfst-9-3-1

10.12691/ajfst-9-3-1.Crude

Enhong Cao, A. N. R., dza bin hasanudin and asterio Gavrillidis. (2021). Study of liquid- solid mass transfer and hydrodynamica in micro packed bed with Gas-liquid flow. https://doi.org/10.1021/acs.iecr.1c00089

F.Montazeri. (2023). Improving Thermal Performance of Rectangular Microchannel Heat Sinks using Porous Layer: CFD Simulation and Optimization. *Journal of Applied Fluid Mechanics*, *16*(8). https://doi.org/10.47176/jafm.16.08.1745

Feng, L. L. (2023). Investigation of Flow Boiling in Micro-Channels: Heat Transfer, Pressure Drop and Evaluation of Existing Correlations. *Journal of Applied Fluid Mechanics*, *16*(9). https://doi.org/10.47176/jafm.16.09.1840

Fengyan zhang, Y. D., Shuong Lin, Xufeng Gui,Jiwenhu. (2023). Optimization of production process epoxidized soyben oil with oxgen content through response surface methodology.

Firadousi, T. (2025). Comparative Oxidative Stability of Soybean and

Sunflower Oil during Prolonged Storage under Various

Storage Conditions. *Carpathian Journal of Food Science and Technology*, 57-66. https://doi.org/10.34302/crpjfst/2025.17.2.5

Fu, T. (2023). Multiphase flow in micro channels. *science and technology*.

G Marsegila, M. d., P pontes, R Solipa,R.r Souza,L.N Moreira, A smoita. (2024). Enhancement of micro channel heat sink transfer

:comparison between different heat transfer strategies. https://doi.org/10.1016/j.expthermflusci.2023.111052

Gabriel L.O. Carmo, M. S. G., Nata C.L , Katia M.Novack, Wanderson Ramao, Fabiano L. Naves, Cristane M. Finzi-Quniato. (2023). Synthesis and degradation of polyols from thermograded Soybean oil.

Gaikwad, V. P., & Mohite, S. S. (2022). Performance analysis of microchannel heat sink with flow disrupting pins. *Journal of Thermal Engineering*, *8*(3), 402-425. https://doi.org/10.18186/thermal.1117391

Gao, J., Hu, Z., Yang, Q., Liang, X., & Wu, H. (2022). Fluid flow and heat transfer in microchannel heat sinks: Modelling review and recent progress. *Thermal Science and Engineering Progress*, *29*. https://doi.org/10.1016/j.tsep.2022.101203

Giri, A. (2023). Study of two phase flow charachterstics in the interuppted micro channels.

Gobbana, G. M. (2022). Charachterization and optimization of Soybean oil from soybean seed(keta and bilo 19) variety. *68*.

Greener, A. J., Ubysz, P., Owens-Ward, W., Smith, G., Whitwood, A. C., & James, M. J. (2021). Radical anion coupling through reagent: Hydroxylation aryl haliides. https://doi.org/10.26434/chemrxiv-2021-szmqs

Gustavo V, O., Paula A,Meira, Thayana,Henirique M,Okuda, Jacyr V, De quadros Jr,Maui S.A, Palama, Reinaldo,Giudia. (2023). Micro reactorX millireactor:Experimental prformance in epoxidation of soybean oil. *0255-2701*. https://doi.org/10.1016/j.cep.2023.109562

H., H. (2024). Flow instablities in boilling channels and their supperssion methodolgy rev eiw.

Halima kerras, N. a. a. a. h. m. (2023). Materials and clean processs for sustainable and enviromental applications. *26*. https://doi.org/10.5802/crchim.229

Helbling, P., Hermant, F., Petit, M., Tassaing, T., Vidil, T., & Cramail, H. (2023). Unveiling the reactivity of epoxides in carbonated epoxidized soybean oil and application in the stepwise synthesis of hybrid poly(hydroxyurethane) thermosets. *Polymer Chemistry*, *14*(4), 500-513. https://doi.org/10.1039/d2py01318e

Himanshi Soni, M. K., Meonakishi Verma. (2023). Recent advances in production of soap for enviroment remediation. https://doi.org/10.1051/e3sconf/202450903014

Holm, J. (2023). *Bio diesel production from waste cooking oil: Processing,challenges and opportunities in Yemen*

Hong phuoug , p., Trung Dang Bao Hao, Hung Lam. (2023). Epoxidation of soybean oil and its blending with waste cooking oil using H2SO4 as homogeneous catalyst. *106*. https://doi.org/10.3303/CET23106060

Hui ying yong, R. A. a. S. T. A. (2023). Microscopic,Spectroscopic,Thermo analytical Charachterization of modified palm oil and rice bran oil in to biopolymers. *Malasyian Journal of analytical Sciences*, *27*.

Ibrahima Balde, C. K., Abdou K.D.Dime,Samba Balde,khady Ndiaye. (2022). Vegetable oils epoxidation mechanisms. https://doi.org/10.12691/wjac-7-1-1

10.12691/wjac-7-1-1

10.12691/wjac-7-1-1.1

Ibrhaima Balde, C. K., Abdou K.D. Dime,Samba Balde, Khady Ndiaye. (2022). Vegitable oil epoxidation mechanisms. *07*. https://doi.org/10.12691/wjac-7-1-1

10.12691/wjac-7-1-1

10.12691/wjac-7-1-1.1

Ivan Dominguez-Candela, A. L.-C., Salvador Cayentano,Cardena,Jaime Lora,vicent fombuen a. (2022). Physico-chemical charchterstics of novel vegitable oil from chia seed oil. https://doi.org/10.3390/ma15093250

Iyan Sopyian, D. K., Rizka Korhunissa Guntina. (2022). Design of expert:An application tool for optimization in pharamaceutical preparation formulation. *14*. https://doi.org/10.22159/ijap.2022v14i4.45144

10.22159/ijap.2022v14i4.45144.Journal

Jain, D. M. (2023). Determination of diffrent parameters of edible oils.

Jarred Wilhite, C. k. (2024). Fluid and thermal analysis of manifloid micro channel heat sink.

Jermy ong shung sheng, M. s. A. m., Norazila Othman, Mastura Abdula wahid. (2024). Soy bean and waste cooking oil feed stocks for sustaiable bio fuel production https://doi.org/10.11113/jm.v47.474

Ji, Y., Xu, L., Xu, Q., Liu, X., Lin, S., Liao, S., Wang, W., & Lan, D. (2022). Synthesis and Characterization of Epoxidized Silkworm Pupae Oil and Its Application as Polyvinyl Chloride. *Appl Biochem Biotechnol*, *194*(3), 1290-1302. https://doi.org/10.1007/s12010-021-03715-5

Jinhua Yi, X. Y. (2021). The effect of Bisphenol A polyether polyol on the synthesis of hydrophilic epoxy resins. https://doi.org/10.3844/ajbbsp.2021.302.311

Juliana cardenas, B. K., Peter H seeberger,Joe dangand flores, Alvaro (2025). Continious epoxidtion of used cooking oil using an automatated slug flow milli reactor. https://doi.org/10.1016/j.cej.2025.159907

Kahdrawi, A. F. (2024). A SEMI-ANALYTICAL APPROACH TO INVESTIGATE THE VALIDITY OF THE THERMAL EQUILIBRIUM ASSUMPTION IN THE ANALYSIS OF UNSTEADY FREE CONVECTION IN POROUS MICRO-CHANNEL.pdf.

Kai Han, Y. z., Shaoua Ju, Jingxi Zhang. (2022). 3D printing multi channel large micro channel volume for enhanced removal of low concentration of NOX flue gas. *17*, *158*. https://doi.org/10.3390/pr11010158

Kim, T. H., Kim, H. S., & Lee, S. H. (2026). Sustainable Polyurethane Systems: Integrating Green Synthesis and Closed-Loop Recovery. *Polymers (Basel)*, *18*(2). https://doi.org/10.3390/polym18020246

Koosha Karimi, A. F., Nikhli Mahtre, Jay Ravid,David Bosivert and mehdi Javanmarad. (2024). A through review emerging technologies in micro and nano channel fabrication,limitation and application. https://doi.org/10.3390/mi15101274

Kuang, Y., Li, W., Xie, S., Gong, W., Ye, Z., Wang, Y., Peng, D., & Li, J. (2023). Epoxidized Soybean-Oils-Based Pressure-Sensitive Adhesives with Di-Hydroxylated Soybean-Oils Copolymerizing and Antioxidant Grafting. *Polymers*, *15*(12). https://doi.org/10.3390/polym15122709

Lee, J., Darges, S. J., & Mudawar, I. (2021). Experimental investigation and analysis of parametric trends of instability in two-phase micro-channel heat sinks. *International Journal of Heat and Mass Transfer*, *170*. https://doi.org/10.1016/j.ijheatmasstransfer.2021.120980

Leszczynska, M., Malewska, E., Ryszkowska, J., Kuranska, M., Gloc, M., Leszczynski, M. K., & Prociak, A. (2021). Vegetable Fillers and Rapeseed Oil-Based Polyol as Natural Raw Materials for the Production of Rigid Polyurethane Foams. *Materials (Basel)*, *14*(7). https://doi.org/10.3390/ma14071772

M.B, D., Magnini, M., & Matar, O. K. (2024). Numerical modelling of flow boiling inside microchannels: A critical review of methods and applications. *Applied Thermal Engineering*, *257*. https://doi.org/10.1016/j.applthermaleng.2024.124464

Maleki, H., & Bertola, V. (2025). Electrification of ammonia cracking for on-demand hydrogen production: CFD modeling. *Next Energy*, *8*. https://doi.org/10.1016/j.nxener.2025.100324

Mariana del valle, B. v., Viviana Nicholas,Miriam cristin Strumia. (2022). Bio-based polyester from soybean synthesis, charachterization and degradation studies. *9*. https://doi.org/10.22063/POJ.2021.3019.1203

mastroani luca, v. z., eranien kari. (2022). Micro reactor technology in experimental and modelling study of alcohol oxidation on nano gold. https://doi.org/10.1016/j.ces.2022.117920

Mastroianni, L., Vajglová, Z., Eränen, K., Peurla, M., Di Serio, M., Yu. Murzin, D., Russo, V., & Salmi, T. (2022). Microreactor technology in experimental and modelling study of alcohol oxidation on nanogold. *Chemical Engineering Science*, *260*. https://doi.org/10.1016/j.ces.2022.117920

mendonza, J. N. a. j. a. (2025). Impact of micro channel reactor design on thanol synthesis via CO2 hydrogenation:CFD approach. *643*. https://doi.org/10.1051/e3sconf/202564302003

Milena Leszcynska, E. M., Joanna Gloc,Michal Leszczynski,Aleksander Prociak. (2021). Vegitable fillers and rapeseed oil-based polyol natrual raw materials for production of rigid Poly urthane. https://doi.org/10.3390/ma14071772

Mohamed Ezzeldin, M., Ahmed M, Ramdan,Yasser Assem. (2021). Soybean oil-based polyol as a modified natural binder for polyuthane Turf-adhesive. *64*. https://doi.org/10.21608/EJCHEM.2020.31470.2670

Morales-Cerrada, R., Tavernier, R., & Caillol, S. (2021). Fully Bio-Based Thermosetting Polyurethanes from Bio-Based Polyols and Isocyanates. *Polymers (Basel)*, *13*(8). https://doi.org/10.3390/polym13081255

Nasser R.Abd E Rahan, M. B. N. A. N. z. A. (2021). Synthesis and Evaluation of poymeric dispersant based on vegitable oils their application as cutting fluid. *11727*, *64*. https://doi.org/10.21608/EJCHEM.2021.74156.3662

Naveen Anthuvana, K., Josko Valneteincic,. (2024). Mass production of micro mixers: A comphersenive Review. https://doi.org/10.4108/eai.23-2-2024.2346994

Navin Gautam, A. k., Nabin Kahadka, Prakash panta. (2024). Thermal degradation of soybean oil and palm olein during deep fat frying.

Peroline Helbiling, F., Hermant, M.H Petit,Theiry Tassaing,Thomas Vildil, Henri Caramil. (2023). Univeiling the reactivity of epoxides in carbonated epoxidized soybean oil and application in step wise synthesis of hybrid poly (hydroxyurthane) thermosets. *14*, *4*. https://doi.org/10.1039/D2PY01318E

Pierre Albrand, B. L. (2023). Mass transfer rate in gas-liquid taylor flow: Sheerwood from numerical simuilation. *Chemical Engineering science*, *280*.

Pontes. P, M. L. (2022). FLUID FLOW AND HEAT TRANSFER IN MICROCHANNEL DEVICES FOR COOLING APPLICATIONS EXPERIMENTAL AND NUMERICAL APPROACHES.

Putri A.R, R. A. s., W, Riyanto,S. (2020). Determination of acid, Peroxide and Saponification value in patin fish oil by FTIR spectroscopy combined with chemo metrics. https://doi.org/10.26656/fr.2017.4(5).030

Putri, A. R., Rohman, A., Setyaningsih, W., & Riyanto, S. (2020). Determination of acid, peroxide, and saponification value in patin fish oil by FTIR spectroscopy combined with chemometrics. *Food Research*, *4*(5), 1758-1766. https://doi.org/10.26656/fr.2017.4(5).030

Rahmadi, H. Y., Syukur, M., Widodo, Suwarno, W. B., Wening, S., Simamora, A. N., & Nugroho, S. (2024). (1)H NMR analysis of metabolites from leaf tissue of resistant and susceptible oil palm breeding materials against Ganoderma boninense. *Metabolomics*, *20*(5), 89. https://doi.org/10.1007/s11306-024-02160-9

Ramirez, J. C. (2025). Intensification in epoxidation of used cooking oils acid catalyts.

ramirez, J. c. (2025). Intesification in epoxidation of used cooking oils using acid catalyst.

Saadouni, I., El Mrimar, O., & Samoudi, B. (2026). Numerical Investigation of Nanofluid-filled Microchannel Heat Sinks for Improved Heat Transfer of High-power Electronic Devices. *Journal of Applied Fluid Mechanics*, *19*(6). https://doi.org/10.47176/jafm.19.6.4133

Salarvand, E., Omrani, I., Nabid, M. R., & Salehi, M. (2023). https://doi.org/10.21203/rs.3.rs-3062330/v1

Say, M., Heng, P., Kong, S., Ping Tan, C., Phal, S., Nat, Y., & Tan, R. (2024). Characterization of Physicochemical Properties of Cooking Oils Sold in Phnom Penh, Cambodia. *Journal of Food Science and Nutrition Research*, *07*(01). https://doi.org/10.26502/jfsnr.2642-110000149

Shaojie Tan, S. C., Kai wang,xiaoxing,Liu Hui cheng and Jun wang. (2023). The devlopment of micro and small modular reactor in future energy market. https://doi.org/10.3389/fenrg.2023.1149127

Sharma, K. N. R. a. T. (2023). Thermal analysis of PCM based hybrid, micro channl heat sink : A numerical study. *534101*. https://doi.org/10.18186/thermal.1332551

Shen, F., Li, C., Yuan, Y., & Liu, Z. (2023). An easy droplet generation method using an inserted glass capillary into a micro channel. https://doi.org/10.21203/rs.3.rs-2910012/v1

Siti Nurzubadia, R. s. f. N. H. (2021). Pretreatment of used cooking oil followed by transesterification reaction in production of used cooking oil based polyol. https://doi.org/10.24191/srj.v18i2.13749

Subramaniya, P. (2022). Fourier series-based modelling of the effects of the thermal coupling on transient dynamics of componet loops in a coupled natrural circuilation loop.

Suhendra, D., Gunawan, E. R., Handayani, S. S., & Haerani. (2023). Synthesis of Polyol Through Epoxidation and Hydroxylation Reactions of Ricinus Communis L. Oil. In *Proceedings of the 2nd International Conference on Science Education and Sciences 2022 (ICSES 2022)* (pp. 300-307). https://doi.org/10.2991/978-94-6463-232-3_30

Surendera Barhatte, M. L. (2024). Investigations on micro channel heat exchanger using numerical, experimental and ANN networking. https://doi.org/10.54905/disssi.v21i55.e7ije1682

Udom, E. J., & Lappa, M. (2025). Comparative analysis of microchannel heat sinks for different values of the Prandtl and Reynolds numbers. *International Journal of Numerical Methods for Heat & Fluid Flow*. https://doi.org/10.1108/hff-11-2024-0884

Vrushali M, M. a. D. A. A. M. (2024). Shifts in acid and saponification values of oil over time. *10*.

wang, C. (2024). CFD investigation of pressure drop factor and nusselt number for flow in zigzag channel.

Wazed M.A, Y. S., Basak,Rahaman,Hasan,Kahir.Khatun. (2023). Evaluation of physico chemical parameters of edible oils at room temprature https://doi.org/10.26656/fr.2017.7(4).900

Wazed, M. A., Yasmin, S., Basak, P., Hossain, A., Rahman, M. M., Hasan, M. R., Khair, M. M., & Khatun, M. N. (2023). Evaluation of physicochemical parameters of edible oils at room temperature and after heating at high temperature. *Food Research*, *7*(4), 91-100. https://doi.org/10.26656/fr.2017.7(4).900

Wei Han foo, S. S. N. K., Doris ying yingTang,Wen yi chia,kit Wayne chew and au Loke show. (2022). Safety Control of Waste cooking oil: transforming hazard into multi farious products with available pre-treatment process. https://doi.org/10.48130/FMR-2022-0001

Widianto, A. Y., Lorenza, V., Clarisa, C., Valentino, R., Elfa, C., & Sapei, L. (2024). Mass transfer phenomena of partially miscible liquids under liquid-liquid slug flow in a circular microchannel. *Chemical Engineering Research and Design*, *205*, 57-66. https://doi.org/10.1016/j.cherd.2024.03.013

Xu ming, F., Avila,Cabo,miriam,Zeng,Danefi,Zhang,Yifeng,. (2025). Leverging 3D printing in microbial electrochemistry research. https://doi.org/10.1016/j.tsep.2022.101203

Xylem. Determination of acid number and free fatty acids(FFAs) in fats and oils.

Yan, Z., Tian, J., Du, C., Deng, J., & Luo, G. (2022). Reaction kinetics determination based on microfluidic technology. *Chinese Journal of Chemical Engineering*, *41*, 49-72. https://doi.org/10.1016/j.cjche.2021.08.023

Yu, Z.-Q., Li, M.-T., & Cao, B.-Y. (2024). A comprehensive review on microchannel heat sinks for electronics cooling. *International Journal of Extreme Manufacturing*, *6*(2). https://doi.org/10.1088/2631-7990/ad12d4

Zafiah, A. (2023). Waste cooking oils in biodegradable polymer: Conversion process. https://doi.org/10.2991/978-94-6463-134-0_17

Zhang, L., & Yue, J. (2025). Unveiling hydrodynamics in single pellet string microreactors: Insights from gas-liquid slug flow regime and pressure drop. *Chemical Engineering Journal*, *512*. https://doi.org/10.1016/j.cej.2025.162401